Forensic Fire Scene Analysis Using Computational Fluid Dynamics (CFD)

A Major Qualifying Project Report:

Submitted to the Faculty

of the

WORCESTER POLYTECHNIC INSTITUTE

In partial fulfillment of the requirement for the

Degree of Bachelor of Science

by

Francisco Kang

Raeshawn Kennedy

Bernard Rabidou

Dimitrios Savva

Date: April 27, 2016

Approved by:

Professor Milosh T. Puchovsky, Advisor

Professor Christopher B. Wood, Co-Advisor

Table of Contents

Executive Summary

Fire Dynamics Simulator (FDS) is a computational fluid dynamics program developed and maintained by the U.S. National Institute of Standards and Technology (NIST). This project examined the use of FDS as a forensics tool to provide better insight on how changing ventilation conditions within a compartment fire can affect fire growth, flame spread and resulting fire damage.

Fire investigations remain a very complex forensic science. It is not unusual for two fire investigators to examine the same fire scene and reach different conclusions. Heat energy initially in the form of an ignition source, available fuels and their associated physical and chemical properties, an oxidizer such as oxygen in air, and an uninhibited chemical reaction are necessary to initiate and sustain combustion, and are fundamental in understanding flame spread and fire growth. Fuel properties and availability of the oxidizer through varying ventilation conditions such as door openings and failed windows during a fire, as well as the location of fuel sources with respect to the ventilation openings, can significantly affect the fire's outcome and overall resulting fire scene.

Burn patterns and resulting fire damage prompt certain notions about where and how the fire started. However, areas of heavy fire damage do not always correlate with initial areas of fire origin and growth. Key factors such as changing compartment ventilation conditions throughout the fire event can result in substantial localized fire damage and burn patterns remote from actual areas of origin. A computer model that can replicate, with a sufficient degree of accuracy, the stages of a fire event for a range of likely scenarios would prove useful for better informing decisions about a fire scene and facilitate more uniform conclusions.

A series of four fire tests conducted by the Bureau of Alcohol, Tobacco, Firearms and Explosives (ATF), a U.S. government agency responsible for investigating key fire events formed the basis for the project. These tests were performed in identical compartments in which either initial ventilation conditions or initial items ignited varied. In further detail, tests 1 and 2 varied in ventilation conditions, but with the same fire location; tests 3 and 4 varied in fire location, but had the same initial ventilation conditions as test 1. The effect of these ventilation conditions and fire locations on burn patterns and overall areas of substantial fire damage was specifically examined and assessed. During the course of testing, ATF utilized instruments such as thermocouples, heat flux gauges and velocity probes to record data. In addition, they captured visual data with video recording equipment. Fire growth as characterized by heat release rates (HRR) for the overall compartment fires was not measured. However, smaller scale calorimeter tests were conducted to measure specific HRR of individual fuel packages. FDS was applied to recreate the ATF compartment fire tests to determine if and how FDS could reproduce similar results to those measured and observed during the tests.

The physical state and arrangement of the fuel packages, and the individual materials that comprise them need to be sufficiently articulated and quantified for use with FDS. However, in fire scene investigations, the actual fuel packages, their arrangement and specific material

properties are rarely precisely known. This situation held true for this project, as the material properties of the fuels used as part of the ATF tests were not specifically obtained as part of the test program. The fuel packages in the ATF tests consisted of furnishings composed of synthetic fibers such as polystyrene and polyurethane, and natural materials such as wood and cotton. Common material compositions of the fuel packages and pertinent material properties such as density, specific heat, thermal conductivity, heat of combustion and ignition temperature were investigated and estimates for use as input for the FDS calculations were made. The degree to which the material properties used accurately represent the actual fuels involved can have a significant outcome on the resulting calculations.

Various modeling techniques needed to be applied while using FDS. For certain fuel packages, a ramping function was employed to mathematically match the heat release rates to those measured during the ATF calorimeter tests. While FDS contains a subroutine to calculate flame spread and resulting fire growth based on certain input parameters, the results of these calculations did not match well with measured test results. The associated physical phenomenon is not sufficiently understood nor is it mathematically well characterized. Even so, numerical approaches exist and were applied. FDS approximates a compartment or building as a series of user specified small three-dimensional rectangular control volumes or computational cells. FDS computes changes within and among the cells throughout a computational domain. The numerical flame spread model relies upon user specified material properties as they influence how cells, in this case those that represent the surface of a fuel, absorb energy and heat up. The cell mathematically ignites when the entire cell reaches a user specified ignition temperature.

The temperature, heat flux and velocity measurements recorded during the ATF tests were compared to the results calculated by FDS. For certain full-scale FDS simulations, the temperature and velocity data showed reasonable agreement in terms of trends and magnitude to the data measured in the ATF tests. However, all of the simulations showed some discrepancies, which could be due to a delay in fire growth and flame spread. Additionally, Smokeview, a program coupled with FDS for visualizing numerical calculations was employed to evaluate the results of FDS with the video data obtained. However, the video footage showed to be of limited value as the test fires progressed because visibility into the compartment was drastically reduced due to smoke production. As a result, performing visual comparisons of fire growth and flame spread between the model's calculations and the live tests could not be made. Although the video footage could not be fully utilized, the ATF provided photos of the resulting damage for each individual test allowing us to perform a damage analysis. In doing so, additional features of FDS including boundary, slice, and vector files were applied to show the fire conditions that may have led to the cause and formation of the resulting damage to the compartments.

From the aforementioned FDS results and analysis, ventilation was identified to be a key factor in fire growth as characterized by heat release rates (HRR). FDS was able to provide HRR data through mathematical calculations. A relationship between the effects of dynamic ventilation and HRR was identified such that when a window failed, the HRR increased contributing to fire growth leading to the transition of flashover. In all four FDS simulations,

flaming combustion was observed only in areas proximate to oxygen supplying vents in the post flashover environment. This same observation was made by ATF in their tests as regardless of where the initial ignition was located, flaming fire conditions existed only in areas of ventilation openings during the post-flashover environment.

This project puts forth recommendations for areas of further effort and study to improve upon the analysis of resulting damage. The resulting damage of certain fuel packages caused by fire conditions may provide more insight on identifying area of origin. In order to do so, further examination of the materials used in the fuel packages could lead to better characterization of their material properties for use with FDS. Future work should consider performing small-scale bench tests on the materials of the fuel packages using a cone calorimeter or other test devices to derive the actual material properties. In addition, a better characterization of the thermal properties could allow for a more accurate prediction of flame spread.

Abstract

The ATF conducted four identical compartment fire tests to observe the difference in fire conditions and resulting damage when varying the ignition location or initial ventilation conditions. Fire Dynamics Simulator (FDS) was applied to simulate the fire tests to determine the degree to which the fire conditions and resulting outcome from the tests could be replicated. The data measured during the experiments was analyzed against the results calculated by FDS and demonstrated reasonable agreement for certain scenarios.

Acknowledgements

We would like to thank the following professors who provided guidance and support throughout the duration of the project:

Professor Milosh Puchovsky, Advisor
Professor Christopher Wood, Co-advisor

We would also like to thank the Bureau of Alcohol, Tobacco, Firearms and Explosives for the opportunity to work on this project. In particular, we would like to thank the following people, who provided us with the materials necessary to complete the project:

Andrew Cox
David Tucholski

We would also like to thank the WPI Information Technology department for providing us with resources essential to the completion of the project. In particular, we would like to thank the following person:

Siamak Najafi

List of Figures

List of Tables

List of Abbreviations, Acronyms, and Units

Abbreviation or Acronym	Description
ATF	Bureau of Alcohol, Tobacco, and Explosives
CFD	Computational Fluid Dynamics
FDS	Fire Dynamics Simulator
FPI	Fire Propagation Index
HOC (kJ/kg)	Heat of Combustion
HOR (kJ/kg)	Heat of Reaction
HOV (kJ/kg)	Heat of Vaporization
HRR (kW)	Heat Release Rate
HRRPUA (kW/m^2)	Heat Release Rate per Unit Area
MLRPUA (kg/m^2)	Mass Loss Rate per Unit Area
NIST	National Institute of Standard and Technology
OBST	Obstruction
SFPE	Society of Fire Protection Engineers
SURF	Surface
TC	Thermocouple
TRP	Thermal Response Parameter

Unit	Description
°C	Degrees Celsius
°F	Degrees Fahrenheit
ft.	Feet
gpm	Gallons per Minute
in.	Inch
kg	Kilogram
kPa	Kilopascal
kW	Kilowatt
L	Liter
m	Meter
min	Minute
mm	Millimeter
MW	Megawatt
psi	Pounds per Square Inch
sec	Second
W	Watt
μm	Micrometer

1 Introduction

1.1 Problem Statement

Over the past 40 years, the fire investigation community has developed scientifically proven investigative techniques, expertise, and resources to aid in the analysis of fire and explosion incidents. A product of this effort was the creation and development of *NFPA 921: Guide for Fire and Explosion Investigations* [1]. Despite all the advancements made over this time, fire investigations remain one of the most complicated forensic sciences. Depending on the fire scene, two qualified fire investigators may assess the same fire scene evidence and reach different conclusions regarding area of origin, and ultimately the cause of the fire. In order to reduce this disparity, fire investigators must have a solid grasp of the physics and variables that influence a fire's growth and flame spread across a room [2].

The principle influencing variables that affect this growth and spread include melting, pyrolysis and burning and of fuels as well as initial and dynamic ventilation conditions. In an attempt to gain insight into these key variables, the Bureau of Alcohol, Tobacco, Firearms, and Explosives (ATF) completed four separate tests in 'identical' compartments with variations in the fire origin and initial ventilation conditions. The intent of the tests was to better understand how changing the initial ignition location and initial ventilation conditions impact a fire's development, spread, and subsequent damage pattern. Instrumentation placed throughout the compartment, including temperature, velocity, and heat flux devices, helped quantify the effects of each test. In addition, video recordings were utilized to note significant visual observations.

Fire Dynamics Simulator (FDS), a computational fluid dynamics program, was used to provide further insight on how changing the initial ignition location or initial ventilation conditions affects fire growth, spread, and resulting damages. The tasks that were necessary to achieve this goal included the recreation of similar fuel packages, compartment geometry and instrumentation devices in FDS to replicate the ATF test data. FDS facilitated further analysis on the damage assessments of the full-scale models using planar slice files and boundary files, which measure instantaneous wall temperature and heat flux. In addition, Smokeview, a separate visualization program that displays the results of an FDS calculation, allowed the ability to compare the visuals of the simulation to the observations of the video recordings.

1.2 Organization of the Report

This report is organized into eight chapters as follows:

Chapter 1 introduces the problem statement and outlines the overall approach used for this project.

Chapter 2 provides relevant background information, details about key factors in compartment fires and further information about the applications of FDS.

Chapter 3 presents the compartment tests conducted by the ATF and the descriptions of the material composition of the fuel packages.

Chapter 4 discusses the procedure for modeling the fuel packages and the full-scale tests. This chapter also addresses the complications of modeling certain phenomenon using FDS.

Chapter 5 shows the FDS modeling results for comparison with the ATF test measurements and observations.

Chapter 6 provides an analysis of the FDS calculations and keys in on certain features of the computer model that can provide for additional insight about the fire tests.

Chapter 7 concludes the overall report and summarizes our findings.

Chapter 8 provides recommendations for potential future work.

2 Background

2.1 Bureau of Alcohol, Tobacco, Firearms and Explosives

Over the past 40 years, the Bureau of Alcohol, Tobacco, Firearms and Explosives (ATF) has developed investigative capabilities that have positioned them as a well-known source for fire investigative knowledge and assistance [3]. ATF fire investigators routinely assess and interpret fire scene patterns and damages in an effort to develop hypotheses, and eventually draw conclusions about where a fire may have started and how that fire spread throughout a compartment or structure. In addition, the ATF conducted compartment burn tests to better understand the fire dynamics of these events.

2.2 Key Factors in Compartment Fires

In order for a fire to exist, the presence of heat, fuel, an oxidizer, and an uninhibited chemical reaction are all required; this is known as the fire tetrahedron [2]. From this characterization of the fire phenomenon, two major fire science principles play a significant role in understanding flame spread and fire growth in compartment fires [2]. The first principle has to do with the state of the fuels and their material properties. In other words, the first principle is about what is burning and how. The thermal properties of the materials used for the fuel packages affect the initial ignition and the associated heat release rate (HRR). The second principle pertains to ventilation or the supply of oxygen to the compartment fire. Oxygen flow and the direction of ventilation profoundly affect a fire in terms of heat generation and spread rate. Both of these principles also pertain to the project goal of simulating flame spread and fire growth because they highlight the importance of accurately representing the material properties of the fuel packages and the significant influence of changing ventilation conditions.

2.2.1 Solid Fuel Packages

Before flaming combustion can be achieved, solids must first be transformed into an ignitable gas. In order for this phase change to occur for a solid, sufficient heat needs to be applied creating potential fuel for flaming combustion. This heat vaporizes the fuel package into a gas then ignites at a certain temperature [2]. This material-based property is known as the ignition temperature. It is important to note that the solid to gas phase transformation begins prior to reaching this temperature. Although this material property has a strong influence on how long a fuel package takes to ignite, there is usually a certain level of uncertainty related to its value. This is so because it depends on the manner in which the material is heated, the rate of energy transfer to the material, and the physical and chemical composition of the material [4]. This concept becomes particularly important in the pre-flashover environment because the entire compartment is filled with a hot upper gas layer. The heat energy from these gases radiates downwards and causes pyrolysis of solid items distant from the actual flames; a phenomenon that can be described as flame spread. The fuel packages then begin to vaporize and produce more gaseous fuels creating a fuel-rich environment that tends to flashover once a change in

ventilation has occurred. Flashover is the moment in time where all ignitable items have ignited. During the transition to flashover, the energy from the upper gas layer radiates down toward any exposed solids. The resistance to ignition and fire propagation for these previously uninvolved fuel packages is assessed through the thermal response parameter (TRP) of a material [5]. As expected, this property depends upon the ignition temperature (T_{ig}) and other material properties such as density (ρ), specific heat (c_p) and thermal conductivity (k) as well as the ambient temperature (T_a). The equation for TRP is as follows [4]:

$$TRP = (T_{ig} - T_a)\sqrt{k\rho c_p}$$

This can then be used to calculate the fire propagation index (FPI) of a material, which represents the ease or difficulty of flame spread on the surface of the material beyond the area of ignition [4]. This characteristic, which is important in simulating flame spread, is also dependent upon the thermal properties of the material.

Once a fuel package has fully ignited, its burning characteristics are further governed by the material properties that make up that respective solid. Properties such as the heat of combustion of a material, which is the amount of energy produced for each unit of fuel mass burned, have a direct impact on fire growth [4]. Since the HRR is a measurement of the objects energy production over time, it can be an indication of fire size and is calculated by the following equation from the 4th Edition of the SFPE Handbook:

$$\dot{Q} = \dot{m}\Delta h_c$$

where $\dot{Q}$ is the heat release rate of an object, $\dot{m}$ is the mass loss rate and Δh_c is the heat of combustion. The heat of combustion for a material is determined almost entirely by the chemical composition of the material as well as the air quality at the time of combustion meaning that a reaction with pure oxygen will yield the highest heat of combustion [4]. This thermal property is often controlled by the oxygen supply and subsequently the ventilation parameters of the scenario.

2.2.2 Ventilation Parameters

In compartment fires, the ventilation parameters may control the amount and location of available oxygen for combustion [4]. It was previously stated that flashover fires in a compartment create enough heat energy to effectively pyrolize every exposed solid within a compartment. The resulting fuel gases in the upper layer of the compartment can be 600°C or above, but can only ignite and continue to burn when they mix with the appropriate amount of oxygen; this usually occurs near ventilation openings where fresh air can enter a compartment. In order to continue the combustion process, flames are forced to spread from the fire origin toward the ventilation openings where oxygen is more readily available, ultimately promoting flame spread and subsequently fire growth in this direction. In some cases, the mixing of air and gaseous fuel occurs further away from the ventilation opening creating a cooling effect at the initial point of air entry subsequently reducing the damage at that point [2]. As an example, it is

possible that the influx of fresh air at a ventilation opening has enough velocity to extend fire conditions beyond that vent toward the interior of the compartment [2]. Any solid object that obstructs or interferes with these flows will be the recipient of intense heat fluxes.

In further detail of transitioning to flashover in a compartment, an upper gas layer is formed with increasing thickness and temperature. The position of this upper gas layer affects the ventilation parameters by controlling the size of the vents, which decreases their effective area as the layer descends [4]. This can cause a fire to develop to a point where it produces more gaseous fuels than can be consumed in the compartment with the available air yielding a ventilation-limited fire [4]. Having a ventilation-limited fire with insufficient oxygen causes the HRR of the fire to decrease in a direct relationship to the area (A) and height (h) of the ventilation openings as shown below:

$$\dot{Q} \propto A\sqrt{h}$$

As the resulting upper gas layer from flashover continues to descend, the dimensions of the effective ventilation opening also decrease as does the energy release and size of the fire. These ventilation openings directly control the growth or decay of the fire. A more likely scenario for a compartment fire is to have dynamic ventilation conditions meaning the opening of previously closed vents (for example, window breakage or door opening), which create an increase in compartment ventilation resulting in a fuel-controlled condition. This also increases the HRR and size of the fire with the previously mentioned equation. Dynamic vents also promote flame spread because an opening such as a window could break part way through a compartment fire, altering the direction of incoming air. There can be enough velocity with this flow to push the flames in a specified direction or to draw the flames towards the opening, causing the fire to spread across the compartment. The ventilation parameters of a compartment fire are very influential to the growth and spread of the fire; however, irrespective of where the fire started or where fuel items are located, flaming fire conditions will consistently exist only in areas near oxygen-supplying vents [2].

2.3 Fire Dynamics Simulator (FDS)

Fire Dynamics Simulator (FDS) is a computational fluid dynamics (CFD) model of fire-driven fluid flow. This software numerically solves a form of the Navier-Stokes equations appropriate for low-speed, thermally driven flow, with an emphasis on smoke and heat transport from fires. This report utilized version 6.2.0 of FDS with a compilation date of April 11, 2015 [6]. As a supplementary program to FDS, Smokeview (SMV) is a scientific visualization program that was developed to display the results of an FDS model computation in a three-dimensional animation. Both FDS and Smokeview are free to download open-source software tools provided by the National Institute of Standards and Technology (NIST) [7].

2.3.1 FDS Fire Modeling

The main function of FDS is to solve practical fire problems, as well as provide a tool to study fundamental fire dynamics and combustion. Fire protection engineers and fire researchers use FDS when trying to model low speed transport of heat and combustion products from fire. It is also commonly used to calculate radiative and convective heat transfer between gases and solid surfaces, pyrolysis, flame spread and fire growth [6].

FDS computes the density, velocity, temperature, pressure and species concentration of the gas in each cell as it steps through time. Based on the laws of conservation of mass, momentum, species, and energy, the model tracks the generation and movement of fire gases. All solid surfaces are assigned thermal boundary conditions, plus information about their burning behavior. Computer simulations have been demonstrated to be a credible tool, when properly applied, to help fill in critical details of a fire incident. NIST has previously used FDS simulations to [8]:

1. Examine the effect of fire-induced flow paths (including temperature, pressure, and fire conditions)
2. Simulate and analyze fire phenomena (with associated uncertainties), including fire spread, smoke movement, tenability and operation of active and passive fire protection systems
3. Provide visualizations of the fire behavior that are representative of the conditions that members of a fire departments are likely to experience during the course of their interior operations

With these previous applications, FDS was identified as a suitable tool to provide valuable insight into fire induced flow paths, flame spread, and ventilation induced smoke movement. The results of FDS simulations are exported .csv files that record quantities such as a fire's heat release rate (HRR) output. In addition, Smokeview has the ability to take FDS results and display contours of its calculation results such as temperature, velocity and gas concentration in planar slices.

2.3.1.1 FDS Experiment Validation

The FDS validation guide divides the various examples of validation studies into two classes. The first being design applications for which the heat release rate (HRR) of the fire is specified as an input to the model and secondly forensic reconstruction for which the HRR is predicted by the model [9]. Design applications are generally used for existing or new building designs to predict the transport of heat and combustion products throughout an area of interest. However, detailed descriptions of building contents are usually not necessary due to the user prescribed burning rate of the materials [10].

Forensic reconstructions require the model to simulate fire scenes based on information collected after an event, such as personal accounts, unburned materials and burn patterns. The

purpose of the simulation is to connect a sequence of discrete observations with a continuous description of the fire dynamics. Usually, reconstructions involve more emphasis on such phenomena as heat transfer to surfaces, pyrolysis, and flame spread because virtually all objects in a given room are potentially ignitable, especially when flashover occurs. In general, forensic reconstructions are more challenging simulations to perform because they require more detailed information about the room contents, and there is much greater uncertainty in the total HRR as the fire spreads from object to object. [10]

The FDS simulations described in this report have elements of both design and forensic reconstructions. The individual fuel packages, that will be discussed later in the report, were modeled after actual burn tests conducted by the ATF. Subsequently, the HRR of each fuel package was predefined based on the results of those live tests. Modeling the full-scale compartments involved a forensic reconstruction. Even though the individual fuel packages that composed the compartment had specified HRRs, FDS was used to simulate how the fire would spread throughout the room. As stated previously, this involves simulating heat transfer to surfaces and flame spread, which are both elements of forensic reconstruction.

3 ATF Tests

The ATF conducted a series of four separate tests in "identical" compartments to obtain a better understanding of the differences in fire conditions, specifically fire growth, spread and resulting damage due to variation in initial ventilation condition and initial ignition location. In addition, individual fuel packages were burned under calorimeter to measure the heat release rates (HRR), which determines fire growth and development. The fuel packages included a beanbag chair, bookcase, desk, desk chair, dresser, mattress, and an upholstered chair. The ignition source that was used to ignite the individual fuel packages consisted of gauze pad soaked in 250 ml. of gasoline. The ignition scenario for all four compartment tests consisted of the same ignition source adjacent to the beanbag chair. The peak HRR of all the fuel packages measured during the ATF calorimeter tests are displayed in this section. The test set-ups of the fuel packages under the calorimeter hood and the structure of the compartment tests can be seen in Appendix A and B, respectively.

3.1 Individual Fuel Packages

The ignition source used to ignite the individual fuel packages was measured to have a peak HRR of 40 kW.

3.1.1 Polystyrene Based Fuel Packages

The fuel package that consisted of polystyrene was the beanbag chair. Beanbags are commonly filled with little foam beads that are made of expandable polystyrene (EPS). Expanded polystyrene is primarily made of styrene monomer (C_8H_8) and expanded due to heating to form a cellular structure. When EPS is exposed to temperatures above 100°C, it begins to melt, and at higher temperatures the decomposition of the melted products produces gaseous combustibles [11]. This behavior is similar to the observations of the beanbag chair test. Table 1 below indicates the period at which the peak HRR was reached for the beanbag chair:

Table 1: Polystyrene HRR Data

Test	Time to Peak HRR	Peak HRR
Beanbag	2:56	181 kW

3.1.2 Polyurethane Based Fuel Packages

In the ATF tests, the mattress, upholstered chair and desk chair were almost entirely composed of flexible polyurethane foam. The chemical and physical properties of flexible polyurethane foams vary depending on the production process. As a result, it is difficult to determine a general baseline for foam flammability. However, by its chemical nature and physical open structure array, a polyurethane is considered highly flammable. The combustion process of flexible polyurethane foams is generally described as a two-stage-process. Initially, the foam begins to degrade and melt. After the foam is completely melted, the second stage

begins leaving only the pool fire to burn. Similar to polystyrene based fuel packages, the melt-drip is a complicated solid-liquid transition for which the current FDS framework is not able to capture.

During the fire tests, the upholstered chair experienced significant dripping and pooling of combustible material as compared to the other two fuel packages. This initial pooling delayed the time for the chair to reach its peak HRR. The mattress took the longest time to reach its peak HRR as the flame had to spread across the entire bed before it emitted the most heat. Table 2 below indicates the periods at which the peak HRR was reached for the mattress, upholstered chair and desk chair:

Table 2: Polyurethane HRR Data

Test	Time to Peak HRR	Peak HRR
Mattress	8:32	827 kW
Upholstered Chair	5:05	1.79 MW
Desk Chair	1:18	685 kW

3.1.3 Wood Based Fuel Packages

There were three wood-based fuel packages that were introduced in the set of tests; these included a bookcase, desk, and dresser. The wood based fuel packages are made of solid pine (dresser) as well as particleboard (bookcase and desk). As a material, wood is unique in that it is affected by its respective moisture content. In the presence of temperatures near or above 100°C, the water molecules begin to vaporize and migrate to the surface of the wood as well as other cooler parts; however, the internal migration of the water molecules causes the wood to condense [13]. At above 200°C, thermal degradation, or pyrolysis, produces combustible gases and as the temperatures reach near 300°C, the remaining material experiences the formation of char [13]. This charring causes the material's properties to change; char leads to shrinkage cracks and an increase in heat transfer through them therefore increasing the wood's thermal conductivity [13].

Particleboard contains a binder or adhesive to keep all of the small wood particles intact, which allows it to be engineered for specific purposes [14]. This means that by controlling the board density, particle geometry, and amount of adhesive used during the manufacturing process, it is possible to impart specific performance characteristics such as increased fire retardancy [14].

Two phenomena were observed in the tests of the wood-based furnishings. The first was the presence of charring in the areas directly affected by the fire. Charring was not modeled in the FDS simulations as there are a number of variables that could not be obtained that are pertinent to the charring equations in FDS. These could not be obtained because physical charring characteristics were not calculated as a part of the scope in the ATF tests. The other phenomenon observed in the bookcase and desk tests was a structural failure as the fire progressed. In both of these tests, parts of the structure break off, creating geometrical changes that cannot be adequately approximated in FDS without inputting programming changes into the FDS script. This was deemed unnecessary as the primary focus was on matching the initial HRR

curve development of the tests. Table 3 below indicates the periods at which the peak HRR was reached for the bookcase, desk and dresser:

Test	Time to Peak HRR	Peak HRR
Bookcase	2:44	209 kW
Desk	6:16	271 kW
Dresser	5:00	1.51 MW

3.2 Full-Scale

As previously mentioned, there were four full-scale tests involved in analyzing the effects of varying the ventilation and fire origin within a compartment. The following sections discuss the test structure and the instrumentation that were used to collect the data

3.2.1 Compartment Structure

The test structure resembled a bedroom connected to a hallway, as shown in Figure 1. Overall, the interior of the structure measured approximately 4.89 m wide by 6.10 m long with 2.44 m high ceilings. The structure was framed with 2 x 4 dimensional lumber. The interior walls and ceiling were sheathed with gypsum wallboard. All wallboard seams were taped and sealed. The walls and ceiling were painted with a single coat of interior latex paint. The floor consisted of gypsum wallboard coving the concrete floor of the laboratory with a floor finishing composed of nylon carpeting on top of bonded polyurethane foam.
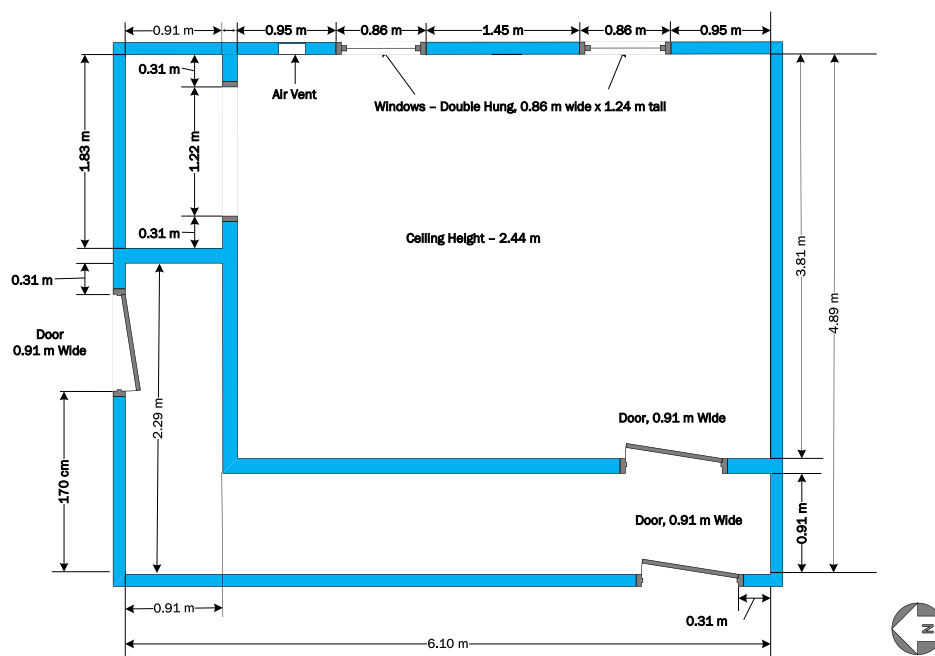
Figure 1: ATF Test Structure

10

Two double hung windows (0.86 m wide x 1.24 m high) were located in the bedroom. A hollow core door (0.91 m wide) separated the bedroom from the hallway. Two hollow core doors (0.91 m wide) were also located in the hallway and opened to the exterior space within the laboratory. One door was directly opposite of the bedroom door, while the other was at the end of the hallway. In each test, the bedroom door remained opened and one of the two hallway doors were open. In addition, both windows were closed at the start of the test. An air vent was also located on one of the bedroom walls near the floor. An adjustable vent was attached to a section of circular heating, ventilating, and air conditioning (HVAC) duct, which was open to the laboratory space. In all but test 3, the vent was is the open position.

For identification purposes, the test structures was divided into two sections: the bedroom and the hallway. Furthermore, the bedroom was further divided into quadrants, which were identified as Quadrants 1-4 on the drawings and figures.

3.2.2 Instrumentation

Each test compartment consisted of several thermocouple trees, heat flux gauges and velocity flow devices. These devices measured temperature, heat flux, and velocity flows respectively at certain points inside the full-scale test compartments. Thermocouples come in different combinations of metal that measures different temperature ranges and are described as Type-J, E, K and T. Thermocouple devices used for the tests had properties consistent with a Type-K temperature probes because of the wide range of temperature it measures (-200°C to 1250°C). Thermocouple trees were placed in each quadrant to measure the temperature change at different elevations (2 ft., 4 ft. and 6 ft. off the ground). In addition, bi-directional velocity probes were located at varying heights (5.5 in, 23.5 in., 40.5 in., 58 in. and 74.5 in.) by the bedroom door to measure gas velocity flow going in and out of the bedroom. Lastly, heat flux gauges were placed on opposing walls at an elevation of 59 in. to measure the heat transfer of the surface over time. The placement of each instrument can be seen in Figure 2 below.

Figure 2: Location of Instruments

11

3.2.3 Contents of Structure

The tests structure was designed to represent a bedroom connected to a hallway. Therefore, various items were included in the structure to depict this scenario. The floor of the entire test structure was covered with carpet and carpet padding. In general, each test structure contained the same type and quantity of furniture, as shown in Table 4. In addition, various miscellaneous items were also included in each structure, as listed in Table 5.

Table 4: Furniture Items

Item	Quantity
Queen Sized mattress and box spring	1
Beanbag Chair	1*
Dresser	1
Bookshelf	1
Upholstered Chair	1
Desk	1
Chair	1

* Note: Two tests used two beanbag chairs: Test 3 & Test 4

Table 5: Miscellaneous Items

Item	Quantity
Laundry Basket	1
Trash Can	3
Foam Padding for Mattress	1
Bedding Set (sheets, comforter, pillow cases)	1
Pillows	2
Plastic Hangers	20
Window Panel	4
Clothing Items (jacket, t-shirts, jeans, sweatpants)	23
Books on bookshelf	varied

3.2.4 Test Scenarios and Results

The ignition scenario of all four tests involved open flame ignition to a standard ignition package, which was placed next to a beanbag chair. Each test was allowed to progress into the transition of flashover (approximately 6 or 8 minutes), burning for an additional 2 minutes. The

initial ventilation conditions of the test compartments, initial ignition location and the general location of the fuel packages can be seen in Table 6 provided below.

Full-scale Tests Scenario

Full-scale Test 1 — **Full-scale Test 2**

Full-scale Test 3 — **Full-scale Test 4**
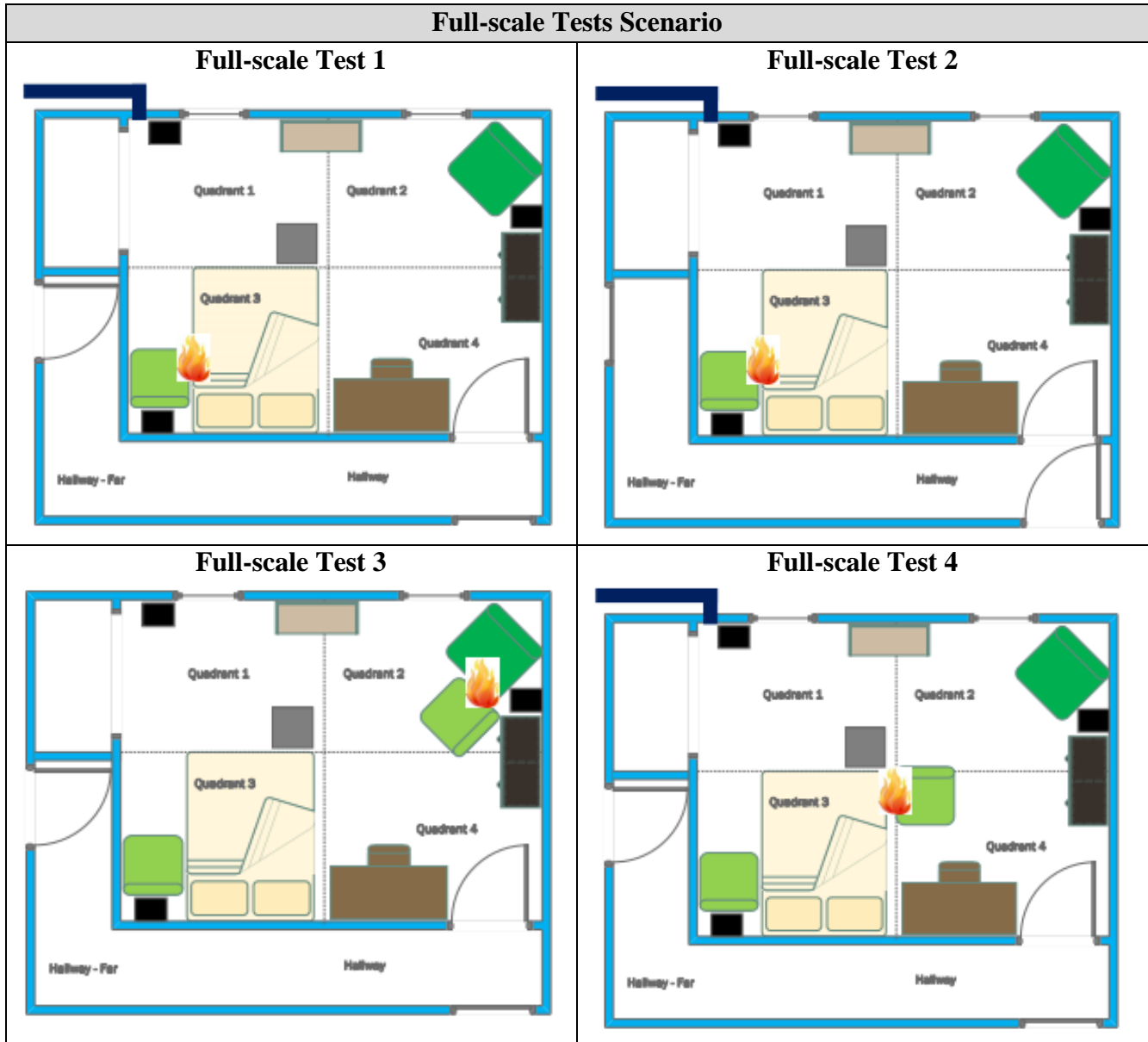
In all four tests, there were a sequence of significant events such as window breakage and burning through of doors that were observed to materially affect fire growth and flame spread. These events are factors of ventilation change and the time to when they opened affected the time of transition into flashover. As shown in Table 7, which provides a summary of the significant events, the earlier the windows broke the earlier the transition phase occurred. For instance, the initial conditions of test 1 and 2 are similar in terms of fire origin, but the door located in the hallway is opened in test 2, which provided better access for combustion air to

13

enter the compartment. Due to these conditions in test 2, the fire developed and spread at a faster rate resulting in a quicker time to flashover of nearly two minutes earlier than test 1.

Similarly, changing the initial ignition location as seen in test 3 and 4 seemed to have an impact on the time to when the windows failed open and the time to transition. Since the initial ignition location for test 3 is closer to the Quad 2 window, the chances of the window breaking is much faster than the window in test 4. This results in an earlier transition time for test 3 because more air is readily available for combustion.

Table 7: Summary of Full-scale Events in Minutes

	Quad 1 Window Break	Flames Out Quad 1 Window	Quad 2 Window Break	Flames Out Quad 2 Window	Transition into Flashover	Suppression
Test 1	4:05	6:20	6:35	6:35	6:35	8:30
Test 2	3:21	4:05	4:30	4:30	4:49	7:00
Test 3	5:15	N/A	2:19	2:19	5:20	7:35
Test 4	6:30	6:45	5:21	N/A	7:46	9:51

4 Modeling Procedures

The modeling approach for this study was broken down into two different parts. The first part was to model the fuel packages individually to match the heat release rates (HRR) data of the ATF tests. The second part was to incorporate the modeled fuel packages into the full-scale model and add instrumentation devices such as thermocouples, velocity probes and heat flux gauges to collect data.

4.1 Numerical Mesh

The computational cell size needs to be specified since CFD models use a numerical grid to solve a form of the conservation of mass, momentum, and energy equations. The non-dimensional expression, $D^*/\delta x$, can be used to estimate how well a flow field is measured. D^* is the characteristic fire diameter and δx is the nominal size of a mesh cell. From the FDS User's guide, [6] the characteristic fire diameter can be calculated by the equation:

$$D^* = \left(\frac{Q}{\rho_\infty c_p T_\infty \sqrt{g}}\right)^{2/5}$$

where Q is the maximum heat release rate of the fire, ρ_∞, c_p, T_∞ is the density, specific heat, and temperature of the ambient air respectively and g is the gravitational force of earth [12]. Based on the validation work performed for the U.S. Nuclear Regulatory Commission, $D^*/\delta x$ ratios ranged between 4 and 16 are used to accurately resolve fires [13]. A ratio of 16 describes finer cell size as a ratio of 4 describes coarser cell size. Finer grid cells allow for more computational cells to span the characteristic fire diameter resulting in better calculations. However, the more cells there are to compute, the longer the calculation will take. The D^*/dx ratios for the fuel package models in our study fell within the range when using 7 cm. grid spacing as shown in Table 8 below. This allowed for quick and accurate simulations. The same grid spacing was used for the full-scale models in order for the fuel packages to produce the same HRR when modeled individually.

Table 8: D*/dx Ratio for all Models

FDS Model	Peak HRR	D*	D*/dx
Bean Bag Chair	181 kW	0.484	6.9
Book Case	209 kW	0.513	7.3
Desk	271 kW	0.569	8.1
Desk Chair	685 kW	0.824	11.8
Dresser	1.51MW	1.128	16.1
Mattress	827 kW	0.889	12.7
Upholstered Chair	1.79 MW	1.21	17.3
Full-scale 1	6.5 MW	2.028	28.9
Full-scale 2	7.0 MW	2.089	29.8
Full-scale 3	7.2 MW	2.112	30.2
Full-scale 4	6.9 MW	2.077	29.7

4.2 Modeling Procedure for Fuel Packages

4.2.1 Geometry

Furniture and other fuels in FDS need to be specified as rectangular blocks with no sloped or curved surfaces. FDS takes the input coordinate values of the furnishings and adjusts them to match the grid cell boundaries of the computational domain. As a result, using exact measurements may affect the geometry of the fuel packages by either growing or shrinking to match the grid. In these cases, the input coordinate values were changed by the user to match the grid for a proportional representation of the fuel packages.

4.2.2 Material Properties

It is essential to specify the thermo-chemical material properties of a solid object in FDS to calculate the fire development and growth for a certain fire scenario. These material properties include density, specific heat, thermal conductivity, heat of combustion and ignition temperature. The density of a material is the ratio of its mass to its volume. As a property, density represents the physical form of a material and affects the ease with which a solid may be ignited by influencing thermal inertia. This characterizes the rate of surface temperature rise for a material when exposed to heat. Low values of thermal inertia lead to increased surface temperatures for a certain heat flux and therefore, to a more rapid ignition [4]. The specific heat of a material describes the amount of heat it absorbs as its temperature increases. Specifically, it is the amount of thermal energy required to raise one unit of mass of the material by one degree [4]. A higher thermal conductivity transfers heat through a material faster, thereby slowing the storage of heat at surface and increasing the time to ignition temperature. Conversely, a low thermal conductivity would mean that the material readily stores heat, lowering the time to ignition [4]. Thermal conductivity depends upon the temperature, composition, and orientation of the structure [14]. Heat of combustion is the amount of energy produced for each unit of fuel mass burned. The effect of chemical composition on "ease of ignition" is affected by the heat of combustion of a material. If the heat of combustion is high, then more energy will be available to sustain flaming after ignition [4]. These thermo-chemical properties influence how fuel surface cells in FDS heat up. Once a specific area of the fuel surface, as characterized by the computational cell size, reaches a user specified ignition temperature, that particular cell will ignite and being to burn.

The thermo-chemical properties for each fuel were not readily determined nor provided as part of the ATF test program. Values were determined through research of reference literature such as the fourth edition of the Society of Fire Protection Handbook [14], the Ignition Handbook [15], and the UMD burning material databases [16]. The list of fuels and their thermo-chemical properties used in the FDS simulations are provided in the Table 9 below. Since the literature sources had different values of material properties, the average value was determined and used. A sensitivity analysis was performed to see the overall effect of the range of values

used on the outcome of the calculations as suggested in the SFPE Guidelines for Substantiating a Fire Model for a Given Application [12].

Table 9: Material Database

Material Property Database at Room Temperature						
Material	Ignition Temperature (C)	Thermal Conductivity (W/ m K)	Density (kg/m3)	Specific Heat (kJ/ kg k)	Heat of Combustion (kJ/kg)	Source(s)
Particleboard		0.14	800	1.3		[16]
Particleboard (HD)		0.17	1000	1.3		[16]
Particleboard (LD)		0.078	590	1.3		[16]
Pine (White)	350 (Dry Douglas Fir)	0.11	435	2.5	18500	[16]
Pine (Yellow)	350 (Dry Douglas Fir)	0.15	640	2.805		[16]
Polyester Fabric	407	0.2	1345	1.15		[16], [17]
Polyurethane Foam (Flexible)	378-416	0.03	30	1.47	21000	[16], [18]
Oak	301 (Oven Dry)	0.17	545	2.39		[16]
Expanded Polystyrene	275	0.034	25	1.5	35600	[19], [20]
Gypsum Plaster		0.48	1440	0.84	3000	[21], [18]
Nylon (Carpet)	405	0.33	1169	0.87		[16]
Melamine	490	0.5	1570	1.2		[20]
Polyurethane Foam (C6.3,H7.1,H,O2.1)	280	0.02	20	1.4	24200	[16], [20]

4.2.3 Heat Release Rate per Unit Area (HRRPUA)

Specifying the HRRPUA value along with the material properties in the FDS input file allows FDS to calculate the heating up and ignition of the fuel, but allows the user to control the burning rate [6]. The HRRPUA value was determined by using the maximum HRR value from the ATF tests and dividing it by the surface area of the fuel burning. Defining the maximum HRRPUA allows the option to use the RAMP_Q function, which enables the ability to match the graph of the HRR with respect to time in the FDS model to that of the actual test. When a surface cell reaches the ignition temperature, that particular surface cell will follow the burning rate that is described using the RAMP function.

4.2.4 Sensitivity Analysis

An informative approach for evaluating the effect of model input is to assess the proportionality of an FDS simulated output to an input parameter. Otherwise referred to as a Power Dependence sensitivity analysis [12]. The input parameters that were tested included thermal properties such as density, specific heat, thermal conductivity, ignition temperature and where applicable heat of combustion. Each thermal property had three iterations which included the actual input value used for the individual fuel package runs and ±10% of that value. By examining the relationship of model outcome to input, the modeler would be able to identify the relative importance of the input. The outcome of this analysis will provide evidence to further investigate specific material and thermal properties in order to reduce uncertainty in further studies. The equation used for this sensitivity analysis is depicted below:

$$x = FDS\ Calculated\ HRR$$
$$y = \pm 10\%\ Thermal\ Property\ Calculated\ HRR$$
$$Power\ Dependence\ \% = \frac{|x - y|}{x} * 100$$

4.2.5 Standard Ignition Package (SIP)

Modeling the SIP was kept simple to recognize its role in the overall event. Since the SIP consists of gauze and liquid, they are going to be merged and essentially act as a single solid fuel package. The SIP was modeled in FDS as an obstruction with a surface that specifies the ramping HRR.

4.2.6 Beanbag

During the beanbag chair burn test, the melting and pooling phenomenon was observed, but these phenomena is not simulated by FDS. There were two ways to modeling the beanbag chair; one way was to attempt to use several functions of FDS to mimic the melting of the beanbag chair and the other way was to simply control the burning rate by using the ramp function in case the melting phenomenon could not be replicated. In an attempt to model the melting phenomenon, the burn away function was used to mimic the melting of the beanbag chair. The burn away function allows a particular cell to disappear once all of the fuel in that cell is consumed. When using this function, the fire spread across the chair when certain cells burnt away, which was observed in the burn test. The pooling of the liquid after the fuel has completely melted was not modeled, but the HRR curve produced by FDS was similar to the ATF test. Therefore, a ramp function was not necessary for the beanbag chair.

4.2.7 Bookcase

There were two phenomena that were observed which affected the changes in modeling strategy. The first of these phenomena is the burning away of the back portion of the bookcase. This piece of particleboard is much thinner than the rest of the frame and shelves, contributing to its faster decomposition. Eventually, though, the entire structure burns away. To model this, the back of the bookcase was allowed to burn away while maintaining the structure of the rest of the frame. This was achieved by specifying two Surface ID's for the fuel, one with burn away and one without.

The second phenomenon is the physical separation between the shelves and the back of the bookcase. In theory, there would be no separation between those obstructions, but when the bookcase was built, there was no sealant introduced to prevent the spread of air between the shelves and the back of the bookcase. This air gap permits smoke and heat to travel up the back of the bookcase, contributing to the spread of fire from the bottom shelf to the top. A small gap was introduced in the model between the middle shelves and the back of the bookcase. This change allowed for a faster spread of heat and gases along the back of the bookcase. Finally, to produce a HRR curve in FDS similar to the one produced by the ATF, a ramp function was used to control the peak energy produced, as well as the decay phase of the simulated fire.

4.2.8 Desk

The desk creates a number of complexities when attempting to model its fire behavior as it is not a solid object, i.e. it is comprised of a number of objects connected at various surfaces and separated by volumes of air space. The process of modeling the desk began with applying the correct material properties identified as particleboard from the manufacturer's data sheet. Since particleboard is comprised of wood, we had to replicate the physical structure of the desk including the air space within the drawers with the use of multiple obstruction lines, as the burning of wood is dependent upon geometrical factors. This idea is further discussed in section 4.2.10 which addresses a solid wood fuel package. The manufacturer was not specific in the type of particleboard used, creating uncertainty as there are multiple types all with different thermal properties. The University of Maryland Burn Database offered properties for a low-density and a high-density form of particleboard as well as a general particleboard.

The three variations of the material had a wide range in density and thermal conductivity therefore, they were all explored and compared to the HRR data provided by the ATF. Ultimately, general particleboard was chosen as its initial HRR growth curve was the most closely approximated to that of the ATF results and because its thermal properties were at an average; low-density particleboard resulted in a very early and low energy steady state fire and high-density particleboard had a very steep growth phase unlike the ATF HRR. Finally, to produce a heat release rate curve in FDS similar to the one measured by ATF, a ramp function had to be used to control the peak energy produced as well as the tail end of the FDS simulation.

4.2.9 Desk Chair

The modeling procedure for the desk chair was more straightforward when compared to other fuel packages. However, its composition of solid oak, polyurethane foam and polyester covering still posed challenges. Due to the polyurethane foam, the desk chair experienced melting during pyrolysis; subsequently forming a pool fire during the ATF calorimeter test. This phenomenon hindered our ability to produce an accurate FDS approximation of HRR. In addition, finding the correct way to input different material layers of a fuel into FDS was a cause of concern.

The initial iterations of the desk chair simulations involved varying the HRRPUA of the chair. The HRRPUA was steadily increased from one test to another. In addition, there were variations in the way the seat and back support of the chair were modeled. Some simulations combined the two parts as one obstruction with a single HRRPUA while other split the two obstruction and distributed the HRRPUA accordingly. In the end, we decided to use a single top obstruction in order to minimize input parameters and simplify our design. To further simplify the design, particleboard and polyester were excluded from input files leaving foam as the main material. This final change ultimately resulted in the most accurate simulations since foam was the main contributor in determining HRR.

4.2.10 Dresser

In modeling the wood dresser, we began with the known values such as the HRRPUA, which was supplied by the ATF's tests. Next, it was necessary to replicate the actual physical structure of the dresser as described in the manufacturer's data sheet (i.e. drawer space) using multiple obstruction lines opposed to a single, solid unit. We did this because wood is a complex composite of natural polymers and is generally anisotropic, heterogeneous and porous meaning that physical properties depend upon structural geometry and thickness [22]. Using individual obstructions over a single one allow us to better replicate this aspect of wood-based fuel packages.

Another challenging aspect of modeling wood-based structures in FDS is the combustion process known as charring which results in heat generation, flame spread, and dramatic changes in material properties. Modeling this behavior in FDS is not only very complex but also requires a lot of very specific information about the type of wood being burned such as the activation energy, the reference temperature, and the pre-exponential factor [9]. Unfortunately, the manufacturer's sheet stated a general "solid pine" as the primary material which limits knowledge of the thermal properties as there are over 115 different species of pine. Through literature research, it was found that yellow pine and white pine are commonly used for home construction or furniture items; however, not all thermal properties could be found which restricted the team from modeling a char effect on the dresser. Although both variations were explored through various FDS simulations, white pine was ultimately applied to the model as it proved to formulate a more accurate peak-HRR; however, ramp functions had to be used to control the growth and decay stages of the HRR produced by the model.

4.2.11 Mattress

There were two mattress tests that were conducted. The first test consisted of the mattress alone and the second test consisted of the beanbag adjacent to the mattress. During both tests, the fire was observed to spread across the mattress at a moderate rate once it was ignited at the corner. The mattress presented different challenges in terms of accurately modeling its fire behavior due to it being composed of a wide array of components with different properties such as springs, multiple core materials, and outside padding materials. To simplify the material composition of the mattress, the only material that was used was polyurethane foam. Rather than modeling a separate obstruction for the bedding, the layer feature of FDS were used to have one solid fuel package with one maximum HRRPUA value.

To model the flame spread across the mattress, certain input variables were scrutinized in more detail for analysis, which included ignition temperature, specific heat and thermal conductivity. When a range of values was tested for specific heat and thermal conductivity, there were minor changes in terms of flame spread and HRR. However, changing the ignition temperature described on the surface affected how the fire spread across the bed. Since the bedding and the mattress were modeled as one solid fuel package the ignition temperature of the mattress and the bedding had to be integrated, which allowed the fire to spread at a similar rate to the actual tests.

4.2.12 Upholstered Chair

During the tests, the upholstered chair was observed to melt into a pool fire underneath before the flames engulfed the entire chair. Due to this phase change, modeling the upholstered chair presented a unique challenge. As stated before, FDS does not perform well when attempting to model phenomenon such as melting of thermoplastics. In addition, the upholstered chair was composed of polyurethane foam, polyester wadding, particleboard and solid pinewood (for the legs of the chair). All of these different materials increased the difficulty of accurately modeling this fuel package in FDS. Lastly, the exact initial placement of the SIP was unknown as indicated in Figure 3 below.

Figure 3: Upholstered Chair with SIP

To begin, the first step to modeling the upholstered chair involved dividing the furniture up into different block obstructions. This had to be done in order to provide realistic dimensions

of the seat cushion and armrests of the chair. Once the geometry of the chair was complete, the first attempts at modeling the chair involved comparing the use of HRRPUA or Mass Loss Rate per Unit Area (MLRPUA) to control fire growth. After iterations of MLRPUA simulations did not produce desired HRR curve outputs, more emphasis was placed on refining HRRPUA controlled simulations. After a few iterations of using HRRPUA, the best results were found when the SIP was placed halfway underneath the seat cushion of the upholstered chair.

Based on the assumed location of the ignition source, ensuing simulations focused on the material and layering aspects of FDS. As stated before, this process was difficult due to the complexity in the initial upholstered chair design. As with the desk chair simulations, after unsuccessful attempts in matching the HRR, it was decided to reduce material inputs to only the polyurethane foam and polyester covering since these were the major contributing fuel sources. This resulted in more predictable simulations that could then be further analyzed.

After that baseline was produced, more focus went into varying thermal properties and input parameters to produce the desired HRR curve. These parameters included soot yield, material thickness, ignition temperature, BURN_AWAY feature, specific heat and density. As stated previously, due to time constraints, some parameters were excluded after only a few simulations. This helped us to not only save time but also reduce model uncertainty by excluding values we were not confident with.

4.3 Modeling Procedure for Full-scale Model

4.3.1 Computational Domain

Since modeling some external space is good practice, it was necessary to extend the domain past the compartment's ventilation openings [23]. A parametric study that was conducted proposed a connection between the hydraulic diameter of ventilation opening and the minimal effective domain extension [23]. The hydraulic diameter is a function of the area and perimeter of the vent opening, which is shown in the following equation:

$$D_H = \frac{4A}{P}$$

This equation was applied to the two exterior doorways and the two windows yielding the computational domain shown in Figure 4 below. The results are as follows:

$$D_{H,DOORS} = 1.261m \; ; \; D_{H,WINDOWS} = 1.009m$$

From the results above, the computational domain extended 1.261m in both the negative x-direction and the negative y-direction to account for the exterior doors. The domain also extended 1.261m in the z direction, measured from the top of the doorways. As for the windows, the vertical domain extension of the doorways was greater than what is required by the windows however, it was still necessary to add 1.009m to the computation domain in the positive y-direction.
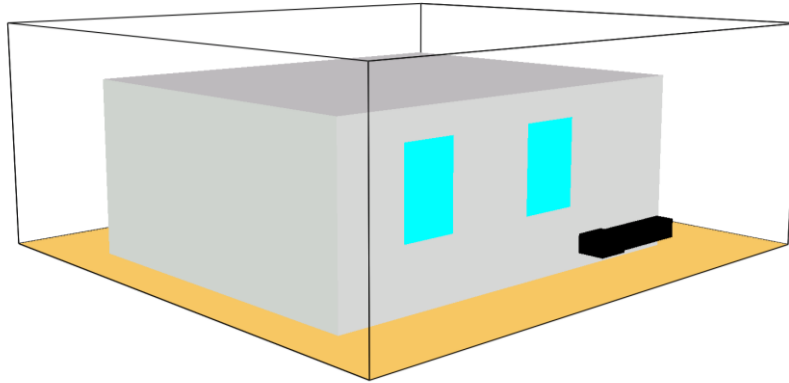
Figure 4: FDS Computation Domain of Compartment

4.3.2 Geometry

We utilized PyroSim, a graphical user interface for Fire Dynamics Simulator, to construct the compartments for our full-scale models. PyroSim is designed to provide immediate feedback to the user and subsequently provide the user with a formatted FDS input. This software provided a simpler way to create the obstructions of the compartment walls. The input geometry of the doors, windows, HVAC units and locations of the fuel packages were modeled through FDS based on documentation provided by the ATF. The compartment was modeled with three different materials: gypsum wallboard, nylon carpet, and glass windows. Figure 5 below provides a bird's eye view of the compartment. Since FDS uses rectangular grids to solve the numerical equations, there was difficulty in positioning the upholstered chair at an angle like in the ATF tests. To simplify, the chair was positioned in line with the computational mesh, leaving considerable space between the chair and walls. This did not significantly affect the outcomes of the simulations as the space allowed for similar gas flows between the chair and walls.
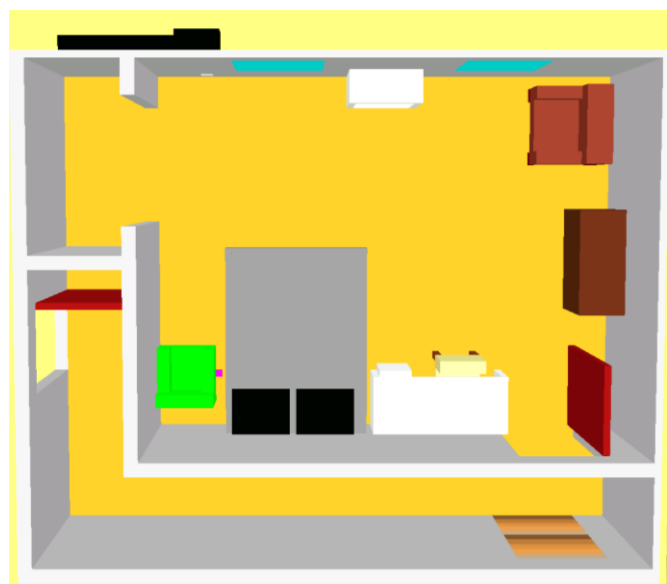

Figure 5: Bird's Eye View of Compartment

4.3.3 Ventilation

Vents in FDS are openings from the compartment to outside ambient conditions. In our simulations, vents allow smoke and heat to leave the compartment and fresh air to enter. Vents may be either simple openings such as open doors or failed windows that allow natural flow to occur, or may produce a specified flow rate such as the flow from a fan. In the full-scale simulations, only natural ventilation occurred based on the buoyancy of the hot gases.

The two major sources of ventilation in the full-scale tests are the windows and doors. There were two windows located on the back wall opposite the bedroom door and three doors placed throughout the compartment. There was also a passive HVAC vent present in tests 1, 2 and 4. A major factor of these ventilation components is their subsequent failure during the course of the full-scale burn tests. This failure was important to model due to significant changes observed in fire conditions following their opening.

The FDS model includes the window as two obstructions to replicate an actual windowpane. This construction also allowed for independent control for each half of the window and a more accurate representation of window breakage. Based on research conducted by Dr. Vytenis Babrauskas, he concluded that for 3 mm thick glass, a gas temperature of 360°C resulted in window failure and at 450°C for 4 mm – 6 mm thick glass [24]. Based on his results, a device located on the center of each window obstruction controlled window failure. Each window in the simulation was set to fail when the device recorded a gas temperature of 450°C.

4.3.4 Devices

The full-scale FDS model incorporated all of the devices previously mentioned in the ATF full-scale tests. The virtual devices were placed in comparable positions and elevations in order to allow for a direct comparison between the ATF tests and FDS model results. Complimentary to the ATF instrumentation, a number of additional virtual thermocouple and velocity devices were utilized to ascertain a better understanding of the simulated fire dynamics inside the compartment. Virtual thermocouple trees were placed in the corner of quadrants 1, 2 and 3 and at the bedroom door at elevations of 2 ft., 4 ft., 6 ft. and 8 ft. Along with these devices, virtual bi-directional velocity probes were placed in each window at 39.8 in., 58.1 in. and 76.4 in. high. In addition, both a virtual thermocouple and velocity probe was inputted into the model at the HVAC opening. These additional thermocouple and velocity devices allowed for a better description of the simulated temperature profile and fluid flows leaving and entering the compartment. The placement of each virtual instrument can be seen in Figure 6 below.
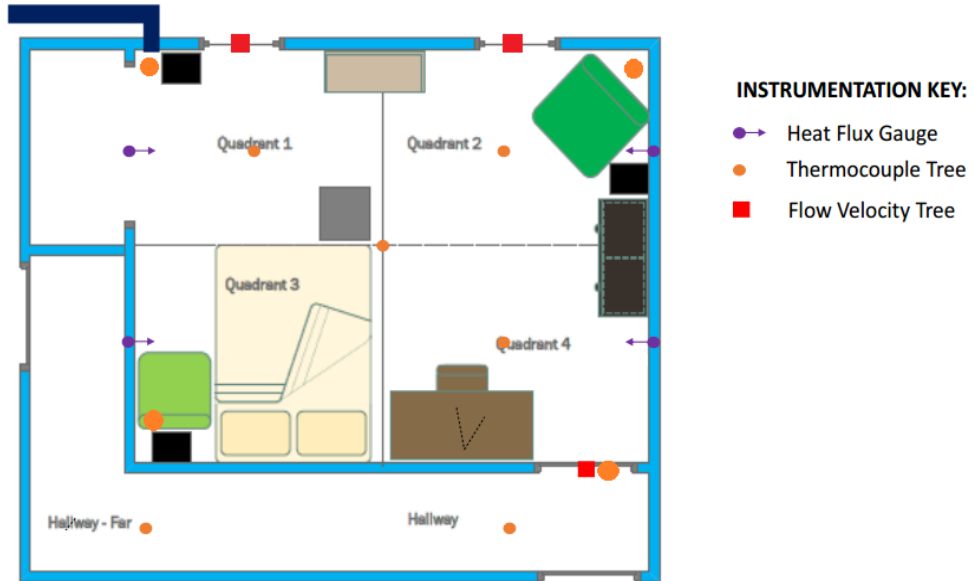
INSTRUMENTATION KEY:
- Heat Flux Gauge
- Thermocouple Tree
- Flow Velocity Tree

Figure 6: Full-scale Location of Instrumentation

5 Results

As described in Chapter 4.2, each individual fuel package was modeled to match the simulated HRR curve to the curve recorded during the ATF tests. This was achieved through the use of RAMP_Q and BURN_AWAY functions. A major factor in the growth of a fire is the thermal properties associated with each of the fuel packages. The exact materials for each fuel package were not given; therefore, properties for the fuel packages were determined through research from reference literature. This presents a level of uncertainty in the inputs and therefore, a sensitivity analysis was conducted to determine the effect that changing the value of the major thermal properties has on the fuel packages. The fuel packages were then inputted into the full scale model, where the ventilation openings were controlled by a temperature dependent function. The following sections outline the results of the FDS simulations as compared to the ATF live tests.

5.1 Sensitivity Analysis

The focus of the sensitivity analysis was to uncover trends between FDS thermal property value inputs and the subsequent calculated maximum HRR. This analysis provides insight that would be helpful in learning how manipulating FDS thermal input values change the simulated HRR graph. In the context of this project, knowing the sensitivity of each thermal property would assist in modeling FDS fuel packages to match ATF calorimeter tests.

The results of the sensitivity analysis are presented in Appendix B. The tables display +10% and -10% values for each thermal property. Both the power dependence and time shift of peak HRR were calculated for each fuel package. The power dependence illustrates how sensitive the maximum HRR prediction by FDS is when a change in thermal property value occurs. In addition, the time shift of the peak HRR gives insight into how the flame propagated over the fuel package.

Ultimately, the sensitivity analysis could not identify a consistent trend in simulated max HRR difference and time to max HRR from varying either the density, the specific heat, or the thermal conductivity. In addition, this analysis found that both specific heat and ignition temperature produced outlier max HRR dependence values. It was noted that in varying the either the heat of combustion or the ignition temperature, an increase for the thermal property constantly led to an increased time to peak while decreasing the value led to quicker peak HRR times. In a broader context, the sensitivity analysis provided information that shows that the thermal properties applied to the surface (T_{ig}) of an FDS model have a more consistent trend to the resulting HRR. This suggests that they have a more prominent role in the associated FDS equations when compared to the material properties (k, ρ, c_p).

5.2 Fuel Package Results

      In this section, the measurements of power from the fuel packages are compared to the values generated by FDS. Since it was challenging to model and match the data of the fuel packages due to certain phenomena such as melting and dripping, it was good common practice in the field of modeling to be within 20% of the desired results [9].

5.2.1 Beanbag

      The HRR of the beanbag chair reached a peak of approximately 160 kW at around 2 minutes. Although both curves reach the peak HRR at different values and time, they both follow similar trends showing agreeable data with the ATF data. Although, the ramp function gives the ability to match the HRR graph accurately, using the burn away function was ideal because it provides a realistic representation of how much fuel is consumed and mimic the melting phenomenon. Since the peak HRR of the FDS model results in a 10% difference to the ATF test, the model is deemed to be acceptable.
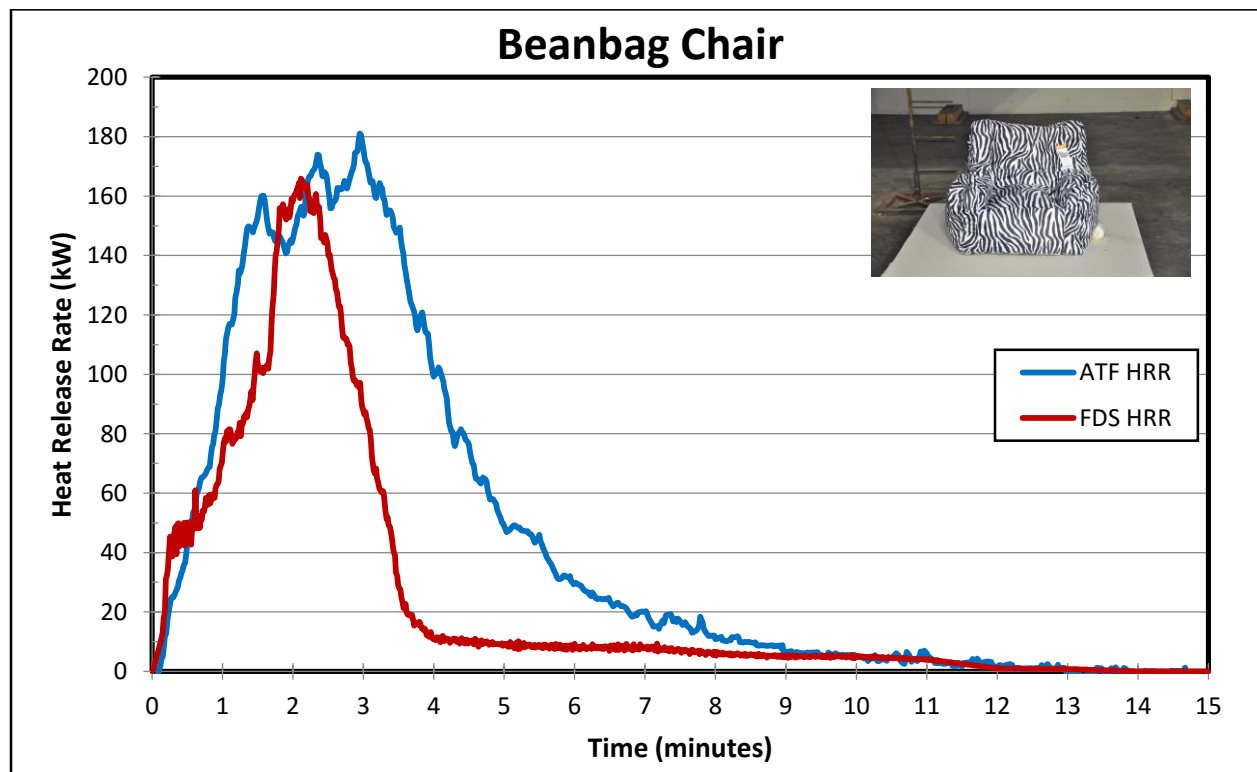

Figure 7: Beanbag HRR Graph

5.2.2 Bookcase

      Figure 8 below displays the comparison between the experimental data and the data from the simulation. The heat release rate in the model is very similar to that of the physical test in the initial growth of the fire. The modeled fire reaches its peak heat release rate about one minute after the physical test reaches its peak. However, the peak HRR of the model (225 kW) comes

within 8% of the peak HRR of the test (210kW). The HRR in the decay stage of the model is higher than that of the test due to the peak occurring later in the simulation. Only the first ten (10) minutes of the test was modeled as the structure began to break, causing secondary spikes in the HRR; this does not occur in the full-scale models, and thus was determined unnecessary to model for the individual fuel package.
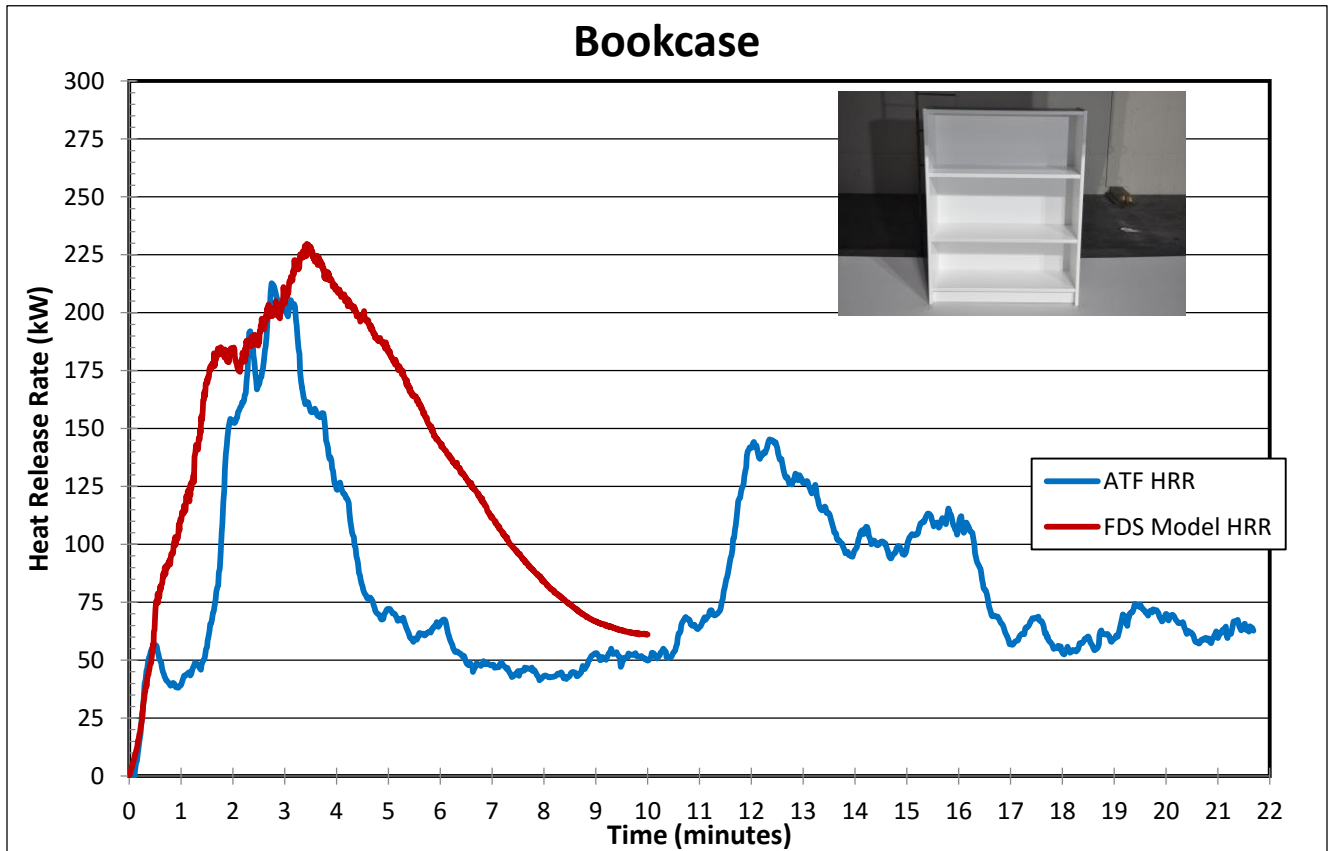

Figure 8: Bookcase HRR Graph

5.2.3 Desk

A large portion of the simulations explored the three different versions of the main material: low density, high density, and general particleboard. As stated in section 4.1.8, the team ultimately chose general particleboard as the applied surface material.

Figure 9 below is a graph comparing the heat release rates captured by the ATF during their tests to that captured by FDS during the simulations. Overall, the modeled desk produces more energy as the produced heat release rate is almost constantly greater than the experimental data recorded by the ATF. The peak HRR of each is much closer though, within 2% as the model reaches a maximum of 269 kW around 7 minutes and the test reaches 274 kW around 6.5 minutes.
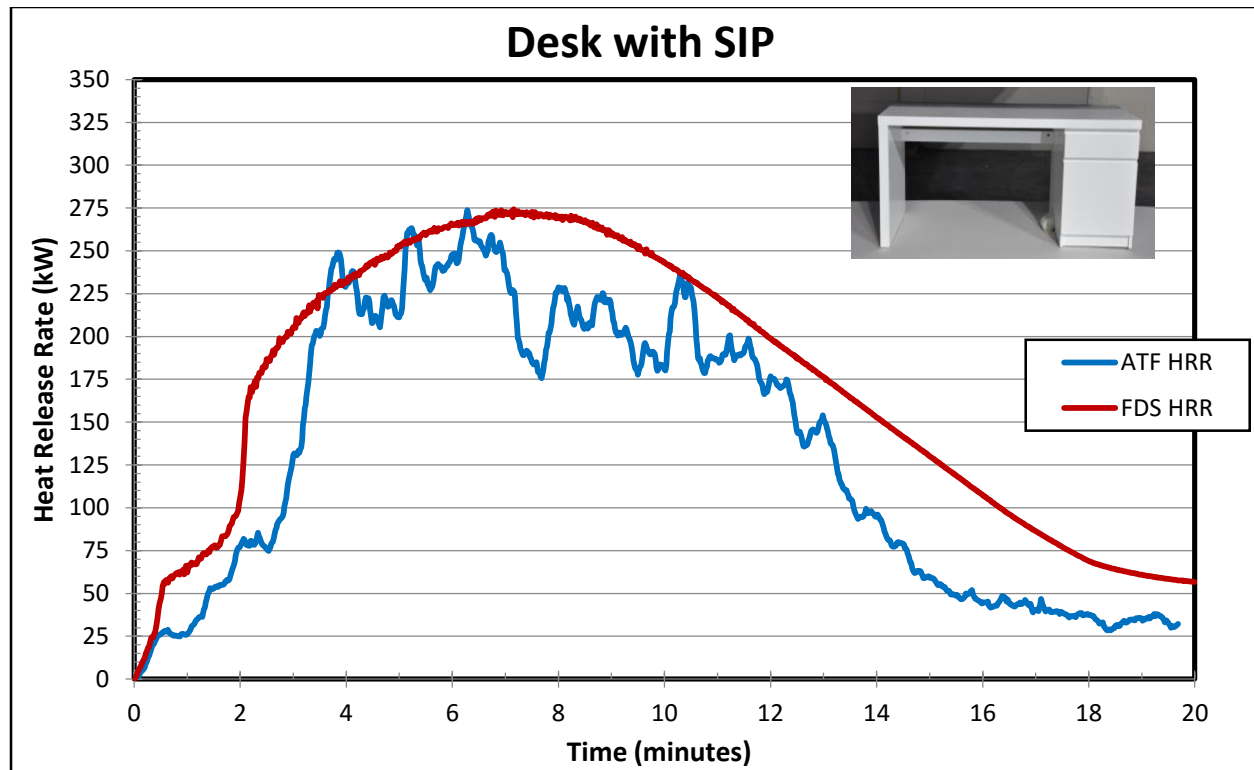
Figure 9: Desk HRR Graph

The incipient and growth stages of the desk fire have the largest differences between the model and test. This means that our model requires less energy to ignite than in reality; possibly influencing flame spread and growth in the full-scale tests, as the desk is located directly next to the mattress, which is a major fuel package for the compartment.

The fully developed stages leading into a decay also differ. The model experiences this stage from roughly the four-minute mark to the eight in which it then enters a steady decay stage when the ATF test is fully developed starting just before four minutes up until it began to decay around the 12-minute mark. During this process, a similar amount of heat energy is produced by both tests as the fluctuations recorded by the ATF fall in line with the positive slope of the fully developed stage and the negative slope of the model decay stage. The HRR produced by the FDS model as a whole is similar to the experimental data but the differences do result in a certain amount of uncertainty for the full-scale tests.

5.2.4 Desk Chair

Results of this best desk chair simulation along with the ATF test are in Figure 10 below. The ATF desk chair reached a peak HRR of 685 kW about one minute after ignition. The FDS calculation reached a similar peak of 668 kW about 2 minutes after ignition. This difference calculated to be about 0.25%, which is extremely low for this application. The only major discrepancy between the two results is the difference in decay times. However, since the FDS graph is only a minute behind the ATF experiment, no further change was needed.
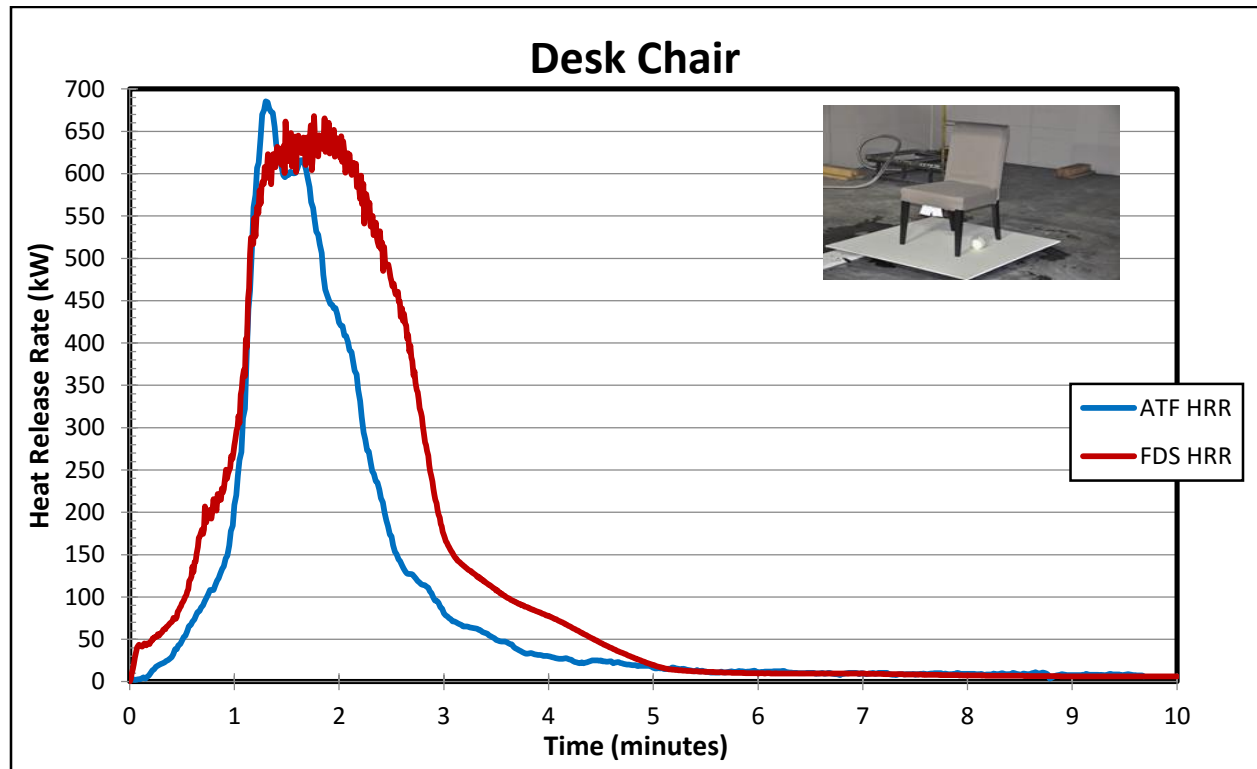

Figure 10: Desk Chair HRR Graph

5.2.5 Dresser

A significant fraction of the tests conducted were explored the different types of pine wood used for the fuel package. As stated earlier in chapter 4, white pine was chosen as the material over yellow pine because it provided a more accurate maximum heat release rate. In regards to heat release rate, Figure 11 below is a graphical representation of the experimental HRR recorded by the ATF when burning the dresser and the model HRR recorded by FDS during the simulation. When directly compared, the two heat release rates follow similar trends such as the fire decay stage and the peak HRR during the fully developed stage; the ATF recorded a peak HRR of 1.51MW and the FDS model recorded a peak HRR of 1.53MW yielding a difference of 1.6%.
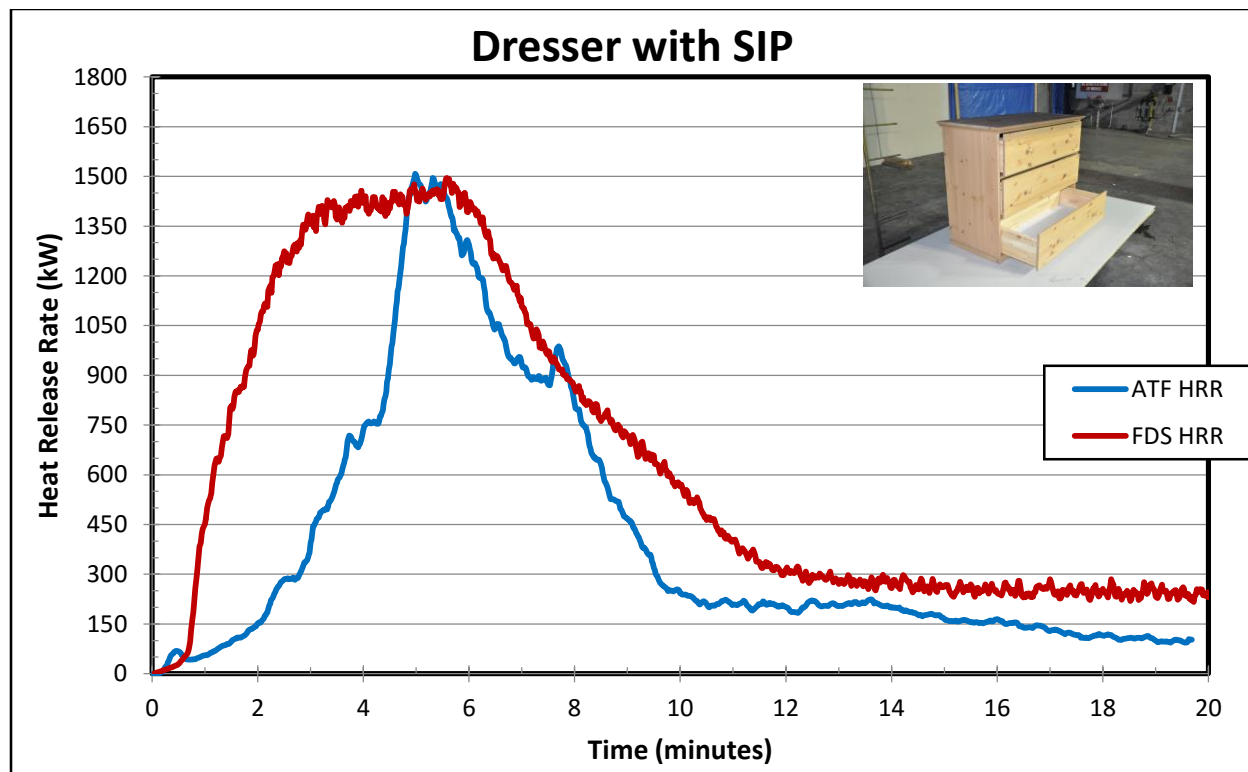
Figure 11: Dresser HRR Graph

As for the differences, the FDS model recorded a much higher total energy output than the ATF test during the incipient and growth stages. This translates to the FDS model being much easier to ignite than the actual ATF dresser; a discrepancy likely caused by the uncertainty of the thermal properties. With the use of ramp functions, a result that meets the industry's standard of achieving a HRR that is within 20% of the desired result is achieved [9].

5.2.6 Mattress

The comparison of the total HRR of the model and the actual test is plotted in Figure 12 below. For the mattress model, the fire spread across the bed at a similar rate as seen in the rise of the HRR. In the model, the entire mattress was involved in fire after 7 minutes reaching a peak HRR of 990 kW. After that time, the fire reached steady-state until all of the fuel was consumed. A possible explanation of the "double hump" characteristic of the ATF data is the role of the bedding (blanket). Since the bedding was ignited at the corner of the bed, the fire slowly spread across the entire blanket while only half of the mattress on the side of ignition was involved in fire explaining the first peak. After that time, the fire began to lose its energy, while leaving smoldering areas of the mattress then eventually re-igniting the mattress explaining the second peak. Since the characteristics of the HRR graph are similar in the beginning and end with a 18.5% difference in peak HRR, the model deemed to be acceptable.

When modeling the mattress and the beanbag, the simulation also produced reasonable agreement in overall magnitude showing similar trends. The comparison of the total HRR of the model and the actual test is plotted in Figure 13 below.
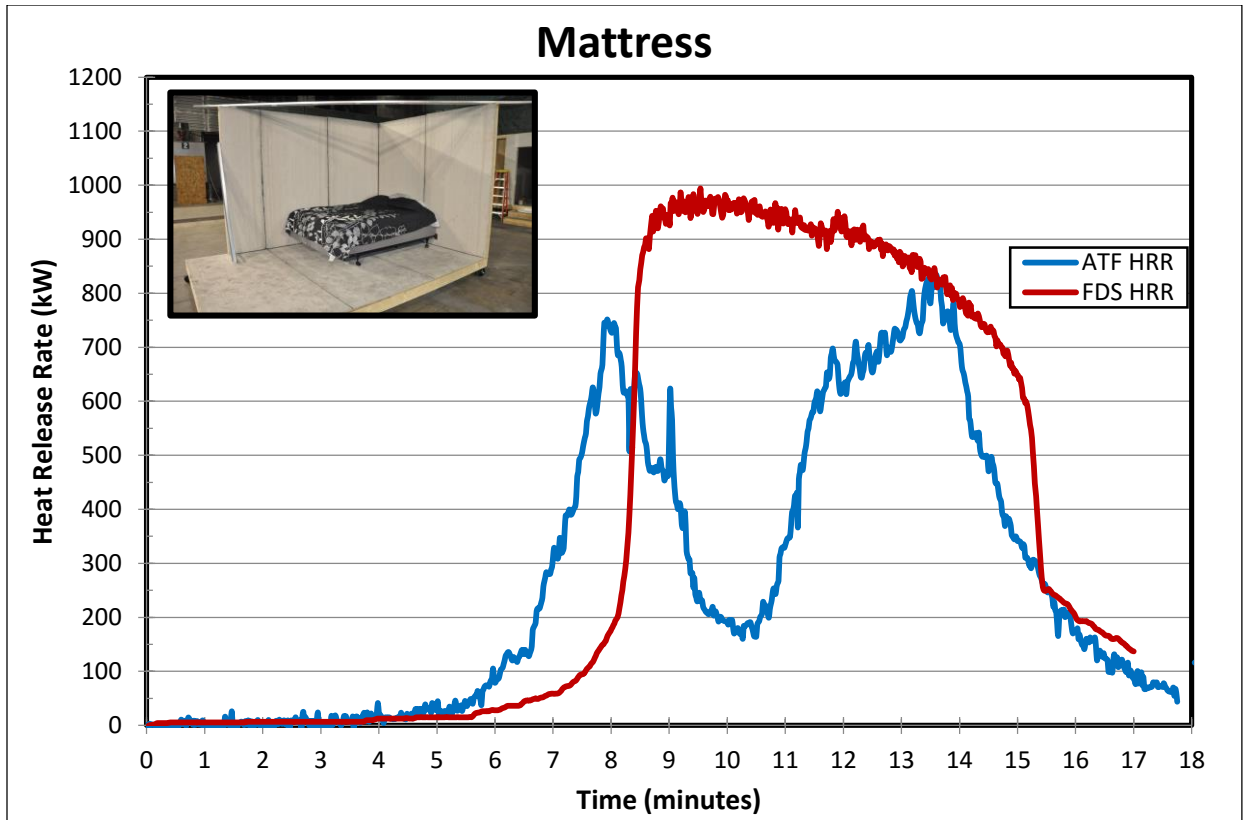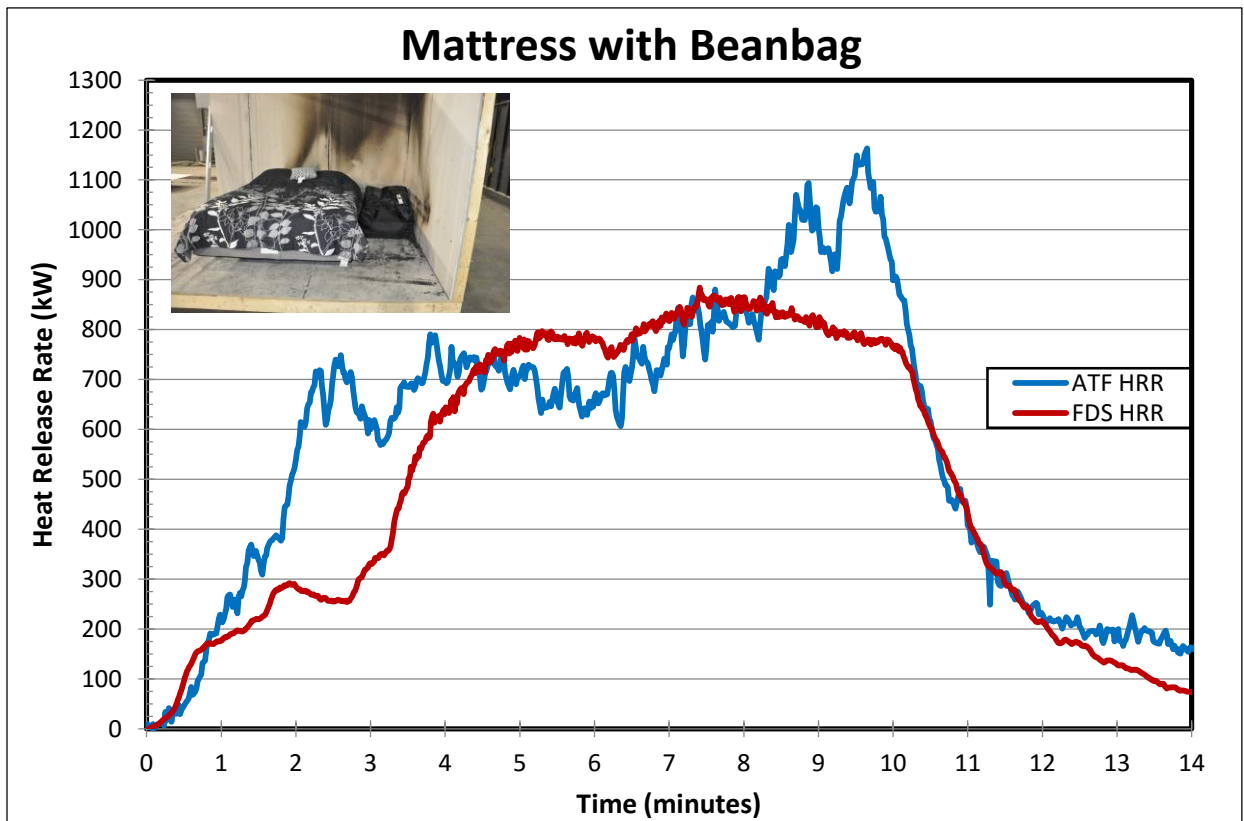
31

Figure 12: Mattress HRR Graph

Figure 13: Mattress and Beanbag Chair HRR Graph

5.2.7 Upholstered Chair

A graph comparing the best FDS simulation to the ATF test is depicted below (Figure 14). In the ATF test, the chair experienced considerable melting and dripping of material underneath the chair. This may have led to the prolonged incipient phase of the growth curve. As for the FDS model, this melting phenomenon cannot be accurately modeled, which led to the spike in HRR at around 3 minutes. The maximum HRR's recorded were 1.7 MW and 1.4 MW for the ATF tests and FDS simulations respectively. This calculates to a total difference of 19%, which is within the acceptable range. Another aspect about the two tests is that the FDS model simulated more energy output than the ATF experiments. The difference in total areas under the HRR curves supports this assertion. However, since the FDS model produced a considerably lower peak HRR, this energy difference was deemed acceptable.
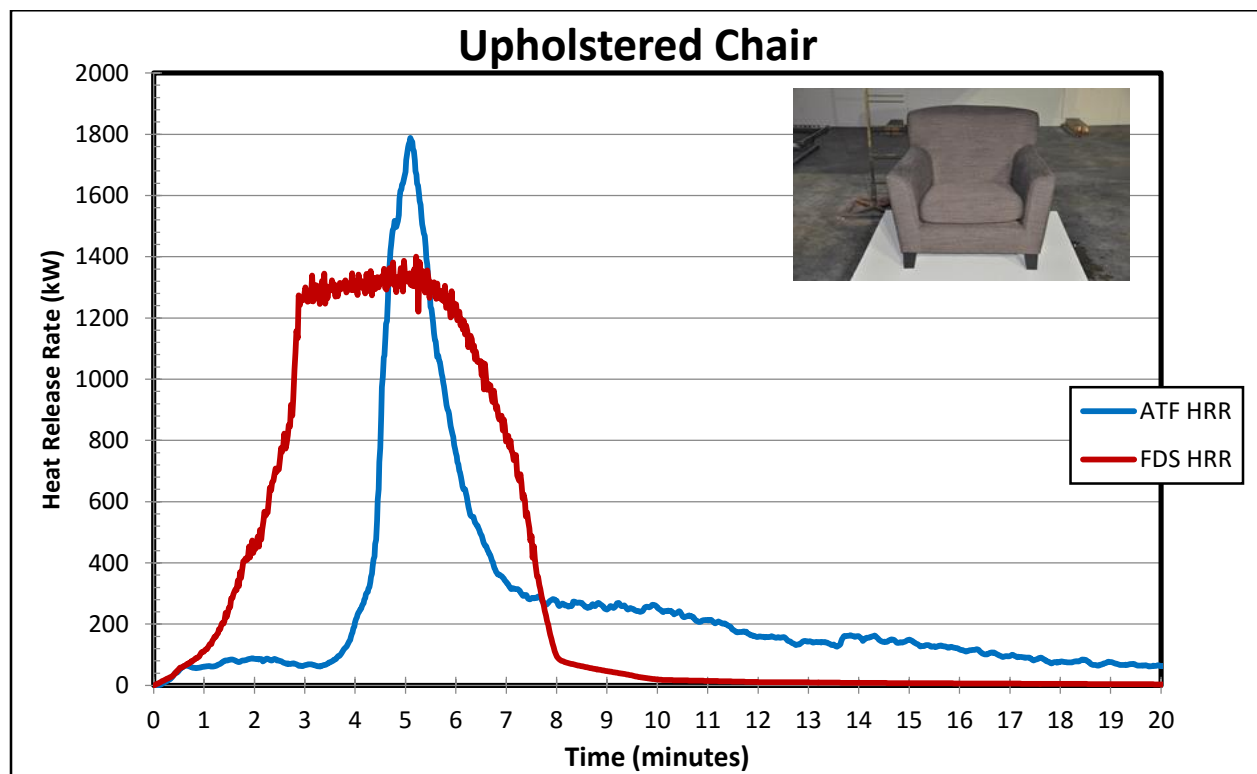

Figure 14: Upholstered Chair HRR Graph

33

5.3 Full-scale Results

In this section, measurements of temperature, heat flux, and gas velocity of the full-scale tests are compared to the values calculated by FDS. The heat release rates for each ATF compartment tests were not measured, so a comparison with the calculated heat release rate by FDS cannot be made. All of the FDS outputs for the full-scales has been smoothed using a 10-point moving average. Images rendered from Smokeview at every minute of all four FDS full-scale models are provided to show the fire growth and flame spread. Since the videos of all the ATF tests show minimal visibility due to smoke production, a visual comparison of fire growth and flame spread cannot be made.

5.3.1 Test 1

Recalling from chapter 4, the initial conditions of the door in the hallway was kept closed with the fire located in the corner of quadrant 3 for test 1. From the timeline shown below, the mattress and beanbag chair becomes fully involved in fire after 2 minutes. At around this time, the top quadrant 1 window opens followed by the top quadrant 2 window. The windows in the FDS simulation opened earlier than the windows in the actual test due to the uncertainties of the method used for the window openings. Between 5 and 6 minutes, all of the fuel packages are ignited and the fire begins to reach the transition point of flashover. After 7 minutes, the flames begin to migrate towards the vent openings, where there is better oxygen supply. Table 10Table 11 below provides a summary of all these events in both the model and the test for comparison.

Figure 15 shows the plotted heat release rate over time calculated by FDS. Events such as the opening of windows were marked as they show direct correlations to the sudden increase in the heat release rate. It is important to note that the heat release rate predicted by FDS provides the instantaneous energy release in the room. For full-scale model 1, the heat release rate reached a peak of approximately 6.5 MW at roughly 8 minutes from ignition. Once the fire reached its peak heat release rate, the fire began to reach a steady state condition due to ventilation control as shown in the images in the timeline.

FDS Full-scale Test 1 Smokeview Timeline		
1 minute	2 minutes	3 minutes
4 minutes	5 minutes	6 minutes
7 minutes	8 minutes	
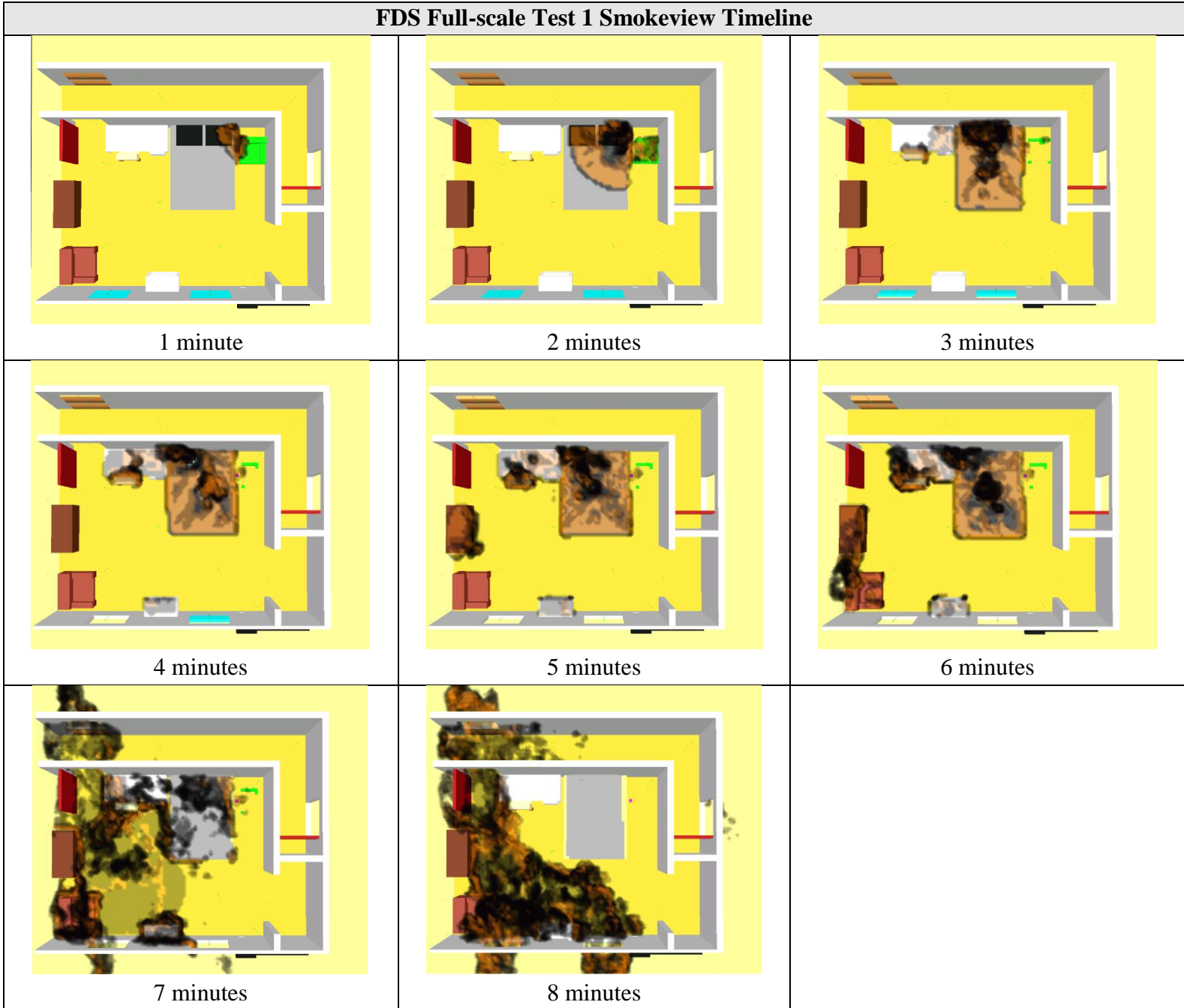
Event	ATF Test 1	FDS Model
Top half of Quad 1 Window breaks	4:05	2:10
Bottom half of Quad 1 Window breaks	N/A	4:58
Flames out Quad 1 Window	6:20	6:51
Top half of Quad 2 Window breaks	6:35	2:35
Bottom half of Quad 2 Window breaks	N/A	3:39
Flames out Quad 2 Window	6:35	6:42
Transition	6:35	
Suppression	8:30	N/A

Figure 15: FDS Full-scale Test 1 HRR

36

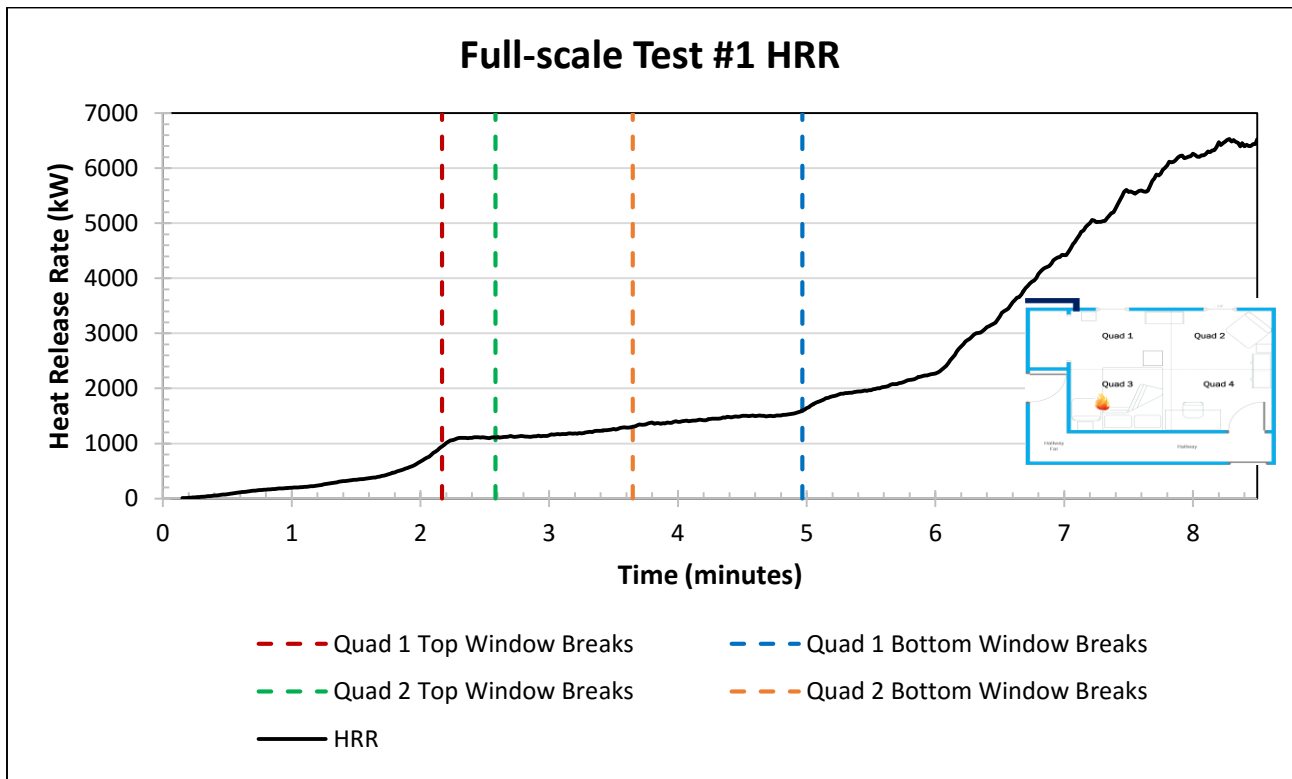Figure 16Figure 19 show the comparison of the temperature data measured in each quadrant of the compartment. As seen from the figures, the FDS temperature data shows reasonable agreement with the measured data following similar trends. In the ATF test, the fire reaches ventilation-limited at approximately 2 minutes as seen from the steady temperature reading of the top thermocouples. The rapid increase in temperature was due to the failure of the quadrant 1 window allowing fresh air to enter the compartment and ultimately, resulting in fire growth and spread. Since the quadrant 1 and quadrant 2 windows in the FDS model breaks at an earlier time, the fire does not reach a state where it is ventilation-limited. This explains why the rapid increase in the temperature data was not simulated. Since there was sufficient amount of oxygen available for combustion the fire growth was dependent on the ignitability and flammability of the fuel packages. This is representative of a fuel-controlled fire. Despite these differences, the full-scale model reached flashover at a similar time to test 1 and the peak temperatures from the test and the simulation show agreeable values.
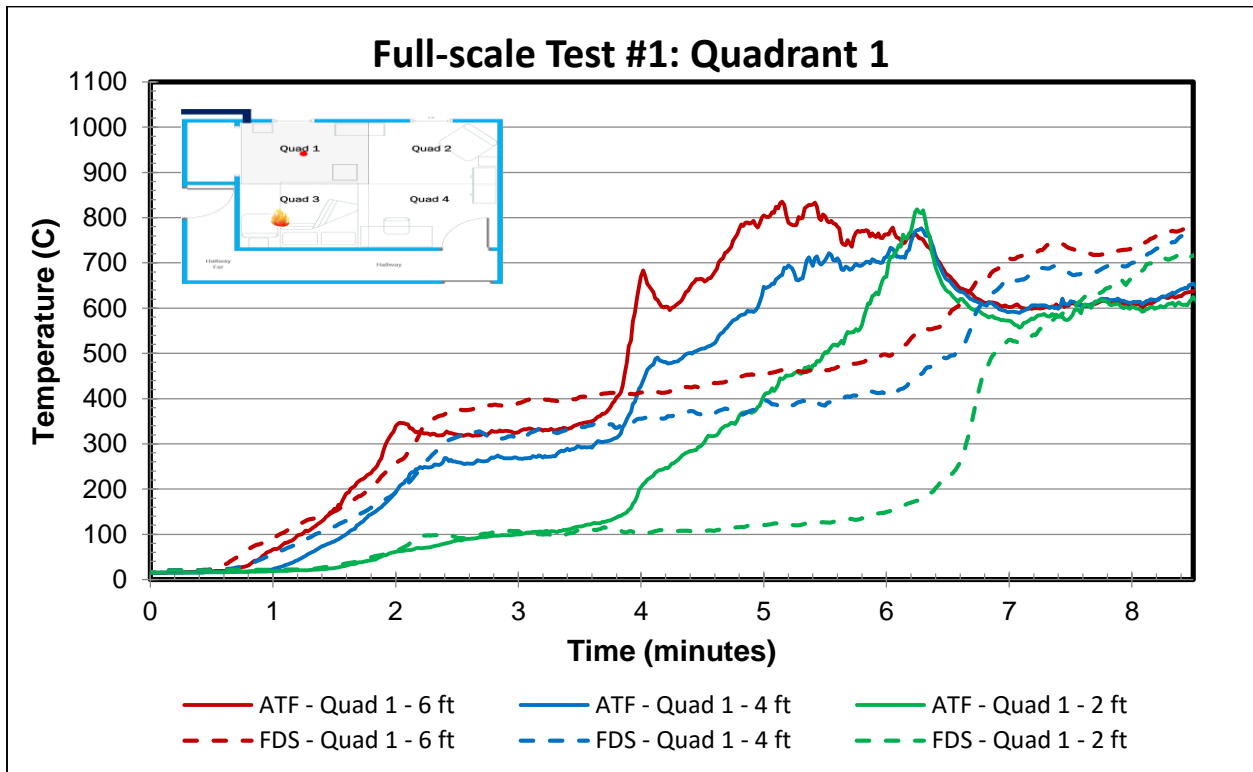

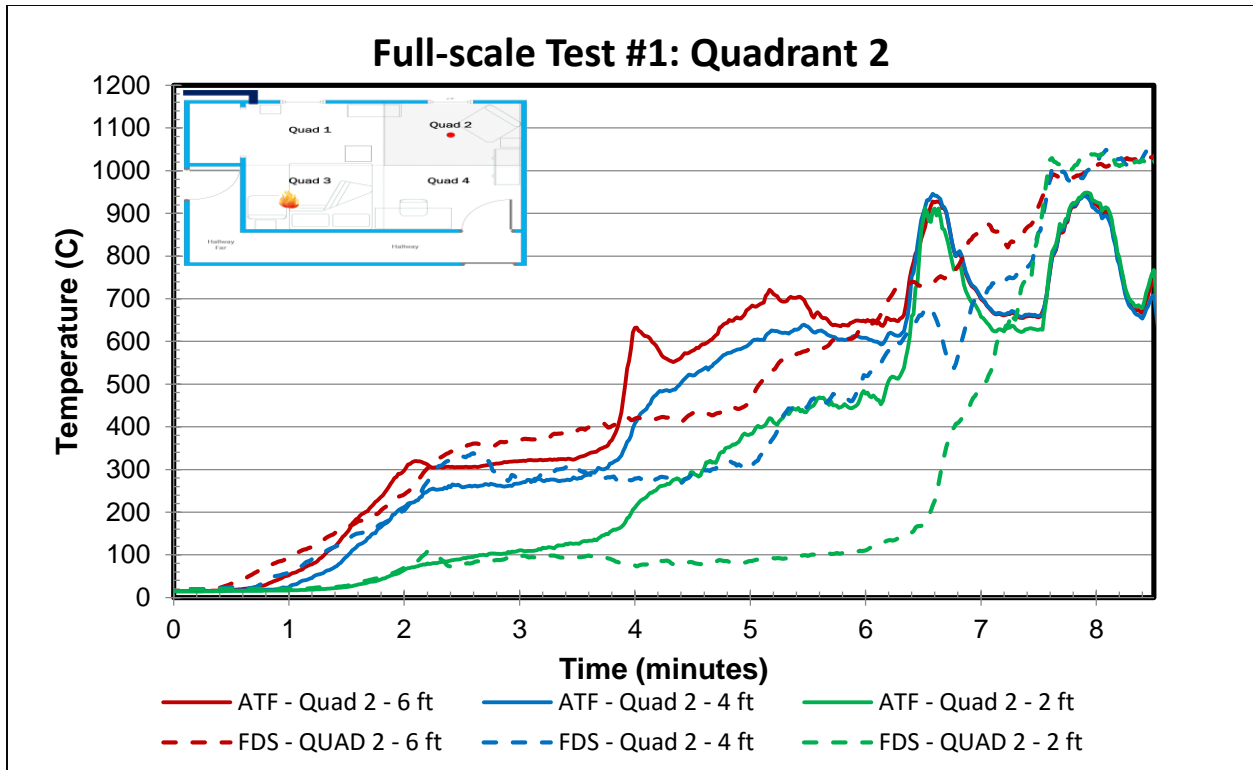Figure 16: Full-scale Test 1 Thermocouple Data - Quadrant 1

Figure 17: Full-scale Test 1 Thermocouple Data - Quadrant 2
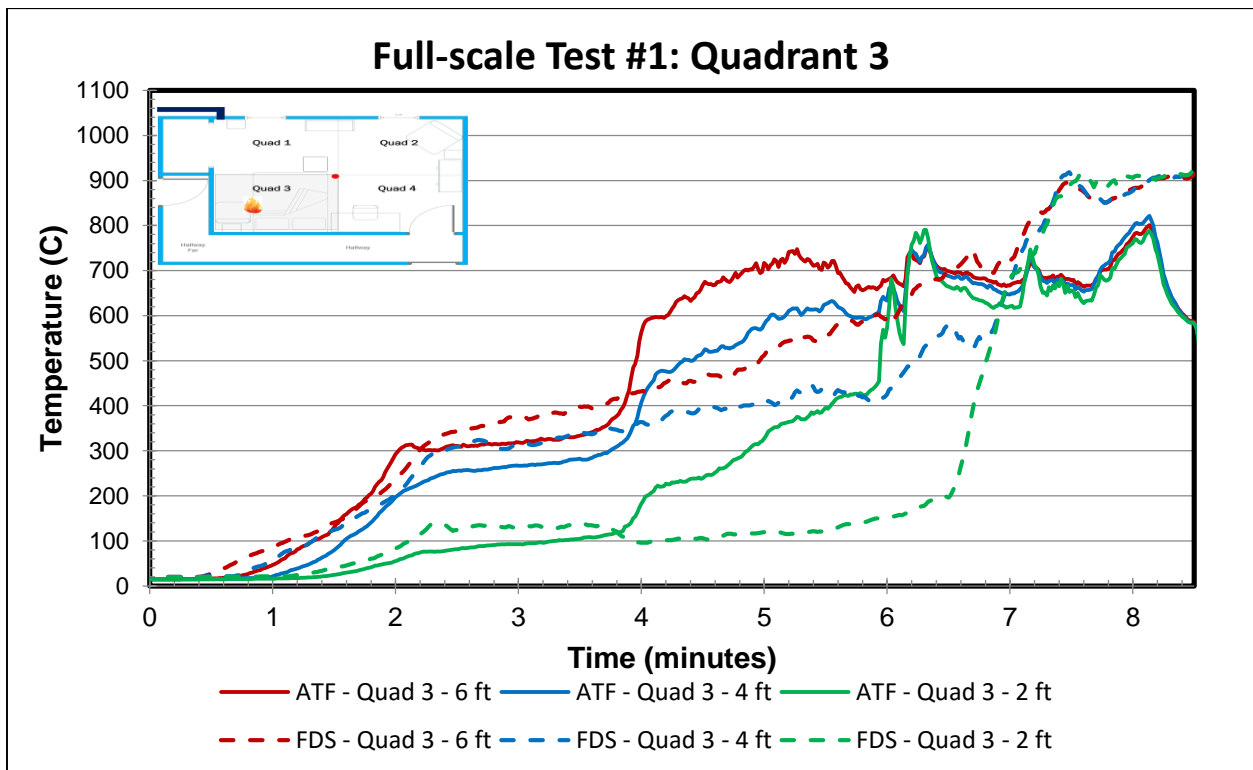
Figure 18: Full-scale Test 1 Thermocouple Data - Quadrant 3
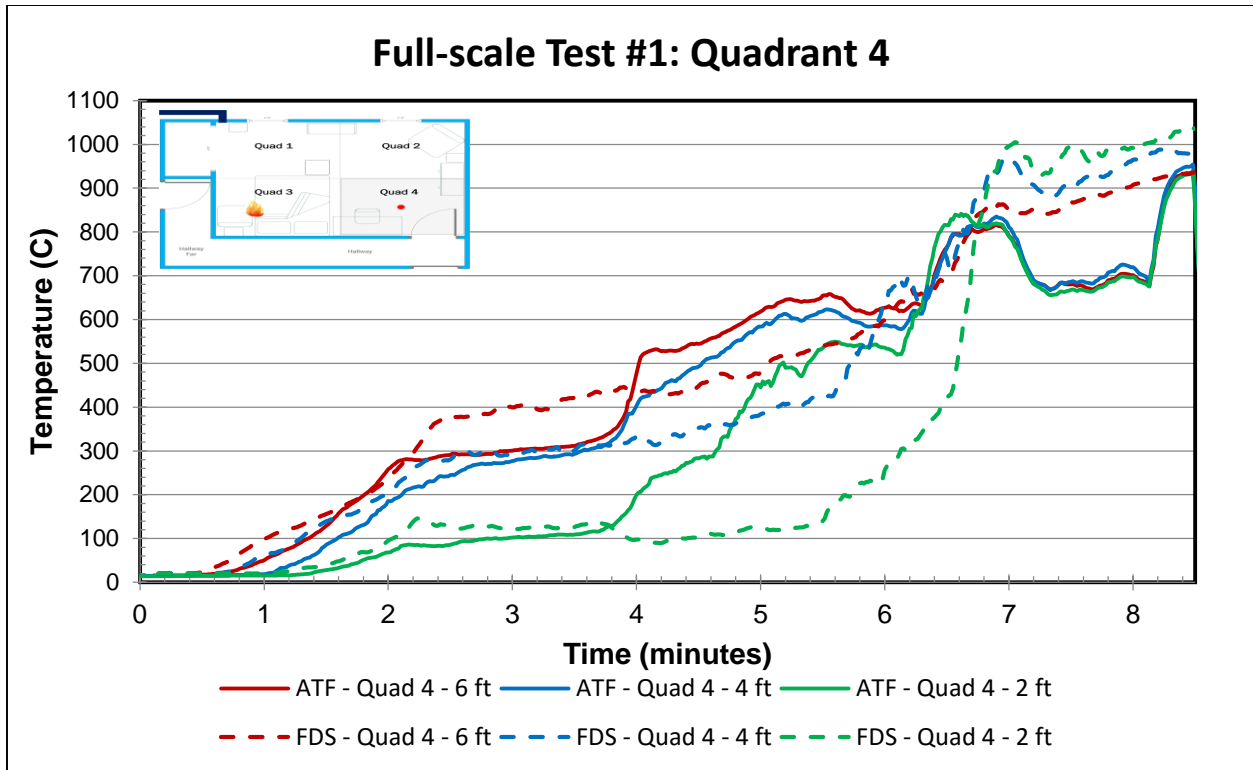
Figure 19: Full-scale Test 1 Thermocouple Data - Quadrant 4

5.3.1.2 Heat Flux

The heat flux gauges used in test 1 only measures up to a maximum value of 75 kW/m². Therefore, a comparison of the peak heat flux between the ATF tests and the FDS simulation cannot be made. In the actual test, heat fluxes initially spike in quadrants 3 and 1 on the origin side of the room. The transition point to flashover results in exposure intensities declining in quadrants 3 and 1 while they are increasing in Quadrants 4 and 2, where the doorway opening is providing fresh air. In the FDS simulation, heat flux initially spikes in quadrant 3, but not in quadrant 1. In all the quadrants the heat flux rapidly increases once the FDS model reaches the transition point of flashover.
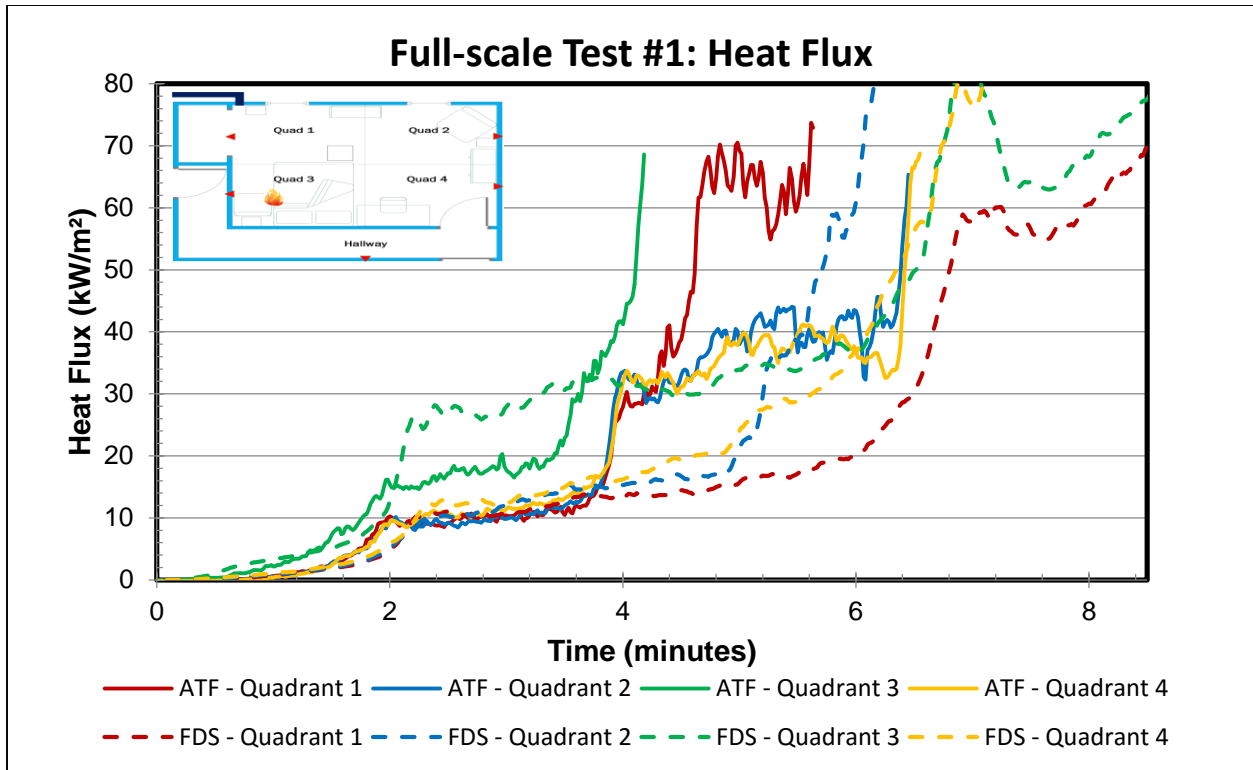
Figure 20: Full-scale Test 1 Heat Flux Data

5.3.1.3 Velocity

A significant detail in the data collected by bi-directional velocity probes is the resulting sign convention for each device; positive result represents flow out of the room while a negative result represents flow into the room in all full-scale scenarios. Besides the proper sign convention of the values calculated by FDS, the overall magnitude show agreement to the measured data. Once the fire reaches its transition phase, all of the velocity probe measures the flow going into the compartment. This trend is not seen in the FDS model.
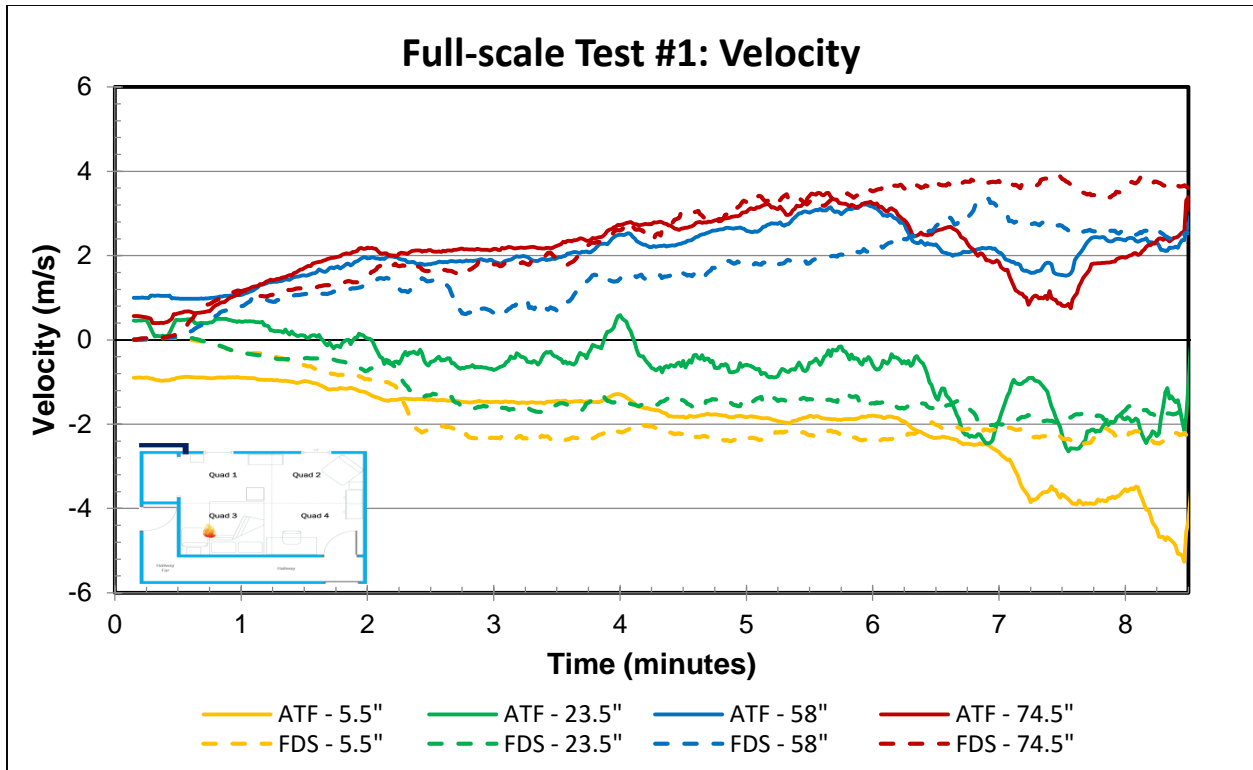
Figure 21: Full-scale Test 1 Velocity Data

5.3.2 Test 2

Full-scale test 2 has optimal initial ventilation conditions when compared to the other three conducted tests. This scenario has both the bedroom door and the opposing door to the outside as initially open which exposes the bedroom compartment to the largest supply of oxygen.

Along with the resulting device data of the FDS model, the time at which specific significant events occurred was also tracked and compared. Table 12 below displays the time for these events for both the ATF test and the FDS model; the most noteworthy event that occurs late in the FDS model is transition to flashover due to the delay in how the fire grew and spread. Other events from Table 12 have been placed as markers on the HRR graph shown in Figure 22 as they directly correlate to the overall fire behavior. In the model, these events coincide with significant details to the HRR graph such as the time of the first ventilation change leading to a stagnated and steady state HRR between roughly 3 and 6 minutes. This then changes at the same time both bottom windows break open correlating with flashover. As shown in the timeline, between the 6 and 7 minutes, this change leads to the spreading of fire resulting in an increasing HRR. The flame spread initiated by the ventilation change allows the fire to enter a ventilation controlled stage which can be seen at the 8-minute mark where fire is only present near areas of incoming oxygen. This fire phenomenon seen in Smokeview is also represented on the HRR graph where the instantaneous energy being released by the fire reaches steady state after the HRR peaked at approximately 7 MW around 8 minutes after ignition.

41

Event	ATF Test 2	FDS Model
Top half of Quad 1 Window breaks	3:21	2:36
Bottom half of Quad 1 Window breaks	N/A	6:01
Flames out Quad 1 Window	4:05	7:17
Top half of Quad 2 Window breaks	N/A	2:40
Bottom half of Quad 2 Window breaks	N/A	5:51
Flames out Quad 2 Window	4:30	6:55
Transition	4:49	7:00
Suppression	7:00	N/A
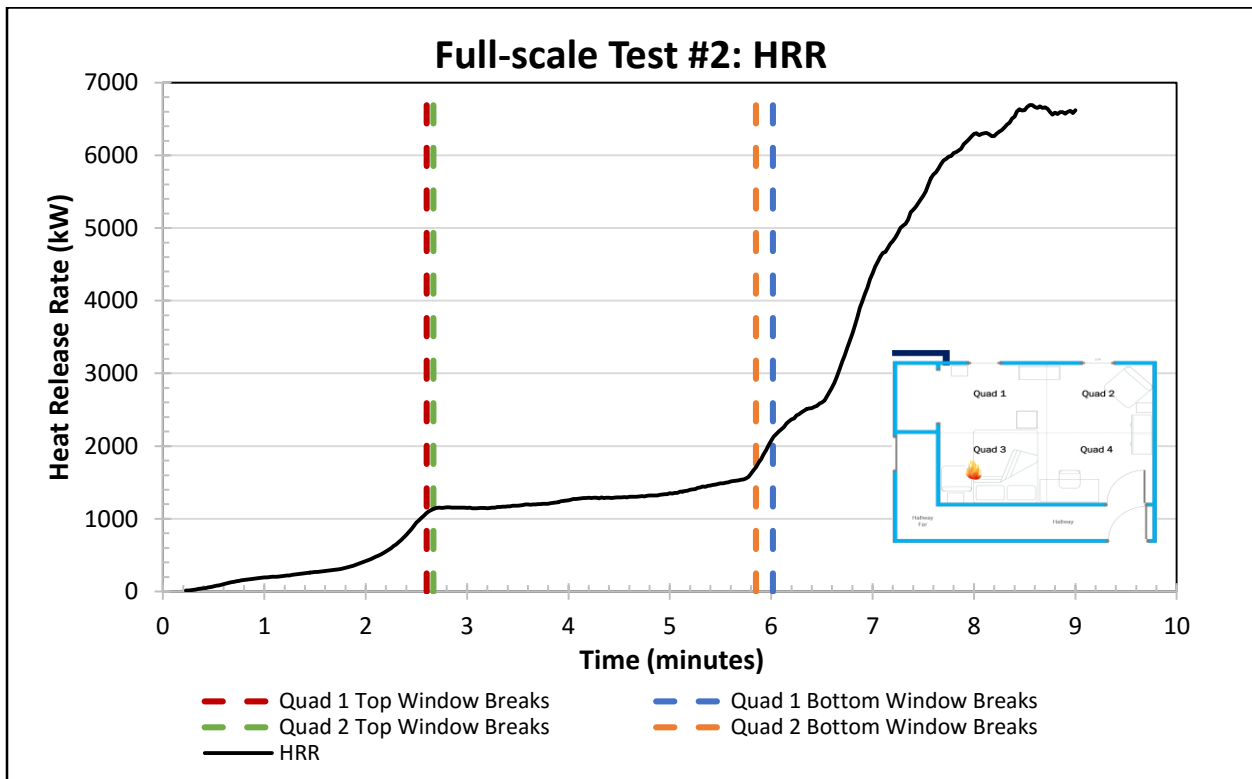
Figure 22: FDS Full-scale Test 2 HRR

FDS Full-scale Test 2 Smokeview Timeline		
1 minute	2 minutes	3 minutes
4 minutes	5 minutes	6 minutes
7 minutes	8 minutes	

Table 13: FDS Full-scale Test 2 Smokeview Timeline
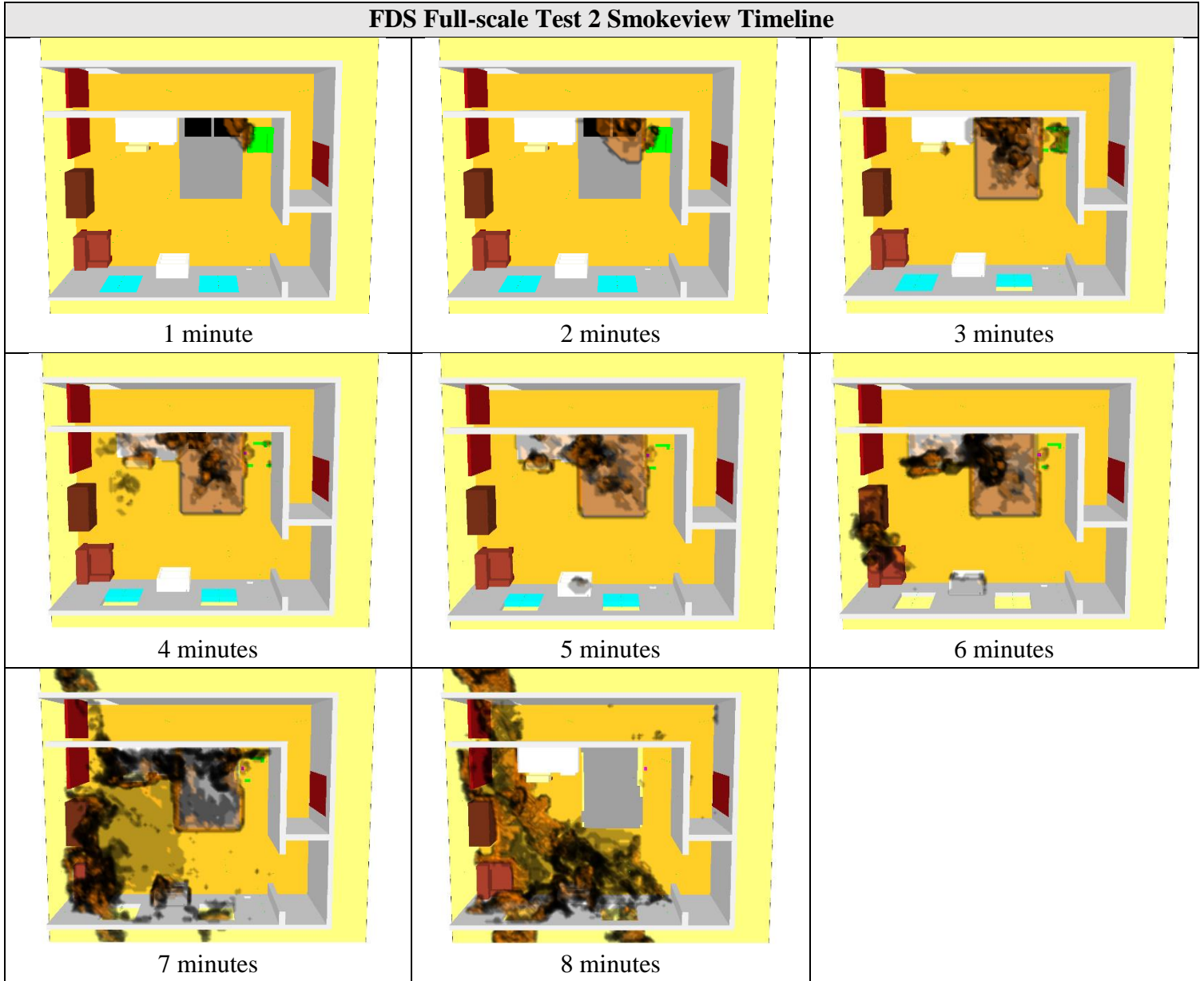
5.3.2.1 Temperature

The FDS model for full-scale test 2 yielded temperature results that were generally and consistently lower than that recorded by the ATF. More specifically, it is the temperatures occurring in the later parts of the model that create a significant discrepancy since the earlier results show some accuracy.

The first two and a half minutes of the model show that the initial growth of the fire resulted in temperatures very similar to the actual test; however, this similarity changes once the FDS quadrant 1 and 2 windows first break open since this event occurs much earlier than the actual ATF test. The difference in timing for this dynamic ventilation change is highlighted in

quadrants 2 and 4 as the FDS thermocouple data stagnates producing steady state temperatures at a much lower temperature than that of the ATF. Quadrants 2 and 4 for the ATF test both stagnate just over 700°C when the FDS model hovers around 400°C for the top most thermocouple and 100°C for the bottom most. This steady-state trend is seen throughout all four quadrants of the FDS model as shown in Figure 23Figure 26, which changes and begins to increase at the 7-minute mark until the end of the simulation; the same time at which the compartment experiences flashover. The disagreement in the temperature value was due to the delay in how the fire developed. Since the initial ventilation conditions for test 2 allow a better access for fresh air, there is an abundance of oxygen within the compartment and the fire growth is then dependent on the flammability of the fuel packages as stated in test 1. Since fire growth and flame spread is one of the major difficulties in fire modeling, the temperature data calculated by FDS show large discrepancies.
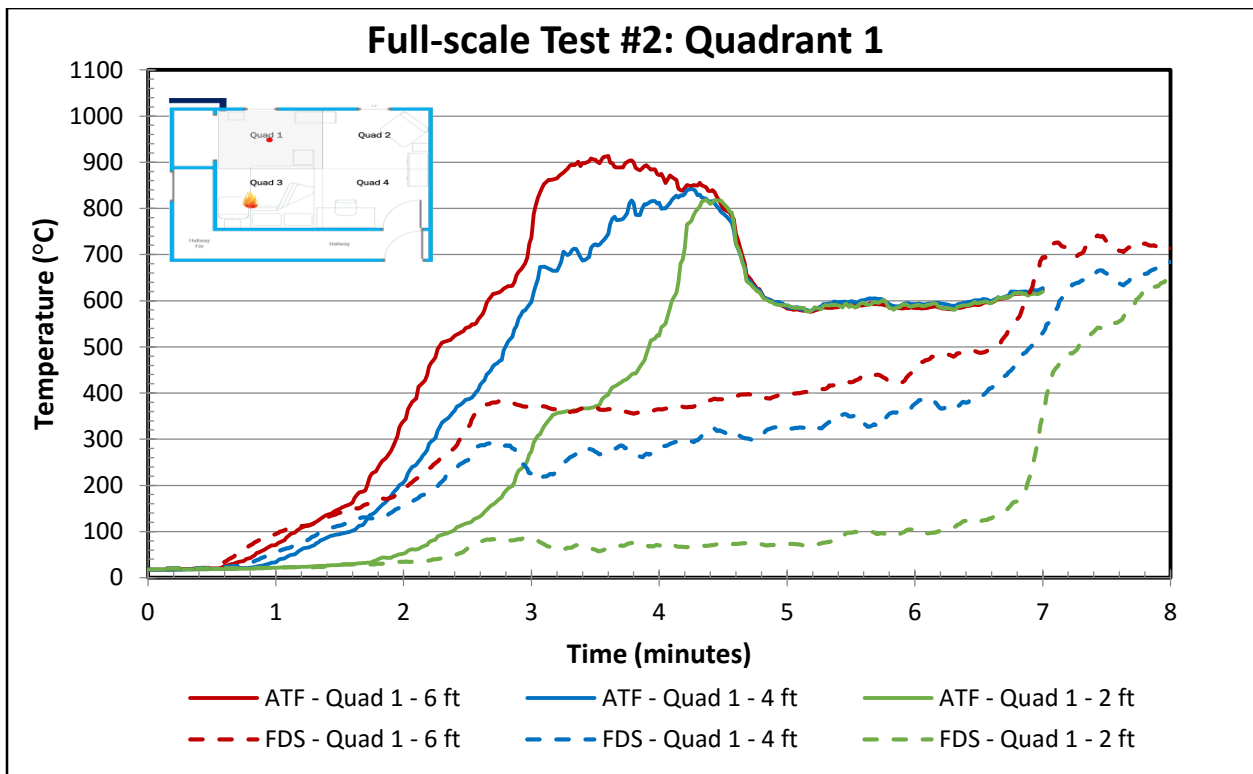
Figure 23: Full-scale Test 2 Thermocouple Data - Quadrant 1
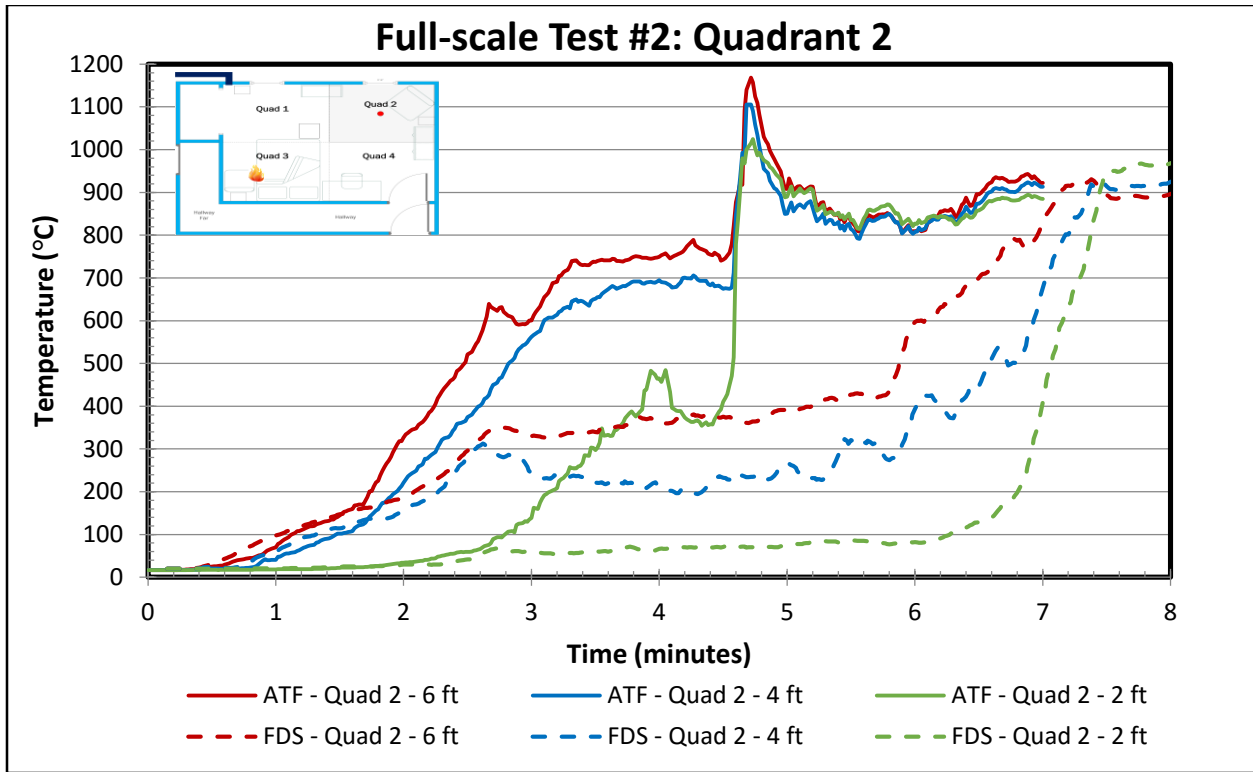
Figure 24: Full-scale Test 2 Thermocouple Data - Quadrant 2
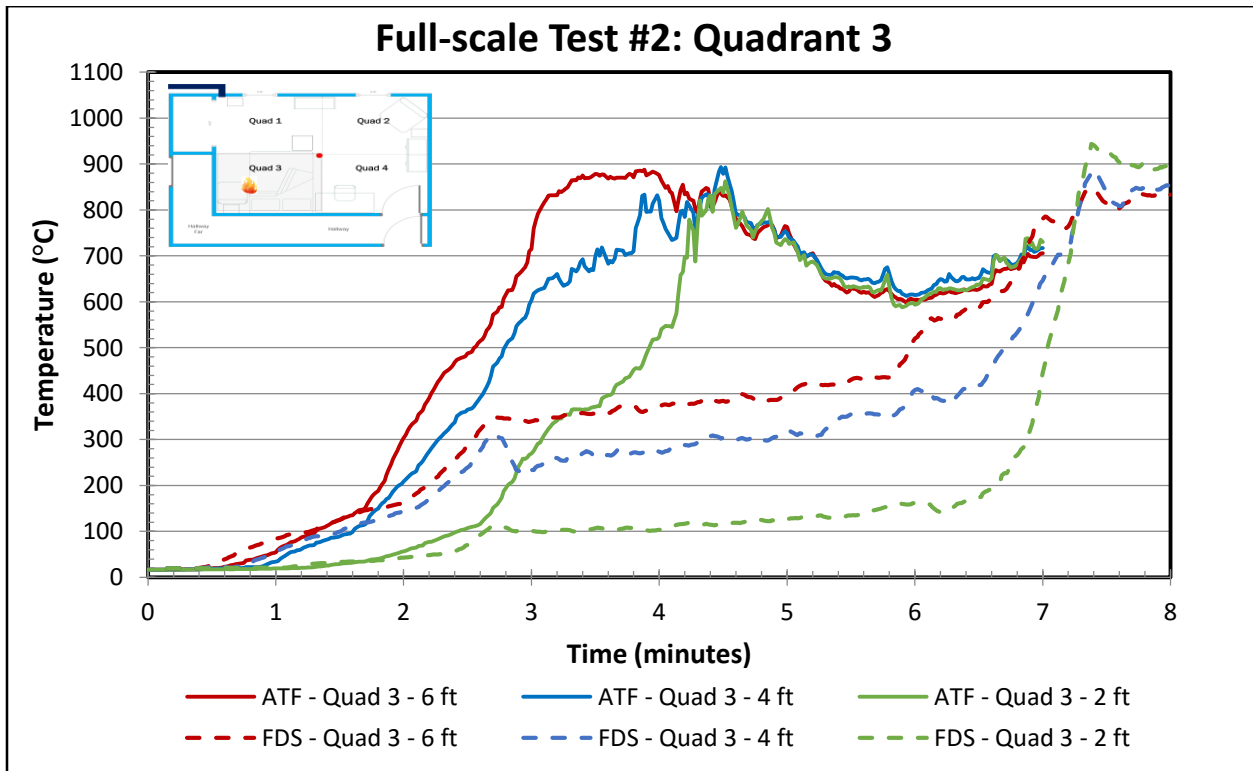
Figure 25: Full-scale Test 2 Thermocouple Data - Quadrant 3
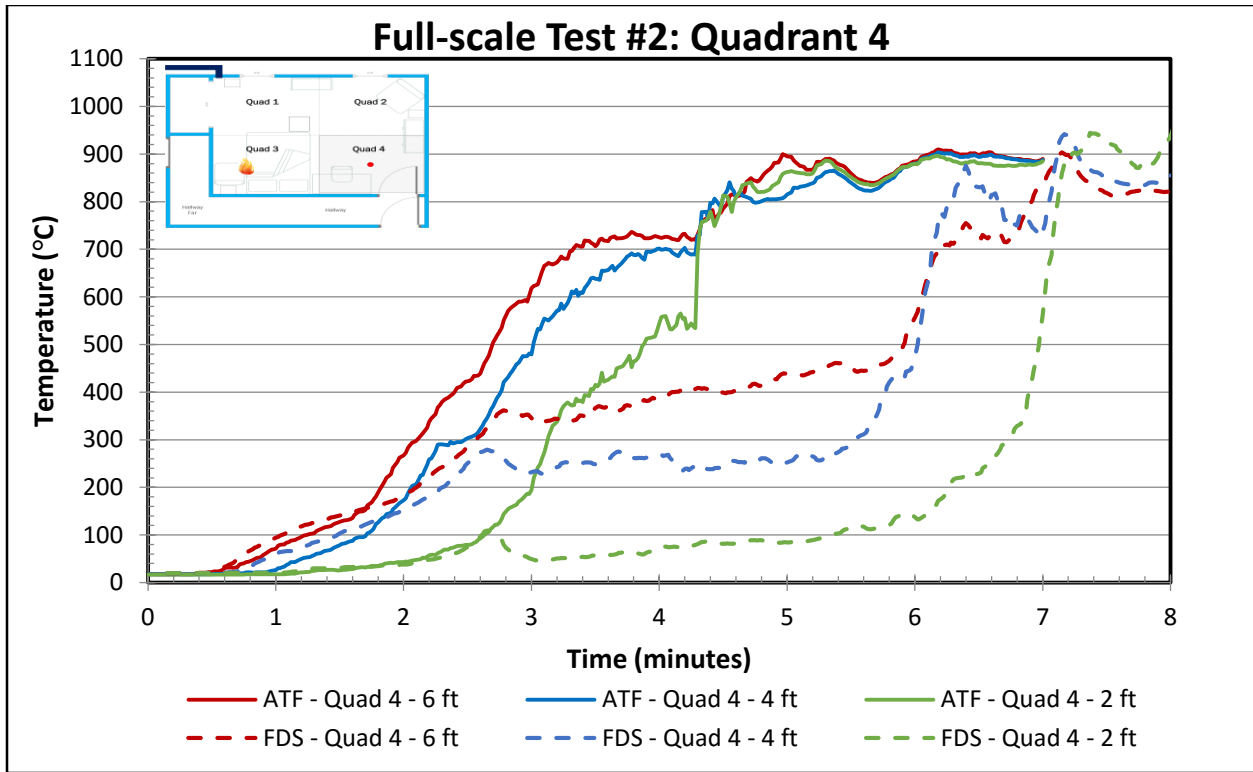
Figure 26: Full-scale Test 2 Thermocouple Data - Quadrant 4

5.3.2.2 Heat Flux

Much like the temperature data, the first two and a half minutes of the model show that the initial growth of the fire resulted in heat fluxes that are very similar to the ATF test. Once the first window breaks open however, the FDS heat fluxes reach a steady state instead of accurately representing the fire conditions like the ATF data. The heat flux gauges for quadrants 1 and 3 should initially spike due to the fire origin location and eventually decay during the flashover transition. Quadrants 2 and 4 should simultaneously be increasing since there is an abundance of ventilation present. This relationship is not seen in the FDS results even though the heat flux data is consistent with the timeline of significant events; quadrants 2 and 4 increase in exposure intensity around 6 minutes which is the same time the quadrant 2 window fully opens. Figure 27 below shows the time history of the heat fluxes for each quadrant of the compartment.

46
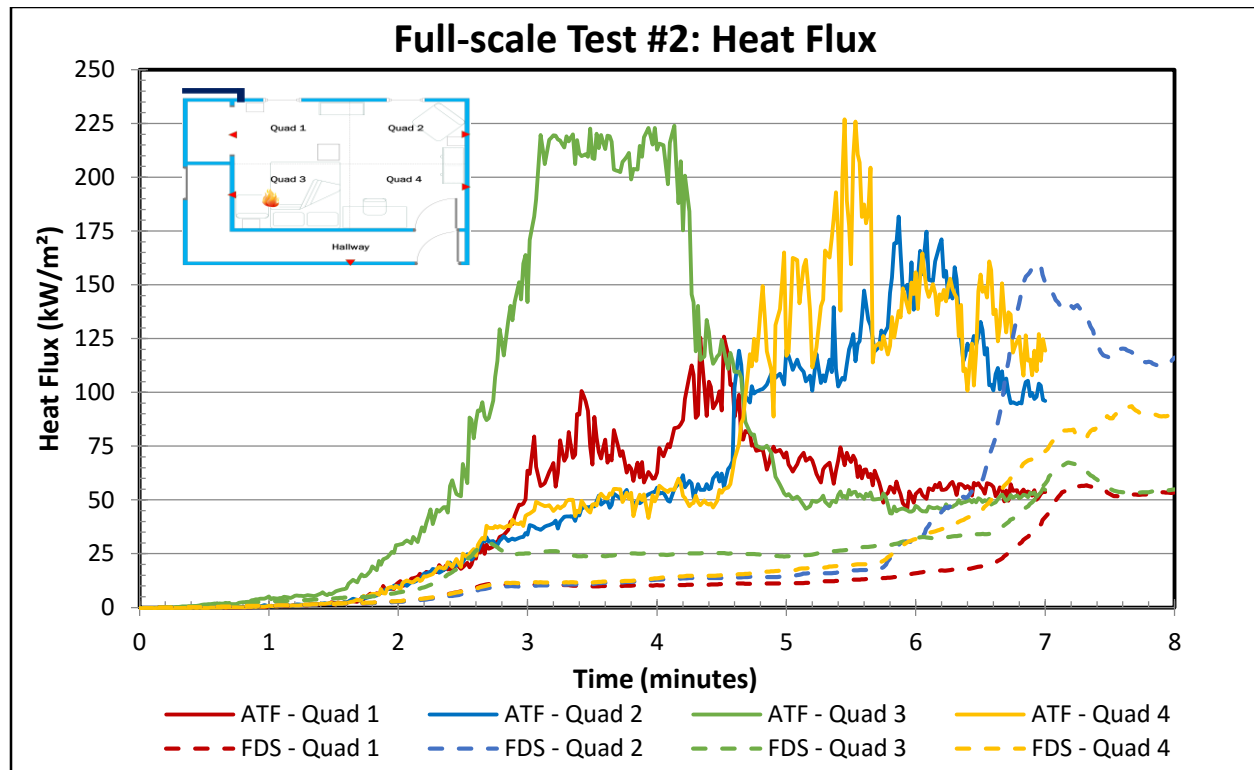
Figure 27: Full-scale Test 2 Heat Flux Data

5.3.2.3 Velocity

The FDS model resulted in data that is very similar to that of the ATF; all four velocity probes placed in the doorway have matching sign conventions and therefore matching directions. Along with proper directional flow, the overall magnitude of the FDS data also correlates with the ATF results. Despite the similarities, there are minor differences such as the drastic dip around 5 minutes for the ATF 74.5" velocity probe which is representative of flashover for the ATF test. This transition requires a large amount of oxygen for complete combustion causing a change in flow at the bedroom door since a large supply of oxygen is being drawn in from that ventilation opening. A similar dip or any other trend connecting the velocities to significant fire events is not seen in the FDS results.
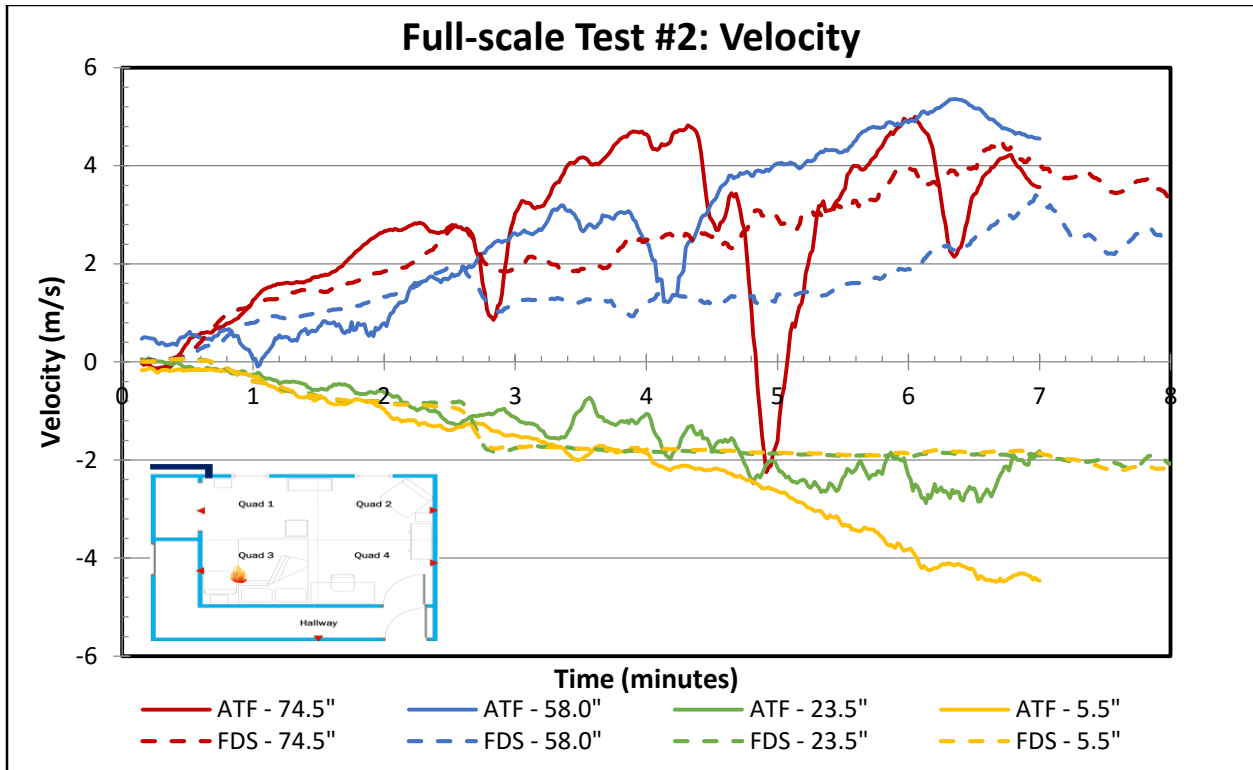
Figure 28: Full-scale Test 2 Velocity Data

5.3.3 Test 3

In full-scale test 3, the fire originated in quadrant 2 by igniting an additional bean bag chair placed next to the upholstered chair in the corner. Table 14 depicts a compilation of photos representing the growth and migration of the fire as it propagates through the compartment. As anticipated, after the fire has spread through the room and all vents have opened, the flaming region is seen to occur in areas of close proximity to these ventilation openings. This flame migration implies that the simulation has reached a ventilation controlled state To get a better understanding of when dynamic ventilation changes occurred, Table 15 shows a comparison between the FDS simulation and the full-scale ATF simulation.

Overall, the FDS simulation predicted the windows to fail earlier than what did actually occurred in the ATF test. The effect of this earlier ventilation change could not quantified; however, one would expect the early influx of fresh air to accelerate the rate of flame spread and growth in the compartment. This trend is represented in Figure 29, which depicts the instantaneous HRR history of the FDS simulation. With each ventilation change, the HRR graph experiences a jump in total energy generated. Once all vents open in the FDS simulation, the HRR begins to rapidly increase and eventually reach its peak of approximately 7 MW around 5 minutes after ignition. Following this peak HRR, the FDS simulation returns to a steady state burning condition.

48

FDS Full-scale Test 3 Smokeview Timeline		
1 minute	2 minutes	3 minutes
4 minutes	5 minutes	6 minutes
7 minutes	8 minutes	
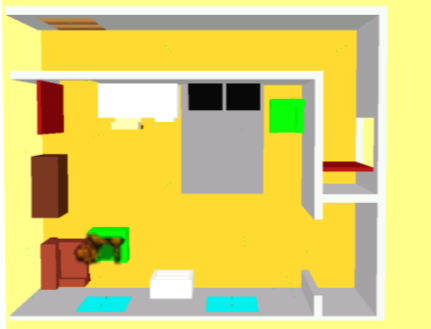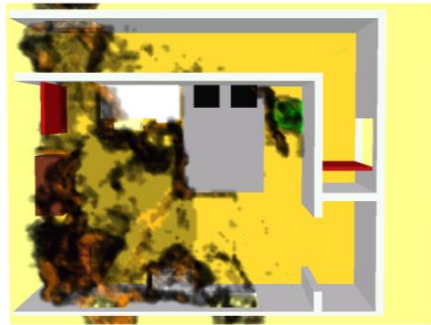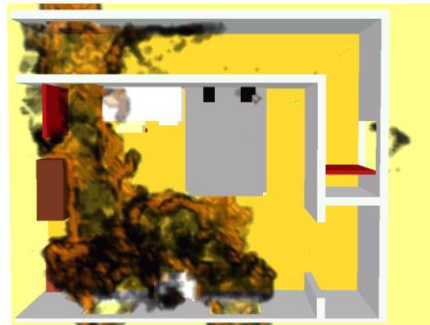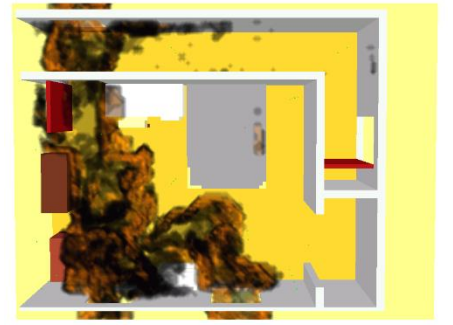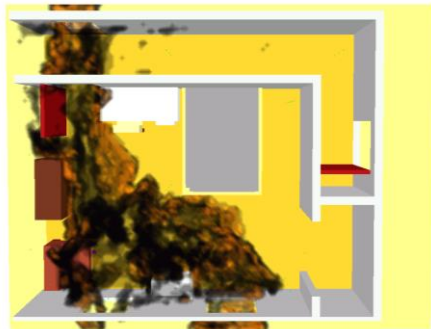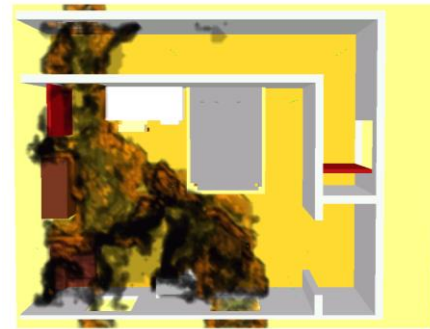
Event	ATF Test 3	FDS Model
Top half of Quad 1 Window breaks	5:15	2:38
Bottom half of Quad 1 Window breaks	N/A	2:40
Flames out Quad 1 Window	N/A	3:50
Top half of Quad 2 Window breaks	2:18	2:07
Bottom half of Quad 2 Window breaks	3:45	1:57
Flames out Quad 2 Window	2:18	3:48
Transition	5:20	3:40
Suppression	7:35	8:00
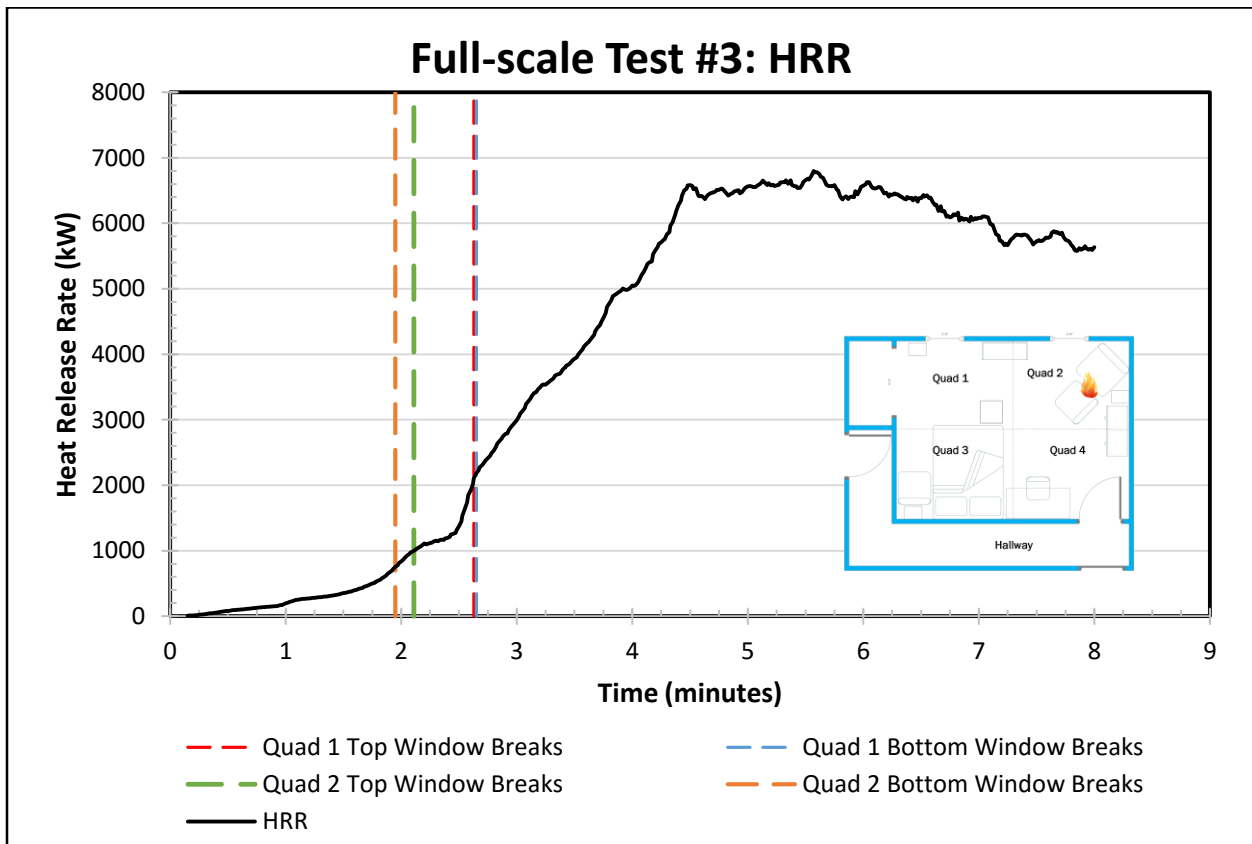
Figure 29: FDS Full-scale Test 3 HRR

Generally, all thermocouple trees in the FDS simulation recorded temperatures above the corresponding ATF thermocouples. Despite this over prediction, the FDS temperature histories followed the same overall trend when compared to the ATF data (Figure 30Figure 33). Both sets of data for all quadrants experienced similar initial growth stage, from ignition to around 2 minutes where the fuel controlled the size and therefore temperature output of the fire. During this growth period, it was noted that the FDS simulation produced both lower temperatures and lagged behind the ATF test data by a couple of minutes. This temperature discrepancy was associated to the difficulties of predicting flame spread in a fire modeling application. After this stage, the FDS simulation saw a rapid increase in temperature that coincided with the quadrant one window opening and allowing fresh air into the compartment. As the fresh air entered the compartment, it mixed with the already hot gases and accelerated the flame spread through the compartment producing a rapid increase in temperature. After this rapid growth period, the FDS simulation began to follow the ATF trends but at a higher temperature.
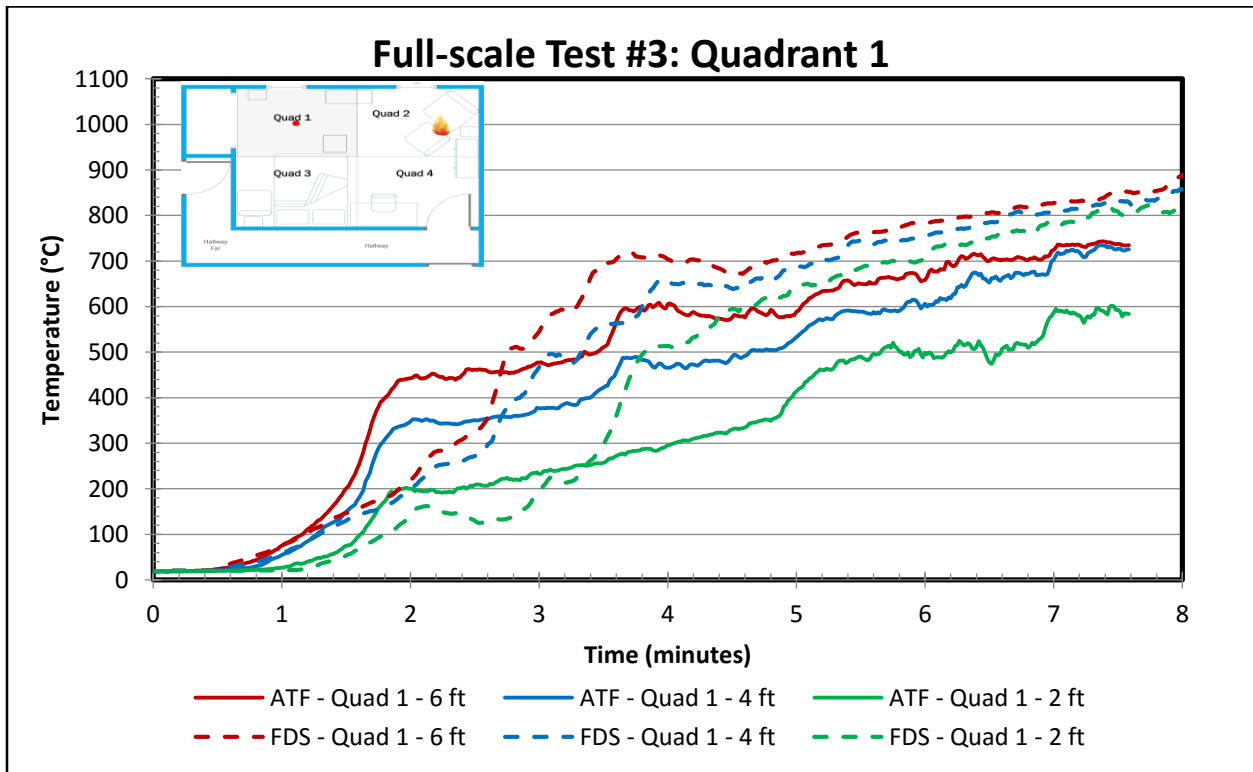
Figure 30: Full-scale Test 3 Thermocouple Data - Quadrant 1
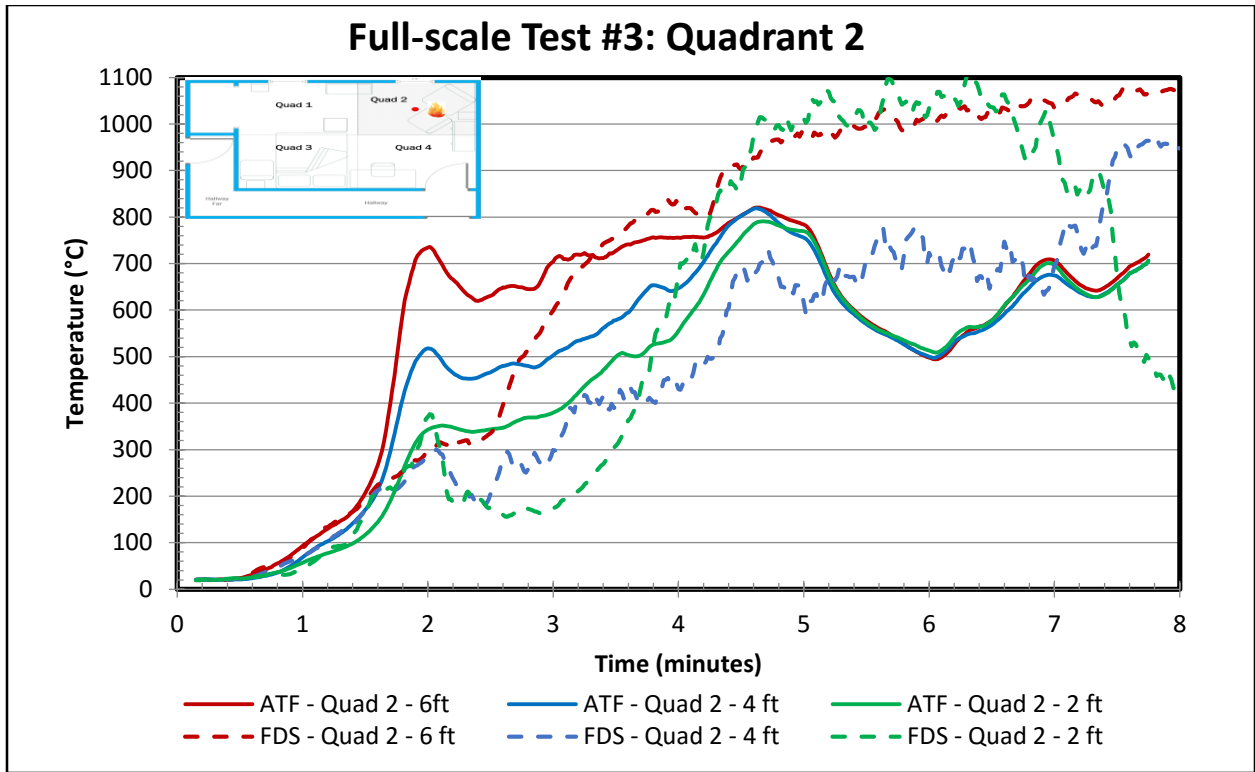
Figure 31: Full-scale Test 3 Thermocouple Data - Quadrant 2
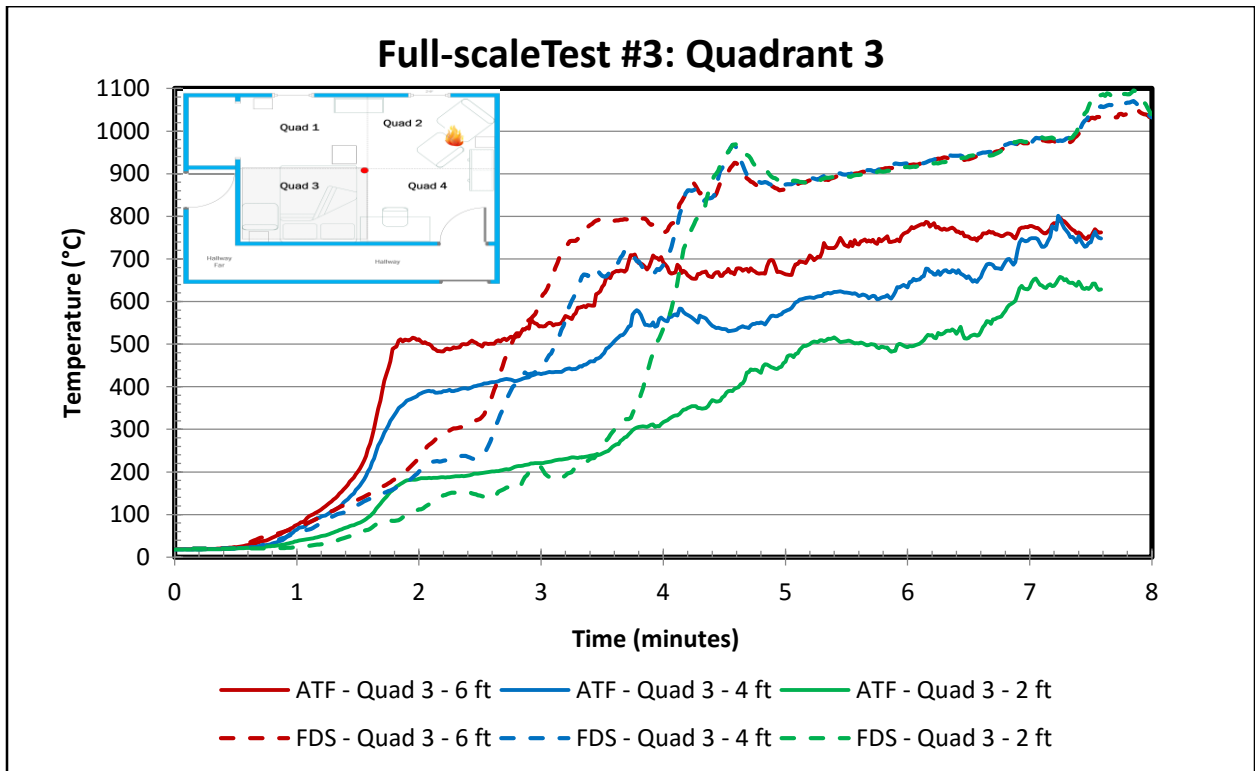
Figure 32: Full-scale Test 3 Thermocouple Data - Quadrant 3

52
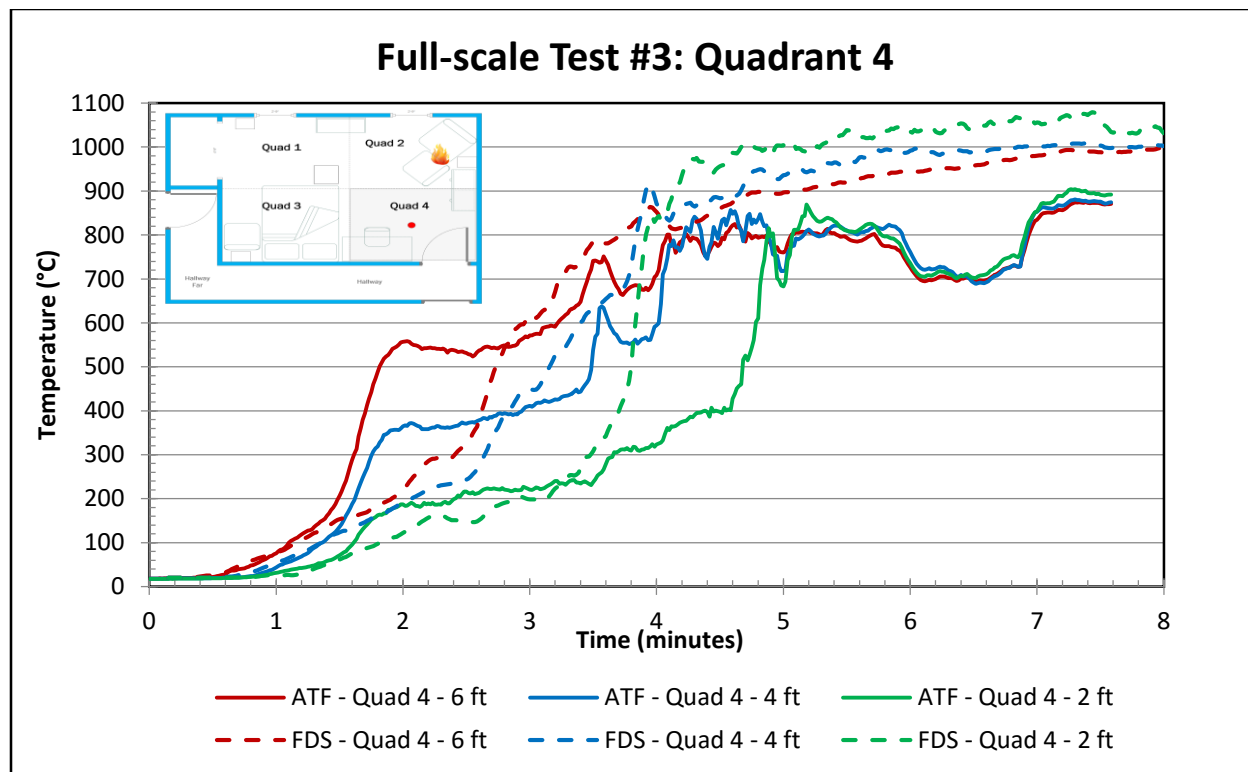
Figure 33: Full-scale Test 3 Thermocouple Data - Quadrant 4

5.3.3.2 Heat Flux

Figure 34 shows the FDS simulated heat flux outputs compared to the ATF tests. Similar to the temperature comparison, the FDS heat flux gauges lagged behind the recorded ATF data during the initial stage of the fire. The quadrant 2 FDS heat flux gauge did not reach its first peak until 3.5 minutes into the simulation while the ATF gauge reached its first peak around 1.5 minutes. This delay was interesting to note since quadrant 2 was the area of origin. However, this heat flux lag was not considered to significantly affect the simulation due to the ignition temperature of the fuel packages driving flame spread in the FDS model. In addition to the time delay, the graph shows that quadrants 2 and 4 in the FDS model did not produce comparable results to the ATF test. This could be a result of flaming being present in these quadrants, which could affect both the ATF and FDS gauges. To further this assertion, quadrants 1 and 3, where flames were not present at the end of the simulation, produced comparable results between the ATF and FDS simulated data.

53
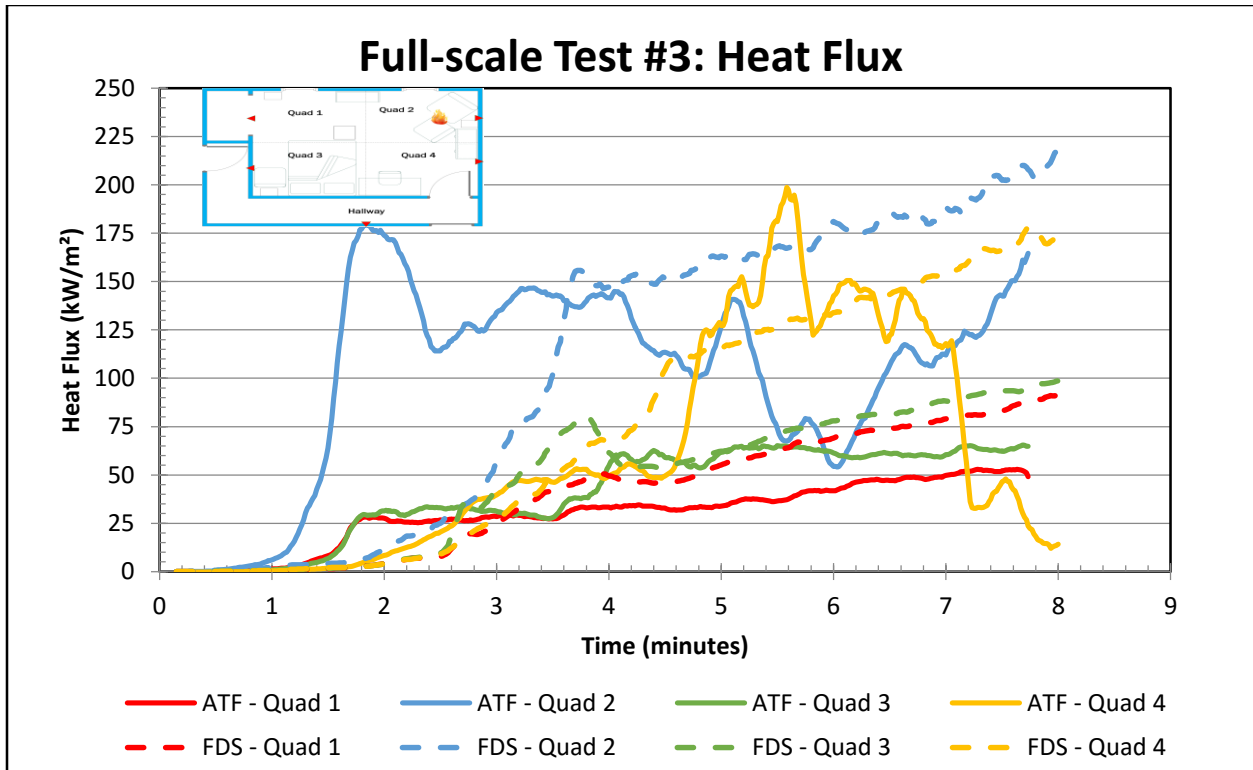
Figure 34: Full Scale Test 3 Heat Flux Data

5.3.3.3 Velocity

The graph below shows bi-directional velocity probe data at the doorway of the bedroom during the fire test. Before the ATF reached transition at around 5.5 minutes, both the ATF and FDS velocity probes recorded similar fluid flow data. However, once the ATF test reached its transition phase, the top two velocity probes dipped and recorded negative values. This brief switch in flow direction indicates that a significant amount of air was being drawn into the room, which could indicate the transition to flashover. Despite the FDS simulation reaching this transition phase, this drastic reversal of fluid flow was not seen.
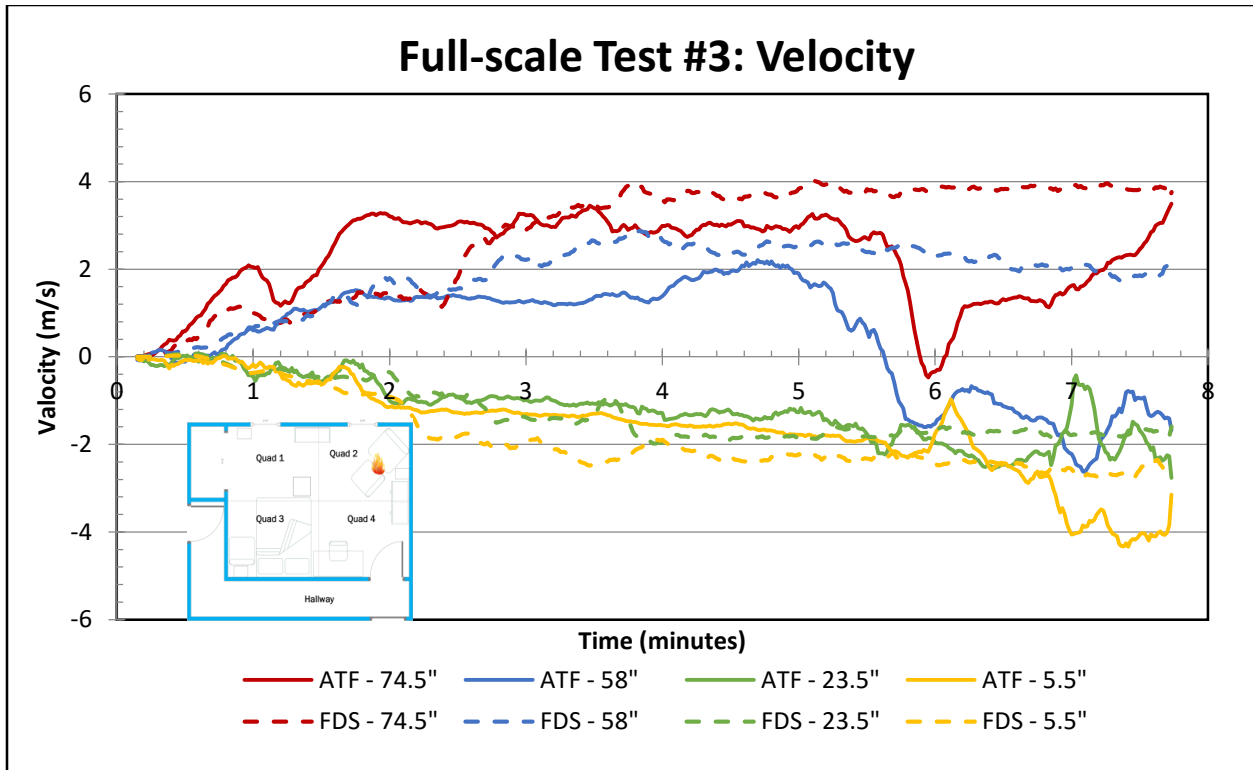
Figure 35: Full Scale Test 3 Velocity Data

5.3.4 Test 4

Table 16 below displays a timeline of the FDS simulation throughout the duration of the fire. Recalling from chapter 4, the fire began in the center of the room between the mattress and second beanbag. The fire spreads across the mattress and ignites the desk and other beanbag. Post-transition, the fire is located near the ventilation openings. Although there is no fire present in quadrant 3 post-transition, the mattress continues to burn away almost entirely. Table 17 displays a timeline of notable events that affected the dynamics of the fire. Of particular interest were the times when the windows broke, introducing more oxygen into the compartment. Most of the events shown in the Table 17 occur roughly 2 minutes earlier in the FDS model than in the ATF tests. Figure 36 displays the instantaneous HRR calculated by FDS. The model reaches a peak HRR of approximately 6.9 MW roughly 8.5 minutes into the simulation. After this point, the fire reaches steady state burning since it is ventilation controlled.

FDS Full-scale Test 4 Smokeview Timeline		
1 minute	2 minutes	3 minutes
4 minutes	5 minutes	6 minutes
7 minutes	8 minutes	9 minutes
10 minutes		
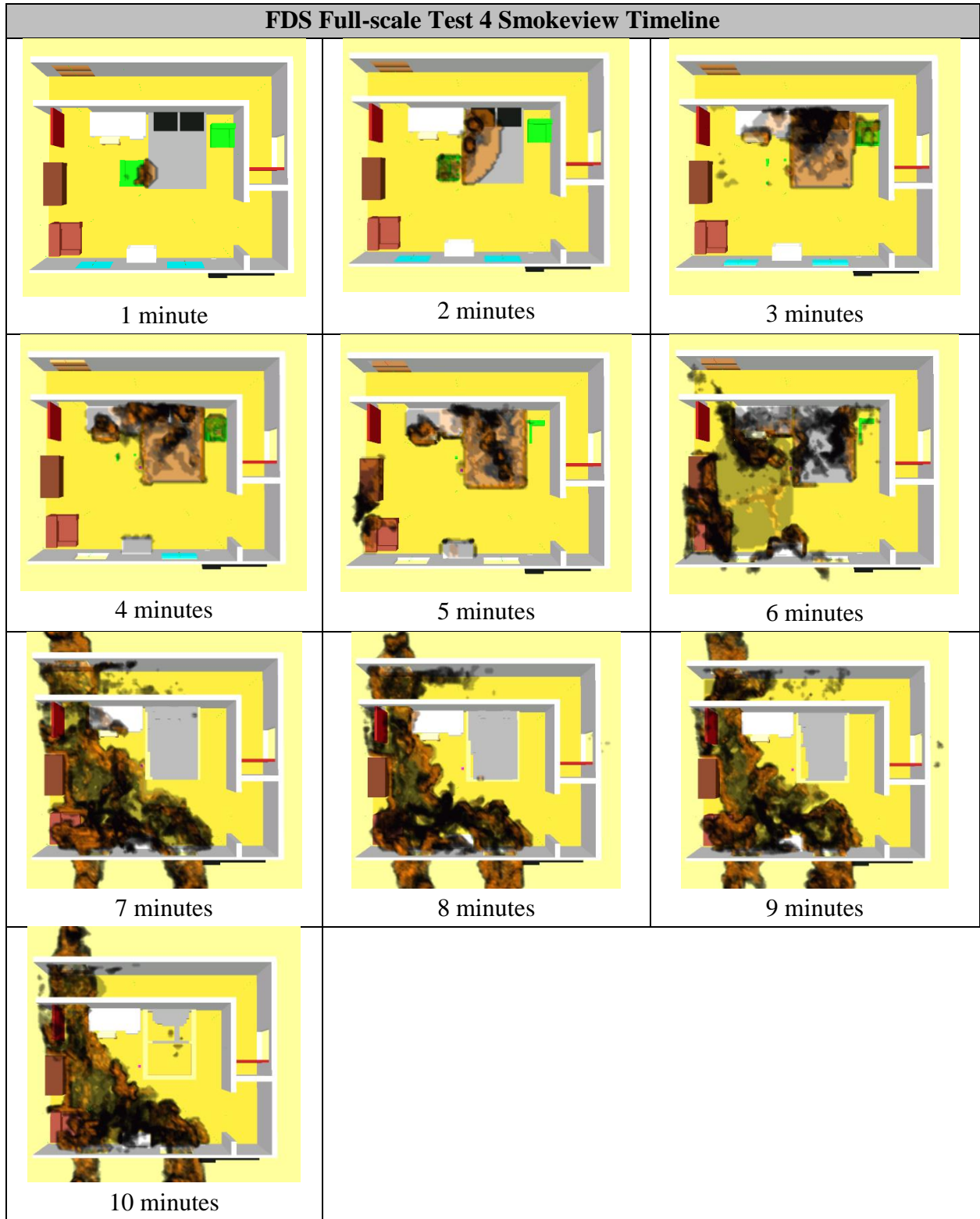
Event	ATF Test 4	FDS Model
Top half of Quad 1 Window breaks	6:30	2:19
Bottom half of Quad 1 Window breaks	7:07	4:13
Flames out Quad 1 Window	6:45	6:00
Top half of Quad 2 Window breaks	5:21	2:40
Bottom half of Quad 2 Window breaks	7:21	3:08
Flames out Quad 2 Window	7:20	5:19
Transition	7:46	5:41
Suppression	9:51	N/A
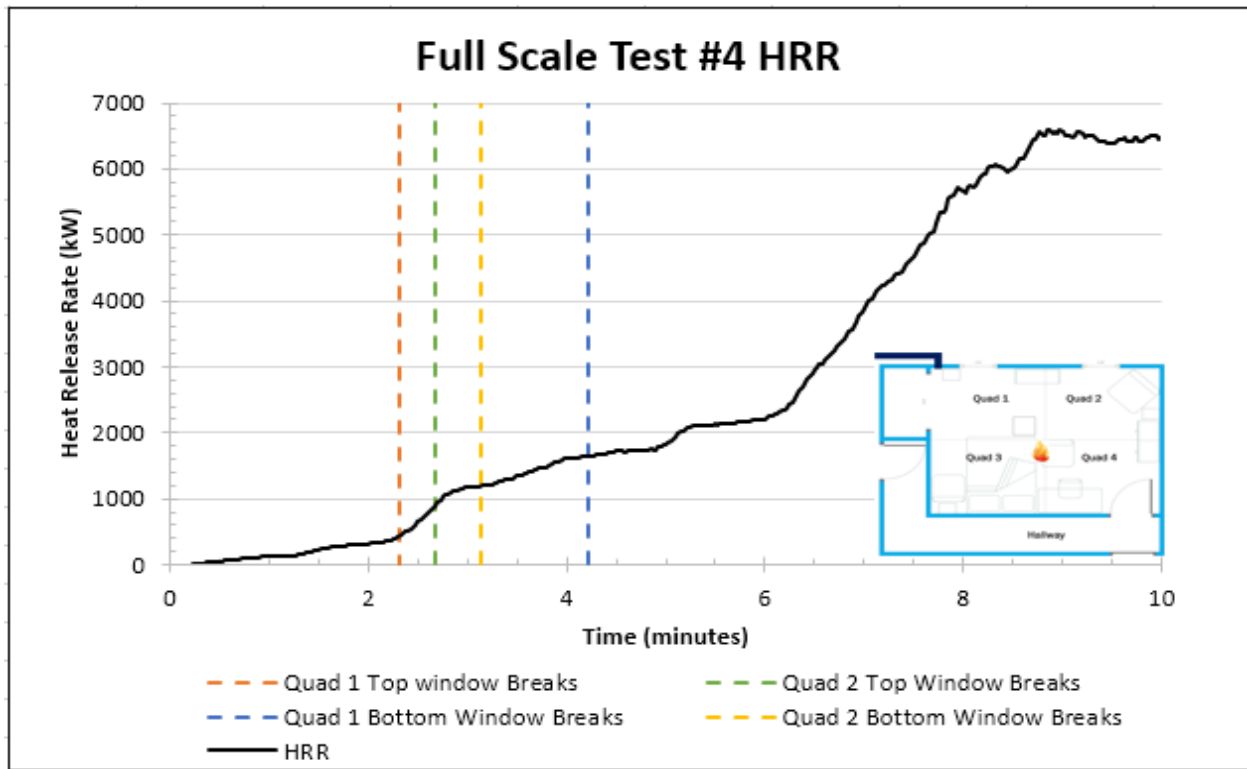
Figure 36: FDS Full-scale Test 4 HRR

5.3.4.1 Temperature

Figure 37Figure 40 display comparisons of the thermocouple results in each of the quadrants within the compartment. The simulated results agree reasonably with the measured results. In each quadrant, the peak temperatures between the simulated and measured is within 200ºC. As mentioned above, the windows and door failed roughly 2 minutes earlier in the FDS simulations than in the ATF tests. This trend correlated with the spikes in temperature in each of the four quadrants. The thermocouples located at 4 and 6 feet above the floor in the simulations record higher temperatures on average throughout each of the quadrants. The thermocouples located 2 feet above the floor in the FDS simulations generally record lower temperatures for the first 6 minutes than those in the ATF experiments. At that point, the FDS simulations transition to flashover and the temperatures recorded by those thermocouples exceed the temperatures recorded in the ATF tests.
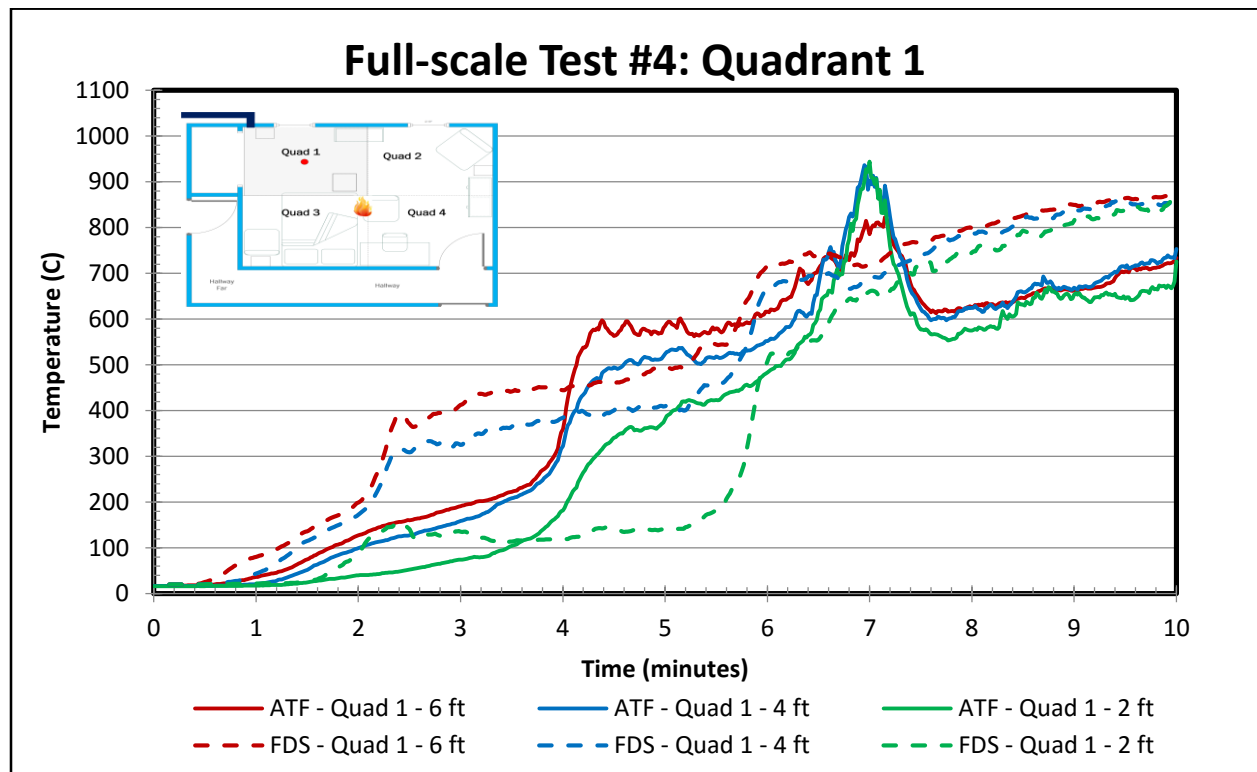
Figure 37: Full-scale Test 4 Thermocouple Data - Quadrant 1
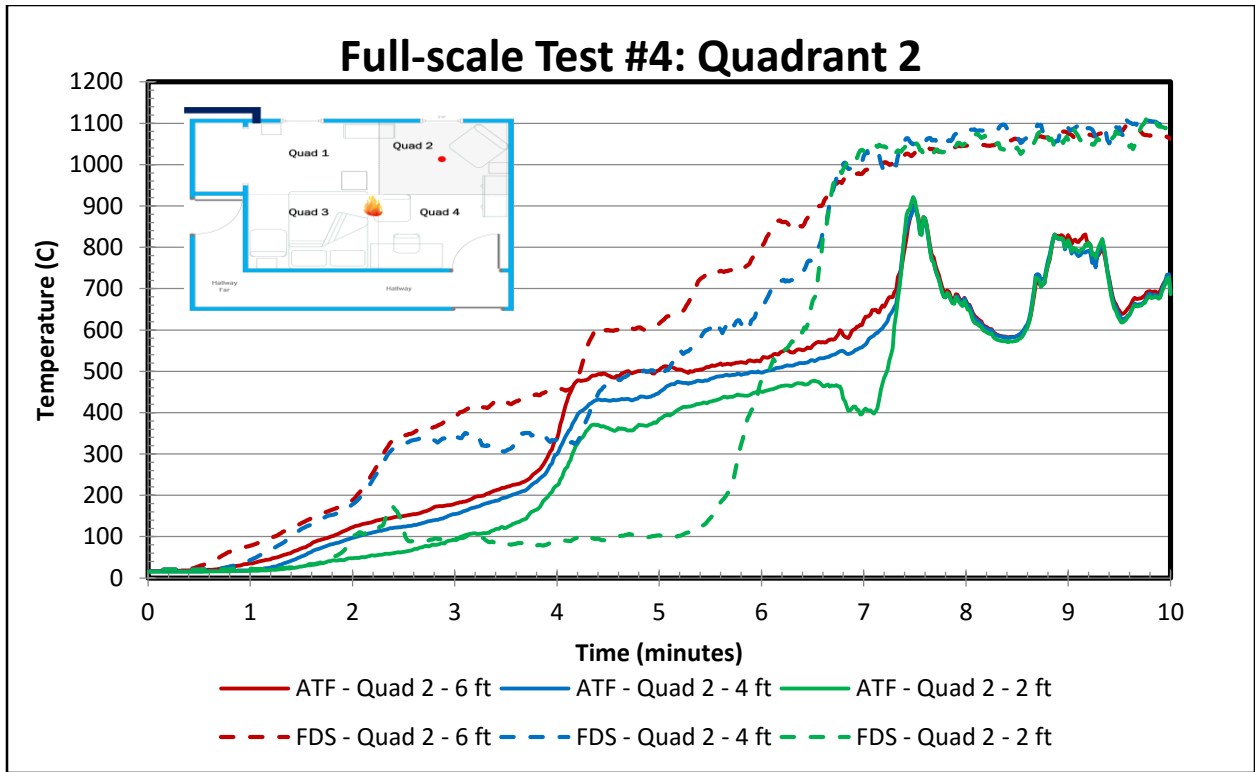
Figure 38: Full-scale Test 4 Thermocouple Data - Quadrant 2
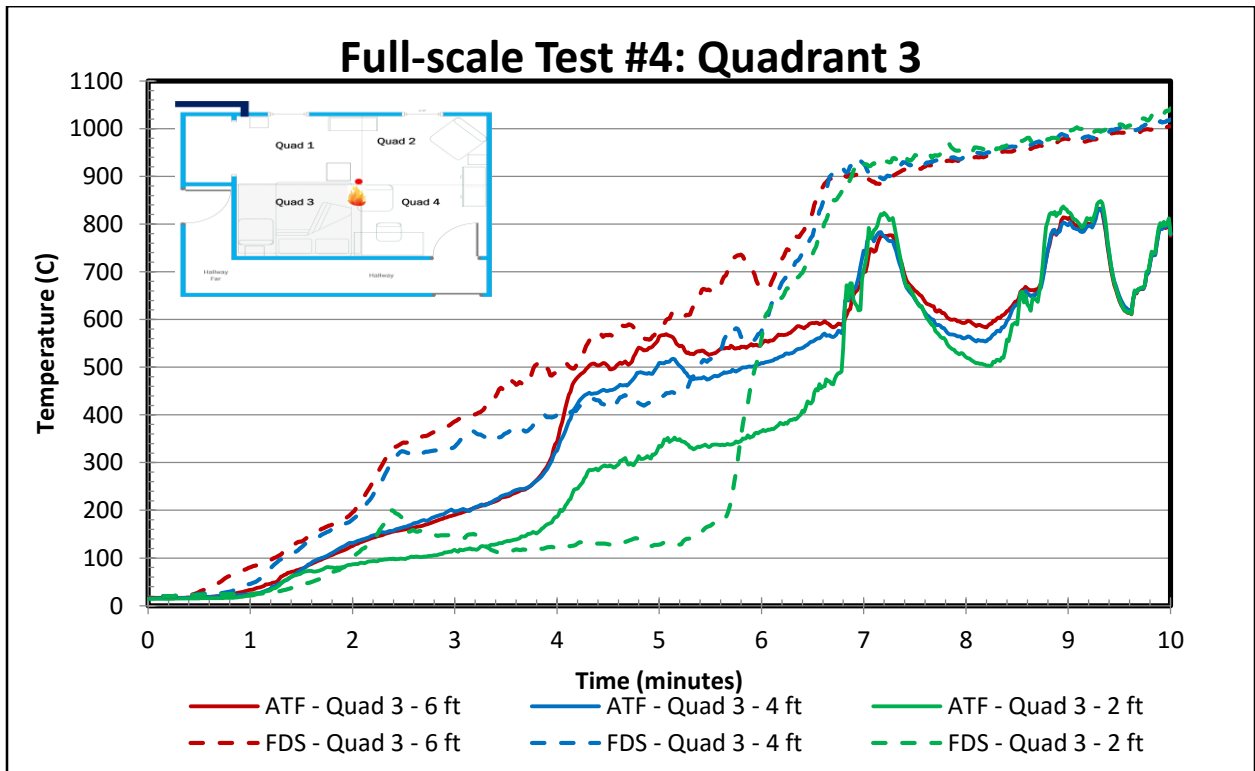
Figure 39: Full-scale Test 4 Thermocouple Data - Quadrant 3

59
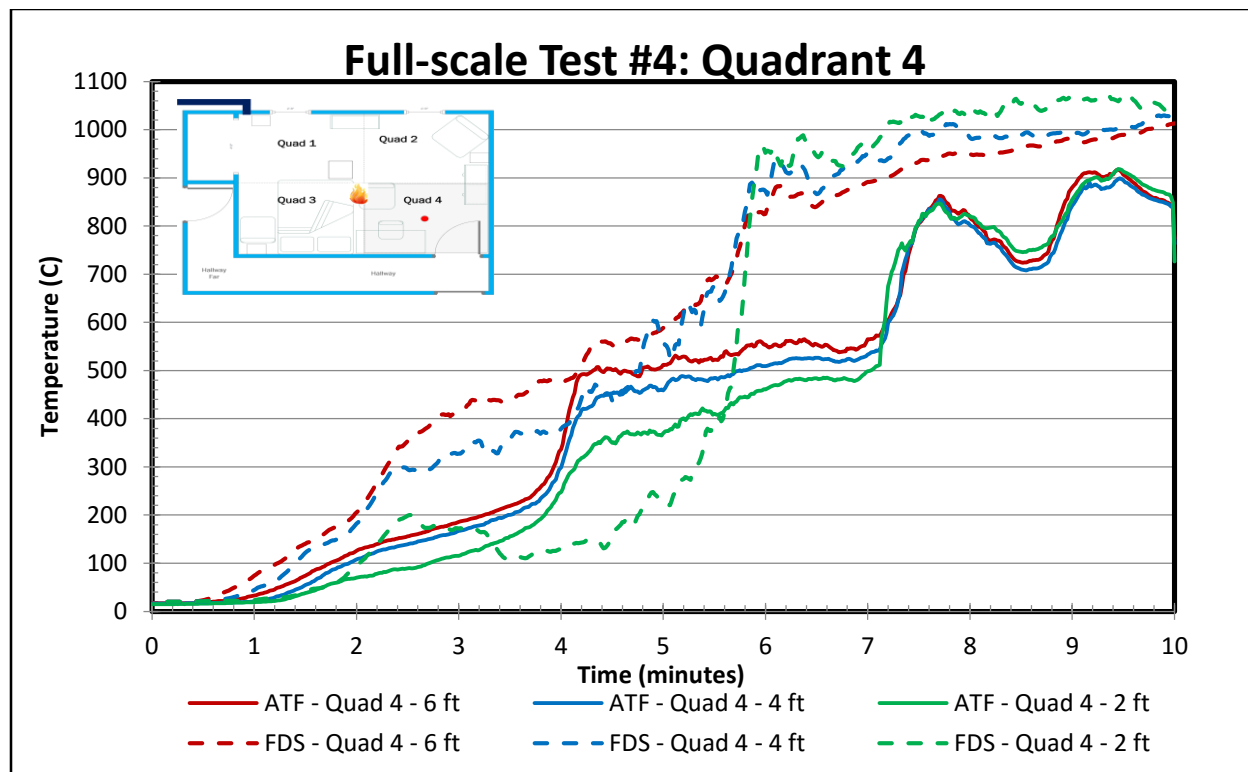
Figure 40: Full-scale Test 4 Thermocouple Data - Quadrant 4

5.3.4.2 Heat Flux

Figure 41 below displays a comparison of the heat flux measurements between the ATF test and FDS model. The data in the FDS model does follow trends similar to those present in the ATF tests. The magnitude of the heat flux between the FDS model and ATF test is very similar in quadrants 1 and 4.

The magnitude of the heat flux, however, differs in quadrants 2 and 3. In quadrant 2, the heat flux calculated is roughly 100 kW/m² greater than that in the ATF test once both tests reach transition. The heat flux in quadrant 3 in the ATF test is much greater than that in the FDS model during the 4-6 minute period. This is most likely because of the flame spread within the compartment. The windows in the FDS model, as stated previously in this section, open earlier than the windows in the ATF test. Therefore, the fire was able to spread toward the ventilation openings and away from the mattress (located in quadrant 3). In the ATF test, the fire was not able to spread that and, therefore, the mattress remained a large component of the fire for a longer period.
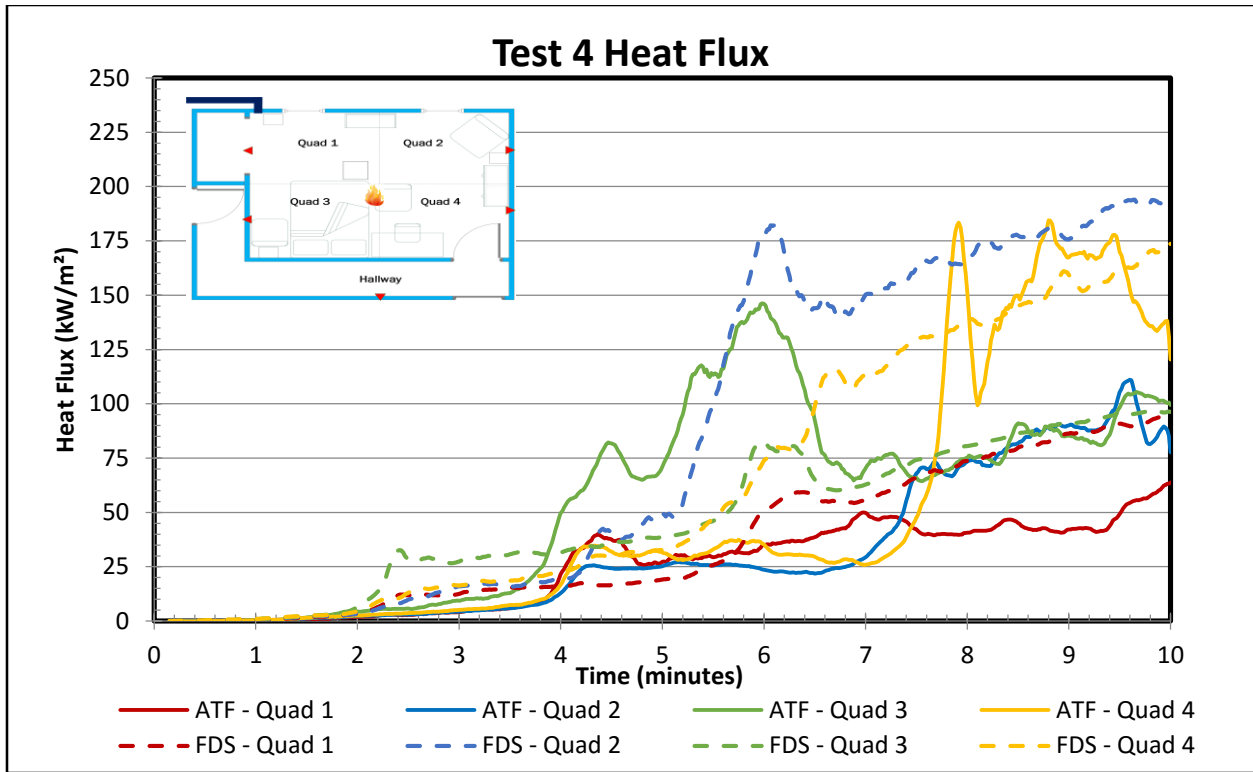
Figure 41: Full-scale Test 4 Heat Flux Data

5.3.4.3 Velocity

Figure 42 below displays a comparison of the velocity measurements at different heights at the bedroom door. The simulated velocity data shows very agreeable measurements until the ATF test reaches transition. After that point, the velocities recorded in the ATF test begin to decrease. The velocity probe at 58", which recorded positive velocities to that point, recorded negative values for a period of time after transition. This means that air was flowing into the room at that height. The lower probes also record velocities that are greater magnitude flowing into the room. This indicates that the doors were acting as the main supply of fresh air post-transition, while the windows were acting as an exhaust for the hot gases.

61
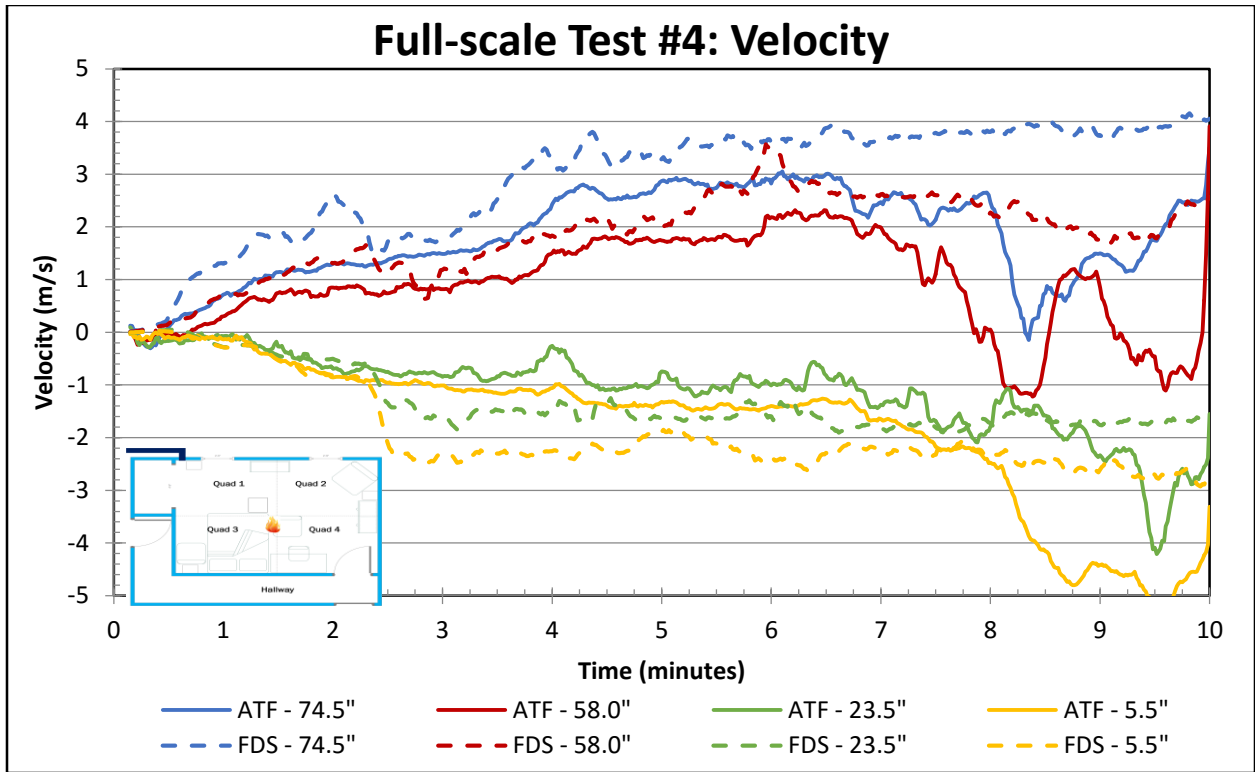
Figure 42: Full-scale Test 4 Velocity Data

6 Damage Analysis

In order to provide some insight on how the resulting damage observed by the ATF were formed an analysis of the full-scale models were performed using features such as slice files, boundary files and vector files. Specifically, we focused on area of fire origin and areas where ventilation may have been a factor in post-flashover conditions such as windows and door ways. A common representation of the damages caused by fire is a clean burn area, which is characterized by areas where soot has burnt away from the surface of the material due to high heat exposures.

6.1 Exterior Window Wall

In the process of performing a damage assessment, the ATF observed that regardless of fire origin location, the quadrant 2 window to the left in Figure 43 showed more significant damage on its surrounding exterior than the quadrant 1 window which is on the right side of Figure 43. Damages such as this occur because of intense heat fluxes over a duration of time.

Figure 43: Exterior Window Wall Damages

The FDS simulations also show this damage through a time-lapse of the heat flux boundary files rendered from Smokeview as shown in Table 18 since FDS cannot display nor calculate cumulative heat flux to surfaces. The simulations also provide insight on the formation of these damages. Table 19 displays the temperature slice file along the windows showing the temperature gradient of the exhausting gases for each model; all of which show that the quadrant 2 window has a hotter upper gas layer than the quadrant 1 window. This suggests that because

the quadrant 2 window is directly across the bedroom entry door, the incoming fresh air immediately reacts with the fire forcing the hot gases and flames out of the exhausting quadrant 2 window. The temperature slice file also shows that these gases can reach temperatures over 1000°C, exposing the exterior side of the wall to a significant heat flux that is a key factor in forming areas of demarcation. The temperature vector files going through both windows, as shown in Table 20, also confirms that the exiting gases of the quadrant 2 window are hotter than those of the quadrant 1 window. This is shown as the quadrant 2 window gases are red, indicating the highest temperature recorded when the quadrant 1 window gases are yellow, representative of a lower temperature.

Table 18: Exterior Window Wall Heat Flux Boundary File Time-Lapse
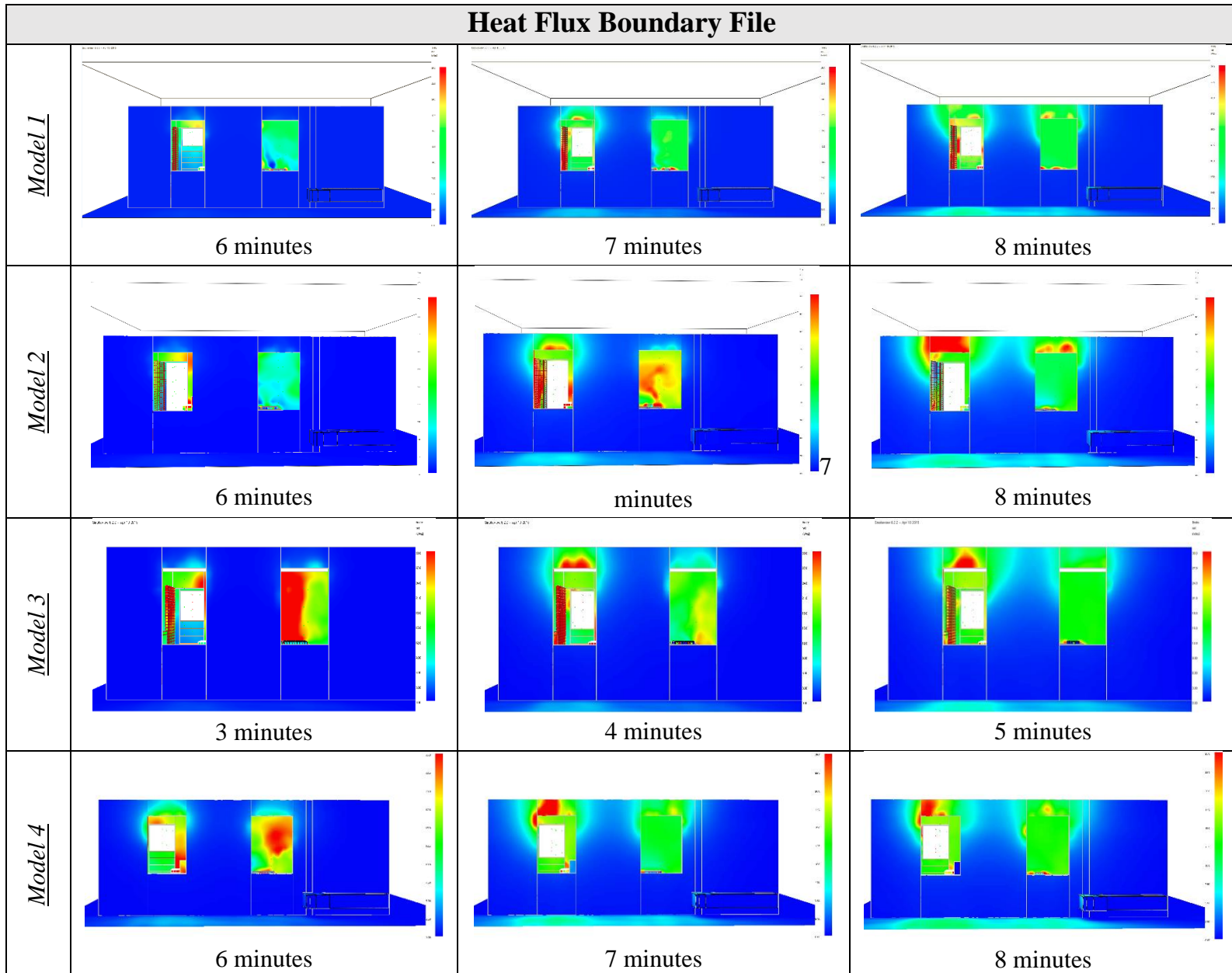
	Heat Flux Boundary File		
Model 1	6 minutes	7 minutes	8 minutes
Model 2	6 minutes	7 minutes	8 minutes
Model 3	3 minutes	4 minutes	5 minutes
Model 4	6 minutes	7 minutes	8 minutes

Temperature Slice File

Model 1	6 minutes	7 minutes	8 minutes
Model 2	6 minutes	7 minutes	8 minutes
Model 3	3 minutes	4 minutes	5 minutes
Model 4	6 minutes	7 minutes	8 minutes

65
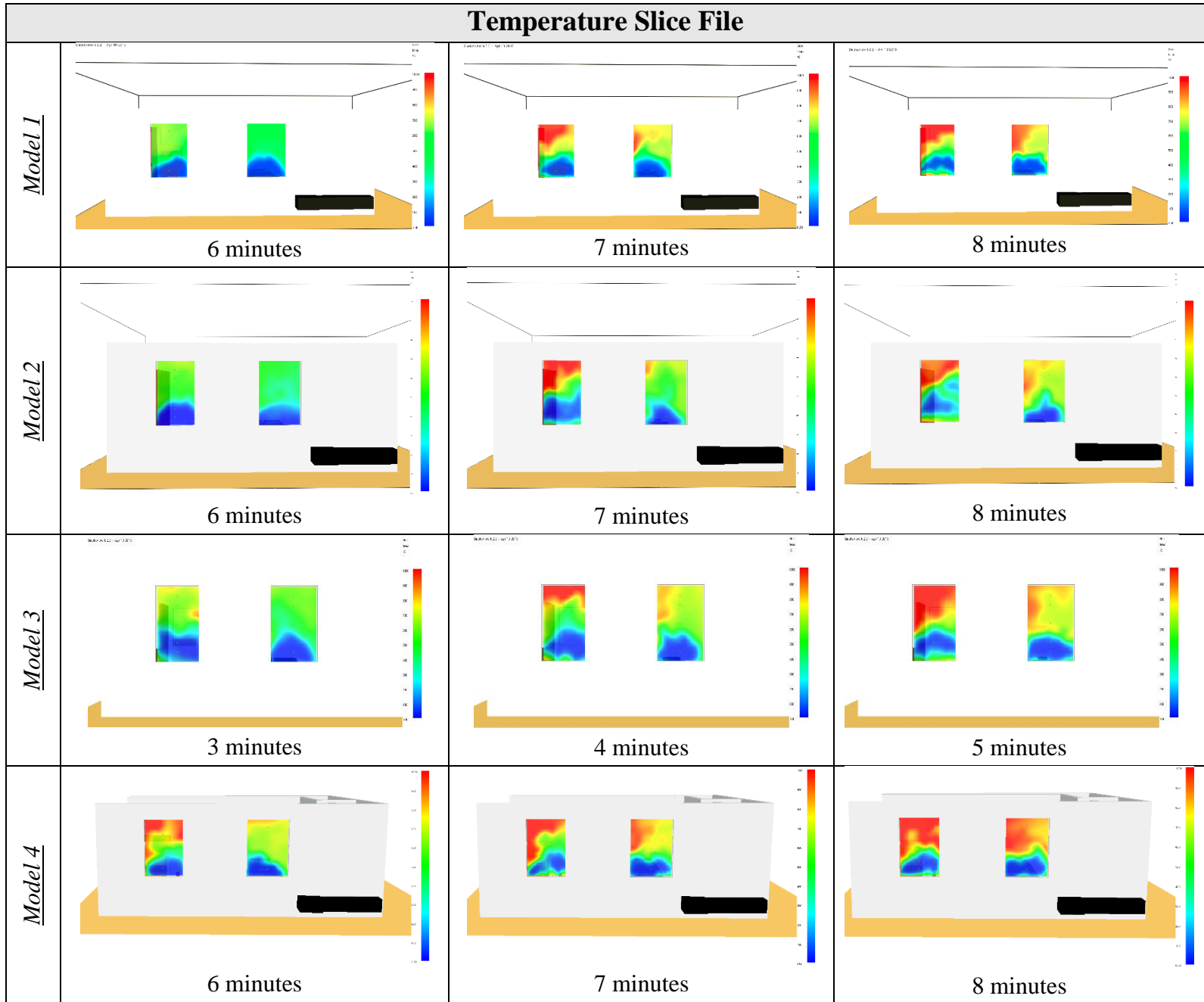
Temperature Vector-Slice File		
Model 1 6 minutes	7 minutes	8 minutes
Model 2 6 minutes	7 minutes	8 minutes
Model 3 3 minutes	4 minutes	5 minutes
Model 4 6 minutes	7 minutes	8 minutes
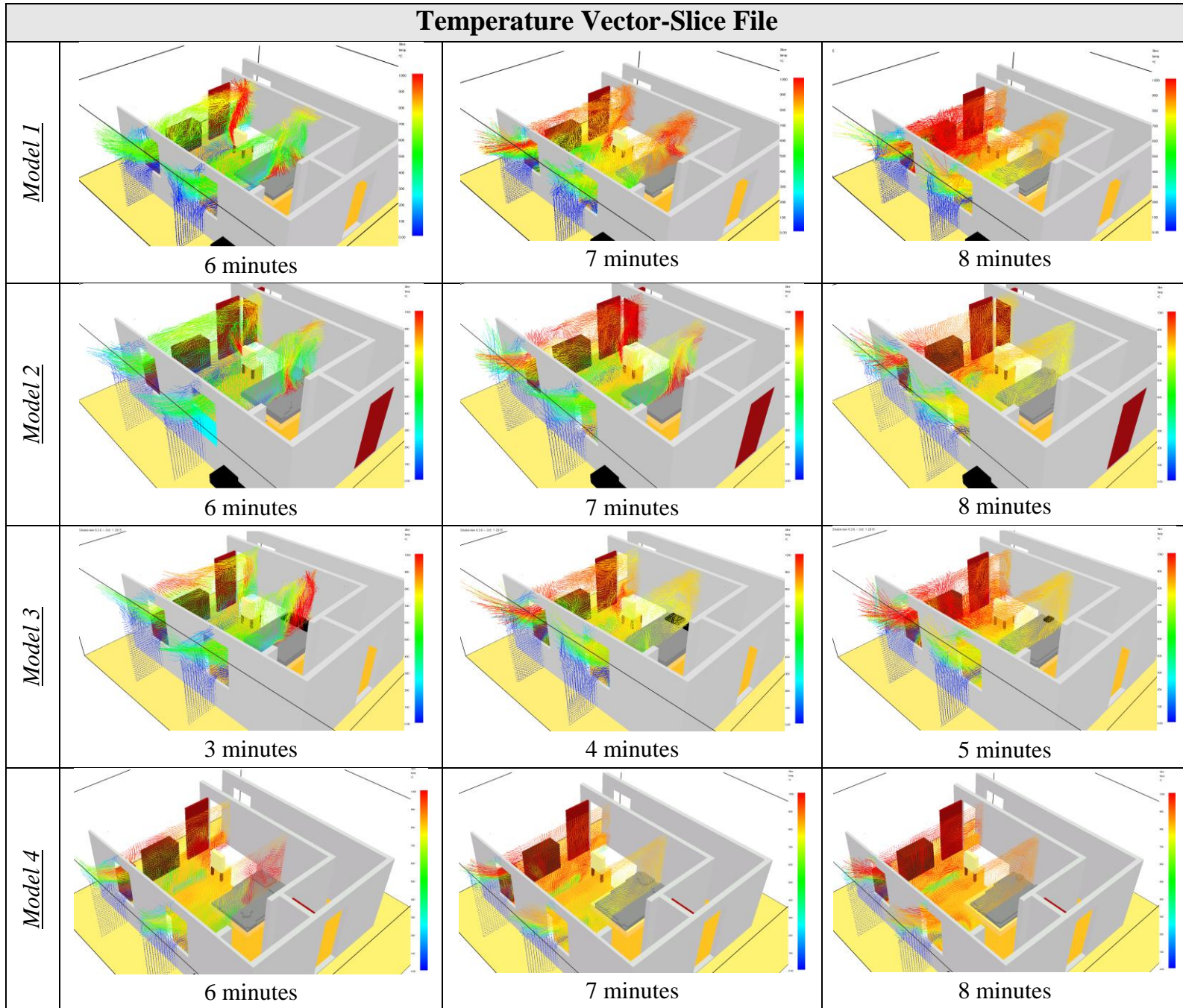
6.2 Interior Window Wall

Figure 44 below displays the back wall in each of the four ATF tests. This area was chosen as it displays different clean burn patterns as the initial ventilation conditions and fire origins change. Test 1 experienced the least amount of damage to the back wall. The most observable clean burns are seen around the quadrant 2 window and along the top of the wall. On the other hand, test 2, which had the same fire origin, contains clean burn damages all along the wall past the quadrant 1 window. This difference may be due to the initial ventilation difference as air was allowed to flow more freely into the room through the bedroom door in test 2.

Test 3 displays a v-shaped pattern coming from the corner of the room as the fire originated in the quadrant 2 corner. This test does not display much of a clean burn past the quadrant 2 window. Test 4, similar to test 2, contains clean burn damage along the wall up to the quadrant 1 window. This may be due to an earlier ignition of the bookcase as the fire originated in the center of the compartment.

Figure 44: Interior Window Wall Damages

Table 21 below displays the FDS simulations two minutes prior to the maximum HRR calculated. The pictures display boundary files that measure the net heat flux at the specified time steps. The simulations for tests 1 and 2 are very similar in their growth; therefore, they do

67

not provide many differences on the back wall of the compartment. The heat flux file for test 2 does begin to resemble the conditions seen at the end of the ATF test.

Test 3 displays the most significant damage in the corner directly above the upholstered chair. The heat flux exposure does not extend past the quadrant 2 window for a long period of time, explaining the lack of clean burn damage near the quadrant 1 window. The boundary files displayed for test 4 do seem to coincide with the damages viewed at the end of the ATF test. The time steps display significant exposure beginning in the quadrant 2 corner and extending to the quadrant 1 window.

Table 21: Interior Window Wall Heat Flux Boundary File Time-Lapse

	Heat Flux Boundary File		
Model 1	5 minutes	6 minutes	7 minutes
Model 2	5 minutes	6 minutes	7 minutes
Model 3	3 minutes	4 minutes	5 minutes
Model 4	6 minutes	7 minutes	8 minutes
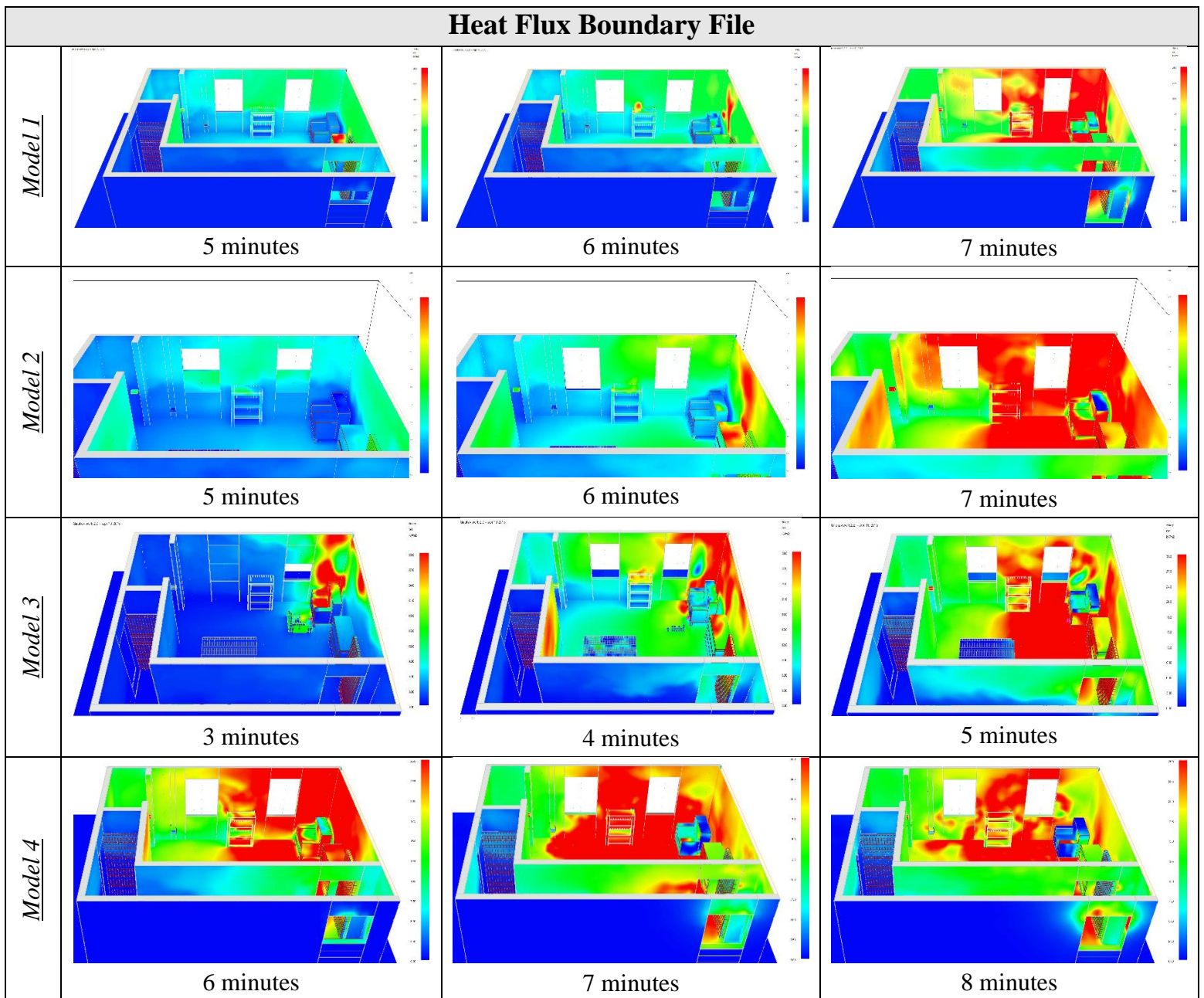
6.3 Quadrant 2: Corner Area

Quadrant 2 was the area of origin for the third ATF full-scale test. The ignition source was a beanbag chair placed next the upholstered chair in the corner of the quadrant. As seen in Figure 45 below, the upholstered chair in the corner of test 3 was completely consumed by the fire. However, in the other three ATF scenarios, the upholstered chair was still visible at the conclusion of the test. In addition, a more prominent V-shape clean burn pattern is visible on the walls in the third test. These observations were a result of the third test having a longer exposure duration since the fire originated in that quadrant. It was also observed that the second ATF test produced clean burns around the corner despite the fire originating in the third quadrant. This may have been caused by the front door of this test being initially open and directly opposite of the quadrant 2 window allowing the air to push flames towards this corner.

As for the FDS simulations, heat-flux boundary file snapshots were taken at 1.5, 2, and 2.5 minutes (Table 22) to show exposure intensity during the initial growth stages of the fire. It was anticipated to observe more heat flux exposure to the quadrant 2 corner wall for full-scale model 3 because initial ignition occurred in that area. In addition, the pattern of heat flux resembles the V-shape damage pattern observed in the ATF post incident photos. In the other the full-scale models, the heat flux exposures to the quadrant 2 corner were due to the heat of the hot gases radiating from the fuel package at a different location. Since the fire in these models had to spread to the upholstered chair in time, the V-shape burn patterns were not as prominent as the pattern observed in model 3.

Figure 45: Quadrant 2 Corner Wall Damages

Heat Flux Boundary File

	1.5 minutes	2 minutes	2.5 minutes
Model 1			
Model 2			
Model 3			
Model 4			
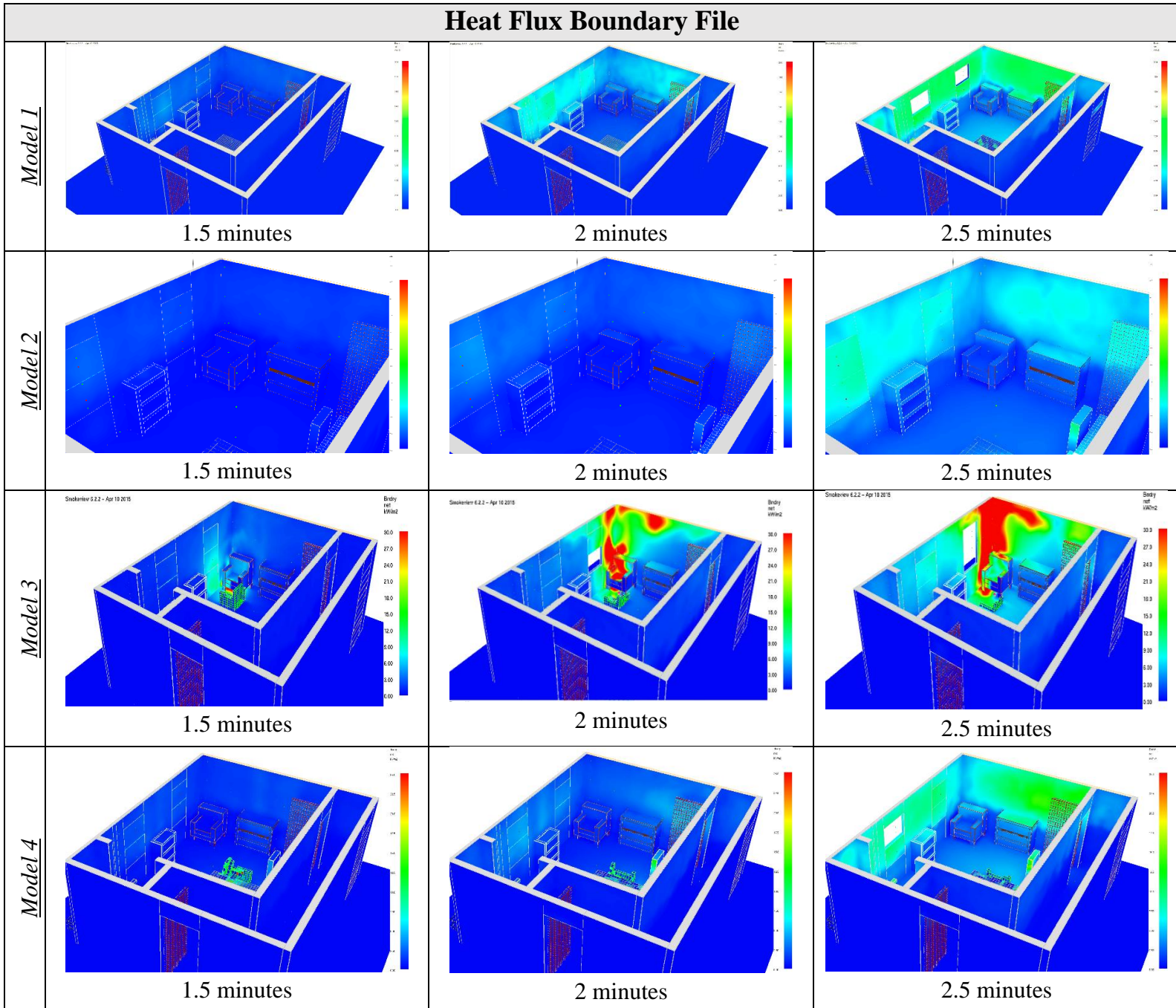
6.4 Quadrant 3: Mattress

Figure 46 below displays the mattress in each of the four ATF tests after suppression. The ATF manually suppressed each fire roughly 2 minutes after the fires transitioned to flashover. The mattress was an integral factor in the growth of the fire in tests 1, 2, and 4 as the fire began adjacent to it. The ignition source was located in the same area in ATF tests 1 and 2. Therefore, it is expected that the damage to the mattress is similar in those two tests because the fire should spread similarly across the mattress, leaving similar burn patterns. It is difficult to make a direct comparison as a ceiling tile fell on the bed in test 2; however, both tests do seem to have more damage to the right side of the bed. This is consistent with what is expected as the fire began on that side.

Test 3 served as the only test in which the fire origin was not adjacent to the mattress; therefore, damage to the mattress in this test would be expected to be influenced by the ventilation conditions. The mattress in this test contains significant burning along the left side of the bed closest to the door. The foot of the bed also contains areas that are completely burnt through as this area is closest to the windows.

Test 4 displays the most damage to the mattress of the four ATF tests. The ignition location in this test, as displayed in the Figure 46, is at the left side of the mattress. Suppression in this test occurred roughly 2 minutes later than in the other tests as this test transitioned to flashover later than the other three tests. This may account for the increased amount of damage.
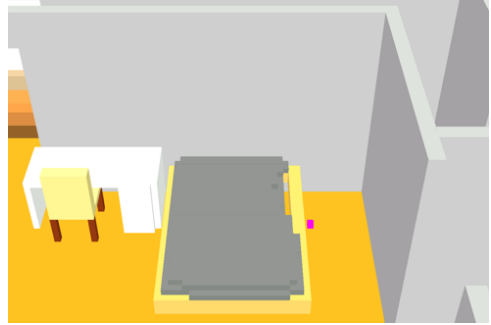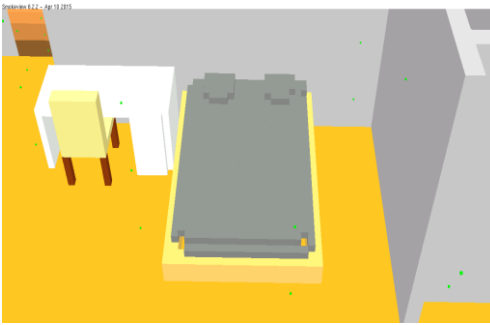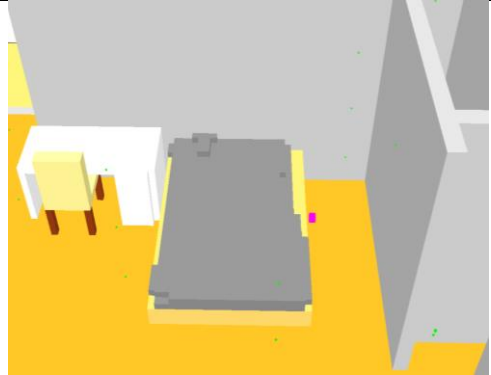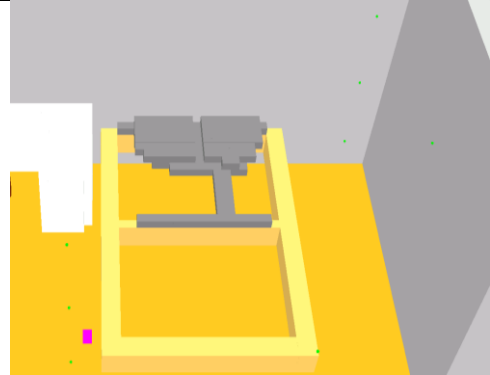
Figure 46: ATF Mattress Damage Comparison

Table 23 below displays the FDS mattress in each of the four tests at the time of suppression. The BURN_AWAY function was used on the mattress; therefore, damage is characterized by a lack of material in the simulations (i.e. no material remaining equated to significant damage). At the end of the simulations, the mattress in tests 1 and 2 display more damage on the right side of the bed, closer to the fire origin. This is consistent with the damage that was observed in the ATF tests.

Test 3 displayed more damage on the left side of the mattress, nearest the ventilation openings. Because the mattress was not a part of the initial growth phase, the bed did not ignite until the fire transitioned to flashover. Therefore, the mattress in test 3 succumbed to damages mainly in the post-flashover environment; most of the damages in this test are near the foot of the bed, closest to the ventilation openings.

The damages in test 4 are very similar to those displayed in the ATF test. Almost all of the ignitable material has burned away at the end of the simulation. The only area where the mattress remains is at the head of the bed nearest the corner of the compartment. This area is farthest from the ventilation openings and, therefore, would not be exposed to the heat those areas.

Table 23: FDS Mattress Damage Comparison

Mattress Damage		
Model 1	 8.5 minutes	Model 3	 8 minutes
Model 2	 8 minutes	Model 4	 10 minutes

6.5 Quadrant 3: Corner Area

The corner of quadrant 3 is an area of interest because it was the origin of fire for test 1 and test 2. As seen from the Figure 47 below, tests 1 and 2 show clean burn damage on the walls of quadrant 3. In tests 3 and 4, where the origin of fire was located away from the wall, the similar fire damage was not seen. The V-shape pattern, formed by the fire plume, is only visible where the origin of fire was located.

Figure 47: Quadrant 3 Corner Wall Damages

Table 24 below shows the exposure intensity of the quadrant 3 corner in all four FDS models. To show which FDS model experienced significant cumulative exposure in the quadrant 3 corner, it was necessary to show the heat flux boundary file at the growth stage of every model which is approximately at 1.5 minutes to 2.5 minutes. As seen from models 1 and 2, there is earlier heat flux exposure to the walls of the corner than in models 3 and 4 resulting in more fire damage. This was anticipated once more since heat flux exposure is intense in areas of initial ignition. Although model 4 shows more heat flux exposure than model 2 at 2.5 minutes, the quadrant 3 corner in model 2 was exposed to intense heat flux at the beginning of the simulation.

Heat Flux Boundary File

Model 1	1.5 minutes	2 minutes	2.5 minutes
Model 2	1.5 minutes	2 minutes	2.5 minutes
Model 3	1.5 minutes	2 minutes	2.5 minutes
Model 4	1.5 minutes	2 minutes	2.5 minutes
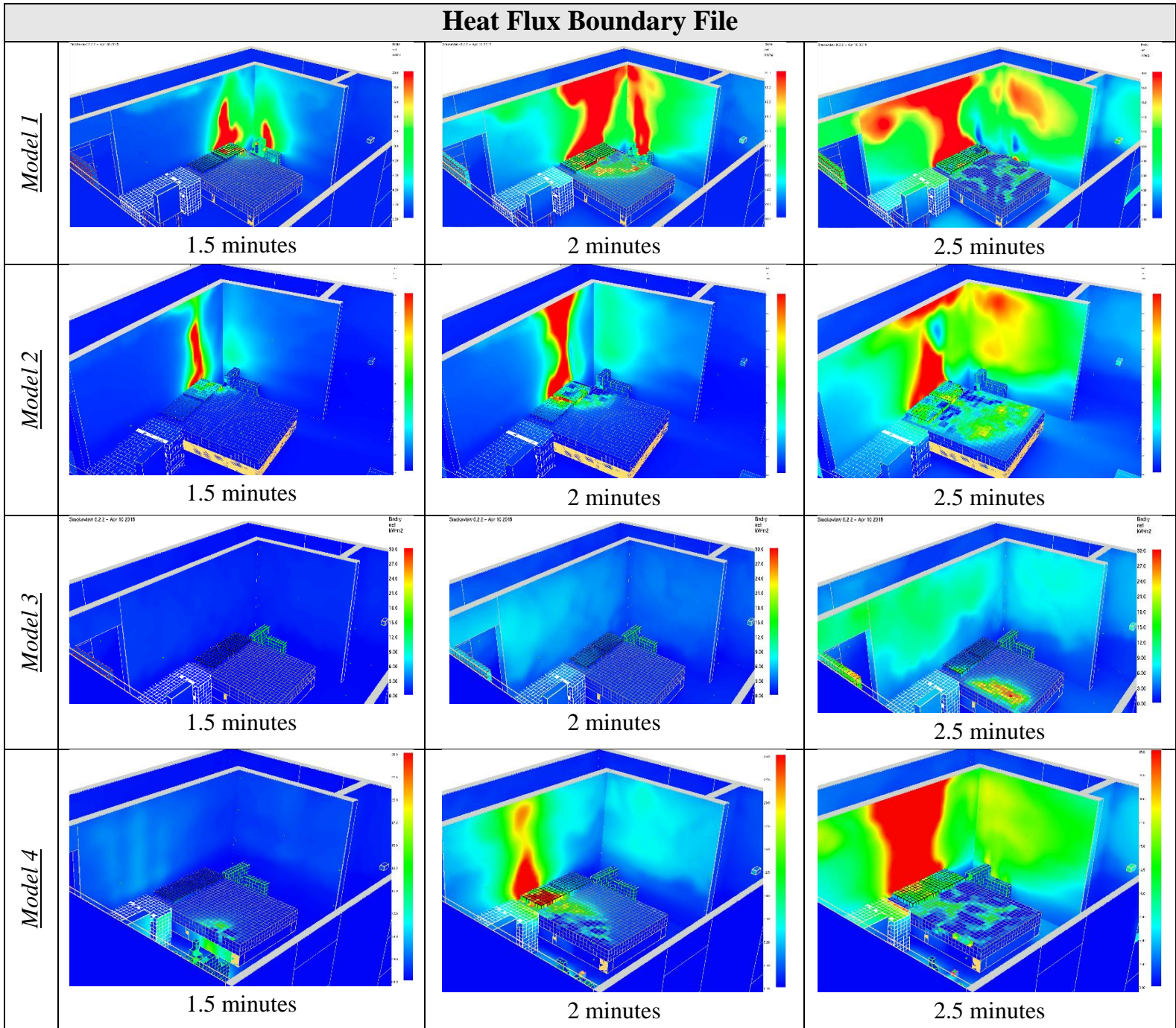
7 Conclusions

FDS was used to simulate a series of four compartment fire tests conducted by ATF to provide further insight on how changing the fire location or initial ventilation conditions affects fire growth, spread, and resulting damage. The analysis of the results calculated by FDS determined that FDS could replicate the tests to a certain degree. In particular, the velocity profiles were shown to be the most accurate results because FDS puts emphasis on thermally-driven flow such as smoke transport. Similar trends and magnitude were also identified when comparing the temperature results between the FDS simulations and ATF tests. From the FDS results, ventilation was identified to be a key factor in fire growth as characterized by heat release rates (HRR). Since the HRR for the overall compartment fire tests was not measured by the ATF, FDS was able to provide this data through mathematical calculations. A relationship between the effects of dynamic ventilation and HRR was identified such that when a window failed, the HRR increased contributing to fire growth leading to the transition of flashover. In the post flashover environment for all four FDS simulations, flaming combustion was observed only in areas proximate to oxygen supplying vents such as windows and the outside door. This same observation was made by ATF in their tests regardless of where the initial ignition was located, flaming fire conditions existed only in areas of ventilation openings during the post-flashover environment. Through the FDS simulations, the provided relationships between the resulting fire conditions, the area of origin and changing ventilation conditions helped inform the scope by which FDS could be used as tool to provide further insight to fire investigators in better understanding a fire scene and the range of conditions that caused the resulting fire damage.

7.1 Future Work

Despite the reasonable agreement in overall magnitude and similar trends with the results and analysis between the FDS simulations and the ATF tests, this project has identified certain areas with room for improvement. The resulting damage of certain fuel packages caused by fire conditions may provide more insight on identifying area of origin. To do so, utilizing the burn away function in FDS would allow assessing and analyzing of cumulative damage to a certain fuel package. Due to the complexity and uncertainty of the exact material properties of the fuel packages used for this project, it was difficult to obtain a desired HRR while using the burn away function. Given more time, further examination of the materials used in the fuel packages could lead to better characterization of the material properties. Therefore, future work should consider the following:

1. Obtain the actual materials of the fuel packages used in the ATF tests to perform small-scale bench tests using the cone calorimeter to gather data or information of the fuel packages such as:
    a. Effective heat of combustion
    b. Ignitibility (Critical heat flux to ignition)
    c. Smoke and soot production

2. Using the cone calorimeter test data, derive material properties such as:
    a. Ignition temperature
    b. Thermal properties (specific heat c_p, thermal conductivity k, density ρ)

In addition, a better characterization of the thermal properties could allow for a more accurate prediction of flame spread. The numerical flame spread for the FDS models relied upon user specified material properties as they influenced how cells, in this case those that represent the surface of a fuel, absorb energy and heat up. The cell then mathematically ignited when it reached the user specified ignition temperature.

Bibliography

[1]   National Fire Protection Association , NFPA 921: Guide for Fire and Explosion Investigations, Quincy, MA, 2014.

[2]   A. Cox, "Origin Matrix Analysis: A Systematic Methodology for the Assessment and Interpretation of Compartment Fire Damage.," Journal of the International Association of Arson Investigators, 2013.

[3]   U.S. Department of Justice, "Arson," [Online]. Available: https://www.atf.gov/arson. [Accessed 12 December 2015].

[4]   A. E. Cote, *Fire Protection Handbook 20th Edition,* Quincy, Massachusetts: National Fire Protection Association, 2008.

[5]   H.-J. Kim and D. G. Lilley, "Heat Release Rates of Burning Items in Fires," American Institute of Aeronautics & Astronautics, Reno, 2000.

[6]   K. McGrattan and F. Glenn, "Fire Dynamics Simulator (Version 6) - User's Guide," National Institute of Standard and Technology, 2015.

[7]   G. P. Forney, "Smokeview, A Tool for Visualizing Fire Dynamics Simulation Data Volume I: User's Guide," National Institute of Standards and Technology, 2015.

[8]   C. G. Weinschenk, K. J. Overholt and D. Madrzykowski, "Simulation of an Attic Fire Wood Frame Residential Structure," National Institute of Standards and Technology (NIST), Chicago, 2014.

[9]   K. McGrattan, S. Hostikka, R. McDermott, J. Floyd, C. Weinschenk and K. Overholt, Fire Dynamics Simulator, Technical Reference Guide, vol. 1 Mathematical Model, National Insitute of Standards and Technology, 2015.

[10] K. McGrattan, S. Hostikka, R. McDermott, J. Floyd, C. Weinschenk and K. Overholt, Fire Dynamic Simulator, Technical Reference Guide, vol. 2 Verification Guide, National Institute of Standards and Technology, 2015.

[11] EUMEPS, "Behavior of EPS in case of fire," 1998.

[12] SFPE, Guidelines for Substantiating a Fire Model for a Given Application, Bethesda: Society of Fire Protection Engineers, 2011.

[13] U.S. Nuclear Regulatory Commission, "Verification and Validation of Selected Fire Models for Nuclear Power Plant Applications," 2007.

[14] M. J. Hurley, *SFPE Handbook of Fire Protection Engineering,* New York: Springer, 2016.

[15] V. Babrauskas, Ignition Handbook, Issaquah: Fire Science Publishers, 2003.

[16] UMD Fire Protection Engineering Department, *University of Maryland Burning Item Database.*

[17] A. Trouve and T. Minnich, "Thermal Property Database," U.S. Department of Justice, 2012.

[18] W. Grosshandler, N. Bryner, D. Madrzykowski and K. Kuntz, "Report of the Technical Investigation of The Station Nightclub Fire," National Insitute of Standards and Technology (NIST), 2005.

[19] European Manufacturers of EPS , "Behavior of EPS in case of fire," Belgium, 2002.

[20] P. J. DiNenno, D. Drysdale and C. L. Beyler, SFPE Handbook of Fire Protection Engineering, Fourth ed.

[21] G. E. Gorbett, "Development and Assessment of a Decision Support Framework for Enhancing the Forensic Analysis and Interpretation of Fire Patterns," 2015.

[22] M. Tabaddor, "Modeling the Thermal and Structural Behavior of Wood Beams in a Fire Environment," Underwriter's Laboratories, 2013.

[23] Y. He, X. Zhang, M. Yang and J. Wang, "Effects of Computational Domain on Numerical Simulation of Building Fires," *Journal of Fire Protection Engineering,* 2010.

[24] V. Babrauskas, "Glass Breakage in Fires," Fire Science and Technology Inc, 1998.

[25] K. McGrattan, S. Hostikka, R. McDermott, J. Floyd, C. Weinschenk and K. Overholt, Fire Dynamic Simulator, Technical Reference Guide, vol. 3 Validation Guide, National Institute of Standards and Technology, 2015.

[26] V. Babrauskas, "Combustion of Mattresses Exposed to Flaming Ignition Sources Part II. Bench-Scale Tests and Recommended Standard Test," 1981.

[27] Composite Panel Association, "Particleboard," 19 February 2016. [Online]. Available: http://www.compositepanel.org/products/particleboard.html/details/.

[28] NFPA Public Affairs, "All About Fire," 2016. [Online]. Available: http://www.nfpa.org/press-room/reporters-guide-to-fire-and-nfpa/all-about-fire#tri.

Appendix

Appendix A: Fuel Package Set-Ups

Ignition Source

Bean Bag Chair

Mattress in Corner

Upholstered Chair

Desk Chair

Bookcase

Dresser

Desk

Appendix B: Compartment Set-Up

Appendix C: Sensitivity Analysis

Density

The table below shows how varying the density thermal property affected each individual fuel package. There was a low power dependence for each fuel package with the most dependent being the dresser at 3.6%. In regards to the maximum HRR time difference, the upholstered chair experienced the greatest time shift of 244-seconds. Despite this large difference, there was no distinguishable pattern for each fuel package. In conclusion, it was determined that varying the density value resulted in a low max HRR difference and no clear trend in max HRR times.

Density			
Thermal Property	**Input Uncertainty %**	**Power Dependence %**	**Max HRR Time Difference (sec)**
Beanbag	+10%	0.66%	-8 seconds
	-10%	0.2%	-5 seconds
Bookcase	+10%	1.9%	+234 seconds
	-10%	0.5%	-42 seconds
Desk	+10%	3.1%	±0 seconds
	-10%	3.5%	±0 seconds
Desk Chair	+10%	1.10%	-52 seconds
	-10%	1.68%	+86 seconds
Dresser	+10%	2.5%	+78 seconds
	-10%	3.6%	-58 seconds
Mattress	+10%	0.74%	+5 seconds
	-10%	1.03%	+28 seconds
Upholstered Chair	+10%	0.28%	+244 seconds
	-10%	1.01%	-168 seconds

Heat of Combustion

There were three fuel packages in which the heat of combustion was specified. There was a low power dependence for each fuel package with the most dependent being the bookcase at 2.8%. The bookcase also had the greatest time shift of 231 seconds. There was no distinguishable pattern seen between the fuel packages. Varying the heat of combustion resulted in a low HRR difference and no clear trend in max HRR times.

Heat of Combustion			
Thermal Property	**Input Uncertainty %**	**Power Dependence %**	**Max HRR Time Difference (sec)**
Beanbag	+10%	1.8%	+9 seconds
	-10%	1.3%	-10 seconds
Bookcase	+10%	2.8%	-163 seconds
	-10%	1.9%	+231 seconds
Dresser	+10%	1.2%	+49 seconds
	-10%	1.9%	-24 seconds

Ignition Temperature

The table below displays how varying the ignition temperature affected each fuel package. As compared to the other variables, varying the ignition temperature generally produced a higher change in the HRR. The most dependent fuel package was the mattress with a power dependence of 33%. The upholstered chair had the greatest time shift between maximum HRR of 528 seconds. In conclusion, it was determined that varying the ignition temperature resulted in inconsistent HRR differences but consistent max HRR times in terms of trends.

Ignition Temperature			
Thermal Property	**Input Uncertainty %**	**Power Dependence %**	**Max HRR Time Difference (sec)**
Beanbag	+10%	11%	+13 seconds
	-10%	5%	-23 seconds
Bookcase	+10%	18.2%	+246 seconds
	-10%	12.5%	-154 seconds
Desk	+10%	18.0%	±0 seconds
	-10%	12.0%	±0 seconds
Desk Chair	+10%	0.99%	+68 seconds
	-10%	0.37%	+260 seconds
Dresser	+10%	1.7%	+48 seconds
	-10%	1.3%	-30 seconds
Mattress	+10%	33%	+83 seconds
	-10%	8.7%	-53 seconds
Upholstered Chair	+10%	5.80%	+528 seconds
	-10%	2.86%	-202 seconds

Specific Heat

The table below displays how varying the specific heat affected each fuel package. There was a low power dependence for each fuel package, with the most dependent being the bookcase at 5.3%. The desk chair experienced the greatest time shift with a maximum difference of 258 seconds. There were no distinguishable patterns that could be seen between the fuel packages. In conclusion, it was determined that varying specific heat resulted in a low HRR difference and inconsistent max HRR times.

Specific Heat			
Thermal Property	**Input Uncertainty %**	**Power Dependence %**	**Max HRR Time Difference (sec)**
Beanbag	+10%	1.22%	-13 seconds
	-10%	0.65%	+3 seconds
Bookcase	+10%	5.3%	+253 seconds
	-10%	3.8%	-181 seconds
Desk	+10%	3.9%	±0 seconds
	-10%	3.5%	±0 seconds
Desk Chair	+10%	1.57%	+177 seconds
	-10%	1.45%	+258 seconds
Dresser	+10%	0.4%	+16 seconds
	-10%	0.7%	-6 seconds
Mattress	+10%	0%	+2 seconds
	-10%	1.62%	+9 seconds
Upholstered Chair	+10%	0.46%	+255 seconds
	-10%	0.61%	+175 seconds

Thermal Conductivity

The table below displays how varying the thermal conductivity affected each fuel package. There was a low power dependence for each fuel package, with the most dependent being the bookcase at 6.7%. In regards to the maximum HRR time difference, the upholstered chair experienced the greatest time shift of 456 seconds. In all but the tests involving the upholstered chair, the time to the peak HRR increased when the thermal conductivity increased; when the thermal conductivity was decreased, the time to the maximum HRR decreased as well. In conclusion, it was determined that varying thermal conductivity resulted in a negligible power difference but seemingly predictable max HRR times in terms of trends.

Thermal Conductivity			
Thermal Property	**Input Uncertainty %**	**Power Dependence %**	**Max HRR Time Difference (sec)**
Beanbag	+10%	1.76%	+4 seconds
	-10%	1.13%	-2 seconds
Bookcase	+10%	3.8%	+254 seconds
	-10%	6.7%	-181 seconds
Desk	+10%	3.1%	±0 seconds
	-10%	3.5%	±0 seconds
Desk Chair	+10%	1.31%	+141 sec
	-10%	2.12%	-37 sec
Dresser	+10%	2.1%	+10 seconds
	-10%	1.0%	-17 seconds
Mattress	+10%	1.7%	+37 seconds
	-10%	1.85%	-18 seconds
Upholstered Chair	+10%	1.26%	-443 seconds
	-10%	1.20%	+456 seconds

Appendix D: Master FDS Input File

&HEAD CHID='FULLSCALE_MASTER_FILE', TITLE='Fullscale Model_Master File'/

&TIME T_END=X /

&MESH IJK=121,114,48, XB=-1.5,7.0,-1.5,6.5,-0.05,3.3 / 7cm grid cells

&MISC THICKEN_OBSTRUCTIONS=.TRUE. /

&DUMP   DT_RESTART=10
      DT_DEVC=1
      NFRAMES=480
      PLOT3D_QUANTITY(1:5)='U-VELOCITY','V-VELOCITY','W-VELOCITY',
'TEMPERATURE', 'VOLUME FRACTION'
    PLOT3D_SPEC_ID(5)='OXYGEN'
      DT_PL3D=30 /

&REAC FUEL='POLYURETHANE'
      C=6.3
      H=7.1
      N=1
      O=2.1
      SOOT_YIELD=0.01
      CO_YIELD=0.025 /

&VENT MB='XMIN', SURF_ID='OPEN' / Open boundary conditions
&VENT MB='XMAX', SURF_ID='OPEN' /
&VENT MB='YMIN', SURF_ID='OPEN' /
&VENT MB='YMAX', SURF_ID='OPEN' /
&VENT MB='ZMAX', SURF_ID='OPEN' /

~~~~~~~~~~~~~~~~~~~~DEVICES~~~~~~~~~~~~~~~~~~~~

&PROP ID='Thermocouple_Props',
    BEAD_DIAMETER=5.1E-4,
    BEAD_EMISSIVITY=0.43,
    BEAD_DENSITY=1.134E4,
    BEAD_SPECIFIC_HEAT=0.128/

&DEVC ID='Q1TC_6ft._FDS', PROP_ID='Thermocouple_Props',
QUANTITY='THERMOCOUPLE', XYZ=2.315,4.0145,1.8288/
&DEVC ID='Q1TC_4ft._FDS', PROP_ID='Thermocouple_Props',
QUANTITY='THERMOCOUPLE', XYZ=2.315,4.0145,1.2192/
&DEVC ID='Q1TC_2ft._FDS', PROP_ID='Thermocouple_Props',
QUANTITY='THERMOCOUPLE', XYZ=2.315,4.0145,0.6096/

&DEVC ID='Q2TC_6ft._FDS', PROP_ID='Thermocouple_Props',
QUANTITY='THERMOCOUPLE', XYZ=4.951,4.0145,1.8288/
&DEVC ID='Q2TC_4ft._FDS', PROP_ID='Thermocouple_Props',
QUANTITY='THERMOCOUPLE', XYZ=4.951,4.0145,1.2192/
&DEVC ID='Q2TC_2ft._FDS', PROP_ID='Thermocouple_Props',
QUANTITY='THERMOCOUPLE', XYZ=4.951,4.0145,0.6096/

&DEVC ID='Q3TC_6ft._FDS', PROP_ID='Thermocouple_Props',
QUANTITY='THERMOCOUPLE', XYZ=3.7,3.0,1.8288/
&DEVC ID='Q3TC_4ft._FDS', PROP_ID='Thermocouple_Props',
QUANTITY='THERMOCOUPLE', XYZ=3.7,3.0,1.2192/
&DEVC ID='Q3TC_2ft._FDS', PROP_ID='Thermocouple_Props',
QUANTITY='THERMOCOUPLE', XYZ=3.7,3.0,0.6096/

&DEVC ID='Q4TC_6ft._FDS', PROP_ID='Thermocouple_Props',
QUANTITY='THERMOCOUPLE', XYZ=4.951,2.1095,1.8288/
&DEVC ID='Q4TC_4ft._FDS', PROP_ID='Thermocouple_Props',
QUANTITY='THERMOCOUPLE', XYZ=4.951,2.1095,1.2192/
&DEVC ID='Q4TC_2ft._FDS', PROP_ID='Thermocouple_Props',
QUANTITY='THERMOCOUPLE', XYZ=4.951,2.1095,0.6096/

&DEVC ID='HallwayTC_6ft._FDS', PROP_ID='Thermocouple_Props',
QUANTITY='THERMOCOUPLE', XYZ=3.69,0.568,1.8288/
&DEVC ID='HallwayTC_4ft._FDS', PROP_ID='Thermocouple_Props',
QUANTITY='THERMOCOUPLE', XYZ=3.69,0.568,1.2192/
&DEVC ID='HallwayTC_2ft._FDS', PROP_ID='Thermocouple_Props',
QUANTITY='THERMOCOUPLE', XYZ=3.69,0.568,0.6096/

&DEVC ID='FarHallwayTC_6ft._FDS', PROP_ID='Thermocouple_Props',
QUANTITY='THERMOCOUPLE', XYZ=0.571,0.568,1.8288/
&DEVC ID='FarHallwayTC_4ft._FDS', PROP_ID='Thermocouple_Props',
QUANTITY='THERMOCOUPLE', XYZ=0.571,0.568,1.2192/
&DEVC ID='FarHallwayTC_2ft._FDS', PROP_ID='Thermocouple_Props',
QUANTITY='THERMOCOUPLE', XYZ=0.571,0.568,0.6096/

&DEVC ID='Bedroom DoorTC_74.5in._FDS', PROP_ID='Thermocouple_Props',
QUANTITY='THERMOCOUPLE', XYZ=5.3381,1.091,1.8923/
&DEVC ID='Bedroom DoorTC_58.0in._FDS', PROP_ID='Thermocouple_Props',
QUANTITY='THERMOCOUPLE', XYZ=5.3381,1.091,1.4732/
&DEVC ID='Bedroom DoorTC_40.5in._FDS', PROP_ID='Thermocouple_Props',
QUANTITY='THERMOCOUPLE', XYZ=5.3381,1.091,1.0287/
&DEVC ID='Bedroom DoorTC_23.5in._FDS', PROP_ID='Thermocouple_Props',
QUANTITY='THERMOCOUPLE', XYZ=5.3381,1.091,0.5969/
&DEVC ID='Bedroom DoorTC_5.5in._FDS', PROP_ID='Thermocouple_Props',
QUANTITY='THERMOCOUPLE', XYZ=5.3381,1.091,0.1397/

&DEVC ID='Bedroom DoorVelocity_74.5in._FDS', QUANTITY='VELOCITY',
XYZ=5.338,1.091,1.8923, VELO_INDEX=-2 /Bedroom Door
&DEVC ID='Bedroom DoorVelocity_58.0in._FDS', QUANTITY='VELOCITY',
XYZ=5.338,1.091,1.4732, VELO_INDEX=-2 /Bedroom Door
&DEVC ID='Bedroom DoorVelocity_40.5in._FDS', QUANTITY='VELOCITY',
XYZ=5.338,1.091,1.0287, VELO_INDEX=-2 /Bedroom Door
&DEVC ID='Bedroom DoorVelocity_23.5in._FDS', QUANTITY='VELOCITY',
XYZ=5.338,1.091,0.5969, VELO_INDEX=-2 /Bedroom Door
&DEVC ID='Bedroom DoorVelocity_5.5in._FDS', QUANTITY='VELOCITY',
XYZ=5.338,1.091,0.1397, VELO_INDEX=-2 /Bedroom Door

&DEVC ID='Q1 Window Velocity.3_FDS', QUANTITY='VELOCITY', XYZ=2.54,5.05,1.942,
VELO_INDEX=2 /Quad 1 Window
&DEVC ID='Q1 Window Velocity.2_FDS', QUANTITY='VELOCITY', XYZ=2.54,5.05,1.477,
VELO_INDEX=2 /Quad 1 Window
&DEVC ID='Q1 Window Velocity.1_FDS', QUANTITY='VELOCITY', XYZ=2.54,5.05,1.012,
VELO_INDEX=2 /Quad 1 Window

&DEVC ID='Q2 Window Velocity.3_FDS', QUANTITY='VELOCITY',
XYZ=4.8415,5.05,1.942, VELO_INDEX=2 /Quad 2 Window
&DEVC ID='Q2 Window Velocity.2_FDS', QUANTITY='VELOCITY',
XYZ=4.8415,5.05,1.477, VELO_INDEX=2 /Quad 2 Window
&DEVC ID='Q2 Window Velocity.1_FDS', QUANTITY='VELOCITY',
XYZ=4.8415,5.05,1.012, VELO_INDEX=2 /Quad 2 Window

&DEVC ID='HVACTC_FDS', PROP_ID='Thermocouple_Props',
QUANTITY='THERMOCOUPLE', XYZ=1.715,5.05,0.3032/HVAC UNIT
&DEVC ID='HVACVelocity_FDS', QUANTITY='VELOCITY', XYZ=1.715,5.05,0.3032,
VELO_INDEX=2 /HVAC UNIT

&DEVC ID='Quad 1_corner.1_FDS', PROP_ID='Thermocouple_Props',
QUANTITY='THERMOCOUPLE', XYZ=1.4905,4.7762,0.6096/Quad 1 Corner
&DEVC ID='Quad 1_corner.2_FDS', PROP_ID='Thermocouple_Props',
QUANTITY='THERMOCOUPLE', XYZ=1.4905,4.7762,1.2192/Quad 1 Corner
&DEVC ID='Quad 1_corner.3_FDS', PROP_ID='Thermocouple_Props',
QUANTITY='THERMOCOUPLE', XYZ=1.4905,4.7762,1.8288/Quad 1 Corner
&DEVC ID='Quad 1_corner.4_FDS', PROP_ID='Thermocouple_Props',
QUANTITY='THERMOCOUPLE', XYZ=1.4905,4.7762,2.4384/Quad 1 Corner

&DEVC ID='Quad 2_corner.1_FDS', PROP_ID='Thermocouple_Props',
QUANTITY='THERMOCOUPLE', XYZ=5.9092,4.7762,0.6096/Quad 2 Corner
&DEVC ID='Quad 2_corner.2_FDS', PROP_ID='Thermocouple_Props',
QUANTITY='THERMOCOUPLE', XYZ=5.9092,4.7762,1.2192/Quad 2 Corner
&DEVC ID='Quad 2_corner.3_FDS', PROP_ID='Thermocouple_Props',
QUANTITY='THERMOCOUPLE', XYZ=5.9092,4.7762,1.8288/Quad 2 Corner
&DEVC ID='Quad 2_corner.4_FDS', PROP_ID='Thermocouple_Props',
QUANTITY='THERMOCOUPLE', XYZ=5.9092,4.7762,2.4384/Quad 2 Corner

&DEVC ID='Quad 3_corner.1_FDS', PROP_ID='Thermocouple_Props',
QUANTITY='THERMOCOUPLE', XYZ=1.4905,1.4618,0.6096/Quad 3 Corner
&DEVC ID='Quad 3_corner.2_FDS', PROP_ID='Thermocouple_Props',
QUANTITY='THERMOCOUPLE', XYZ=1.4905,1.4618,1.2192/Quad 3 Corner
&DEVC ID='Quad 3_corner.3_FDS', PROP_ID='Thermocouple_Props',
QUANTITY='THERMOCOUPLE', XYZ=1.4905,1.4618,1.8288/Quad 3 Corner

&DEVC ID='Quad 3_corner.4_FDS', PROP_ID='Thermocouple_Props',
QUANTITY='THERMOCOUPLE', XYZ=1.4905,1.4618,2.4384/Quad 3 Corner

&DEVC ID='HEAT FLUX GAUGE Q1', QUANTITY='GAUGE HEAT FLUX', XYZ=1.2,
4.15, 1.5, IOR=1 /
&DEVC ID='HEAT FLUX GAUGE Q2', QUANTITY='GAUGE HEAT FLUX', XYZ=6.2, 4.1,
1.5, IOR=-1 /
&DEVC ID='HEAT FLUX GAUGE Q3', QUANTITY='GAUGE HEAT FLUX', XYZ=1.2, 2.3,
1.5, IOR=1 /
&DEVC ID='HEAT FLUX GAUGE Q4', QUANTITY='GAUGE HEAT FLUX', XYZ=6.2, 2.4,
1.5, IOR=-1 /
&DEVC ID='HEAT FLUX GAUGE H', QUANTITY='GAUGE HEAT FLUX', XYZ=4.1, 0.15,
1.5, IOR=2 /
&OBST XB=1.058, 1.138, 4.087, 4.167, 1.48, 1.52, COLOR='INVISIBLE' / Used For Heat Flux
Guage Q1

~~~~~~~~~~~~~~~~~~~WALLS & FLOOR~~~~~~~~~~~~~~~~~~~

&MATL ID='GYPSUM',
    FYI='NBSIR 88-3752 - ATF NIST Multi-Floor Validation',
    SPECIFIC_HEAT=1.09,
    CONDUCTIVITY=0.17,
    DENSITY=930.0/
&MATL ID='YELLOW PINE',
    FYI='Quintiere, Fire Behavior - NIST NRC Validation',
    SPECIFIC_HEAT=2.85,
    CONDUCTIVITY=0.14,
    DENSITY=640.0/

&SURF ID='Exterior Wall',
    COLOR='SILVER',
    BACKING='VOID',
    MATL_ID(1,1)='GYPSUM',
    MATL_ID(2,1)='YELLOW PINE',
    MATL_ID(3,1)='GYPSUM',
    MATL_MASS_FRACTION(1,1)=1.0,
    MATL_MASS_FRACTION(2,1)=1.0,

```
      MATL_MASS_FRACTION(3,1)=1.0,
      THICKNESS(1:3)=0.0127,0.0880,0.0127/
&SURF ID='Interior Wall',
      COLOR='SILVER',
      BACKING='VOID',
      MATL_ID(1,1)='GYPSUM',
      MATL_ID(2,1)='YELLOW PINE',
      MATL_ID(3,1)='GYPSUM',
      MATL_MASS_FRACTION(1,1)=1.0,
      MATL_MASS_FRACTION(2,1)=1.0,
      MATL_MASS_FRACTION(3,1)=1.0,
      THICKNESS(1:3)=0.0127,0.1146,0.0127/

&MATL ID='CARPET NYLON',
          SPECIFIC_HEAT          =0.87,
          CONDUCTIVITY           =0.33,
          DENSITY                =1169.0/

&SURF ID                 ='CARPET'
          COLOR                  ='GOLDENROD'
          MATL_ID                ='CARPET NYLON'
          THICKNESS       =0.02
          HRRPUA                 =86.667
          IGNITION_TEMPERATURE      =405.0/


&OBST XB=0.0,0.1143,0.1143,5.08,-0.05,2.44, SURF_ID='Exterior Wall',  / Left Wall
&OBST XB=0.0,6.3283,0.0,0.1143,-0.05,2.44, SURF_ID='Exterior Wall',  / Front Wall
&OBST XB=6.214,6.3283,0.1143,5.081,-0.05,2.44, COLOR='INVISIBLE', SURF_ID='Exterior
Wall', / Right Wall
&OBST XB=0.0,2.116,5.081,5.1953,-0.05,2.44, SURF_ID='Exterior Wall'/ Back Wall
&OBST XB=2.967,4.417,5.081,5.1953,-0.05,2.44, SURF_ID='Exterior Wall'/ Back Wall
&OBST XB=5.268,6.3283,5.081,5.1953,-0.05,2.44, SURF_ID='Exterior Wall'/ Back Wall
&OBST XB=2.116,2.967,5.081,5.1953,-0.05,0.857, SURF_ID='Exterior Wall' / Back Wall
&OBST XB=2.116,2.967,5.081,5.1953,2.097,2.44, SURF_ID='Exterior Wall' / Back Wall
&OBST XB=4.417,5.268,5.081,5.1953,-0.05,0.857, SURF_ID='Exterior Wall'/ Back Wall
&OBST XB=4.417,5.268,5.081,5.1953,2.097,2.44, SURF_ID='Exterior Wall'  / Back Wall


&OBST XB=1.0457,6.214,1.025,1.157,0.0,2.44, SURF_ID='Interior Wall' / Long Hallway Wall
&OBST XB=1.0457,1.1857,1.157,3.478,0.0,2.44, SURF_ID='Interior Wall' / Short Hallway
Wall
```

&OBST XB=0.114,1.0457,3.033,3.173,0.0,2.44, SURF_ID='Interior Wall' / Long Closet Wall
&OBST XB=1.028,1.168,4.776,5.081,0.0,2.44, SURF_ID='Interior Wall' / Short Closet Wall

&OBST XB=0.1143,6.214,0.1143,5.081,-0.05,0.0, SURF_ID='CARPET' / Floor
&OBST XB=0.0,6.3283,0.0,5.1953,2.44,2.5, COLOR='INVISIBLE', SURF_ID='Exterior Wall',
BNDF_OBST=.FALSE. / Ceiling

~~~~~~~~~~~~~~~~~~~WINDOWS~~~~~~~~~~~~~~~~~~~

&MATL ID='GLASS',
    SPECIFIC_HEAT=0.84,
    CONDUCTIVITY=0.96,
    DENSITY=2803.0 /

&SURF ID='WINDOWS',
    COLOR='CYAN',
    BACKING='VOID',
    MATL_ID='GLASS',
    MATL_MASS_FRACTION=1.0,
    THICKNESS=0.0047625 /

&OBST XB=2.116,2.967,5.0773,5.1953,0.857,1.477, SURF_ID='WINDOWS',
DEVC_ID='Q1_WindowTop' / Quad 1 Window
&OBST XB=2.116,2.967,5.0773,5.1953,1.477,2.097, SURF_ID='WINDOWS',
DEVC_ID='Q1_WindowBottom' / Quad 1 Window Top Half
&DEVC XYZ=2.5415,5.05,1.167, ID='Q1_WindowTop', SETPOINT=450.,
QUANTITY='TEMPERATURE', INITIAL_STATE=.TRUE. /
&DEVC XYZ=2.5415,5.05,1.787, ID='Q1_WindowBottom', SETPOINT=450.,
QUANTITY='TEMPERATURE', INITIAL_STATE=.TRUE. /

&OBST XB=4.417,5.268,5.0773,5.1953,0.857,1.477, SURF_ID='WINDOWS',
DEVC_ID='Q2_WindowTop' / Quad 2 Window
&OBST XB=4.417,5.268,5.0773,5.1953,1.477,2.097, SURF_ID='WINDOWS',
DEVC_ID='Q2_WindowBottom' / Quad 2 Window Top Half
&DEVC XYZ=4.8425,5.05,1.167, ID='Q2_WindowTop', SETPOINT=450.,
QUANTITY='TEMPERATURE', INITIAL_STATE=.TRUE. /
&DEVC XYZ=4.8425,5.05,1.787, ID='Q2_WindowBottom', SETPOINT=450.,
QUANTITY='TEMPERATURE', INITIAL_STATE=.TRUE. /

~~~~~~~~~~~~~~~~~~~DOORS~~~~~~~~~~~~~~~~~~~

&MATL ID='AIR',
    SPECIFIC_HEAT=1.005,
    CONDUCTIVITY=0.0257,
    DENSITY=1.205
    SPEC_ID='OXYGEN'/

&MATL ID='MELAMINE',
    SPECIFIC_HEAT=1.2,
    CONDUCTIVITY=0.5,
    DENSITY=1570.0/

&SURF ID='DOORS',
    RGB=146,9,13,
    BACKING='VOID',
    MATL_ID(1,1)='MELAMINE',
    MATL_ID(2,1)='AIR',
    MATL_ID(3,1)='MELAMINE',
    MATL_MASS_FRACTION(1,1)=1.0,
    MATL_MASS_FRACTION(2,1)=1.0,
    MATL_MASS_FRACTION(3,1)=1.0,
    BURN_AWAY=.TRUE.
    THICKNESS(1:3)=0.003,0.0762,0.003/

&HOLE XB=4.995,5.909,0.0,0.115,1.82799,2.0311, COLOR='TAN',
DEVC_ID='DoorTemp_1/10' / Front Door
&DEVC XYZ=5.452,0.115,1.9295, ID='DoorTemp_1/10', SETPOINT=398.,
QUANTITY='TEMPERATURE', INITIAL_STATE=.FALSE. /Far Hallway Top Device

&HOLE XB=4.995,5.909,0.0,0.115,1.62488,1.82799, COLOR='TAN 1',
DEVC_ID='DoorTemp_2/10' / Front Door
&DEVC XYZ=5.452,0.115,1.7264, ID='DoorTemp_2/10', SETPOINT=398.,
QUANTITY='TEMPERATURE', INITIAL_STATE=.FALSE. /Far Hallway Top Device

&HOLE XB=4.995,5.909,0.0,0.115,1.42177,1.62488, COLOR='TAN 2',
DEVC_ID='DoorTemp_3/10' / Front Door

&DEVC XYZ=5.452,0.115,1.5233, ID='DoorTemp_3/10', SETPOINT=398.,
QUANTITY='TEMPERATURE', INITIAL_STATE=.FALSE. /Far Hallway Top Device

&HOLE XB=4.995,5.909,0.0,0.115,1.21866,1.42177, COLOR='TAN 3',
DEVC_ID='DoorTemp_4/10' / Front Door
&DEVC XYZ=5.452,0.115,1.3202, ID='DoorTemp_4/10', SETPOINT=398.,
QUANTITY='TEMPERATURE', INITIAL_STATE=.FALSE. /Far Hallway Top Device

&HOLE XB=4.995,5.909,0.0,0.115,1.01555,1.21866, COLOR='TAN 4',
DEVC_ID='DoorTemp_5/10' / Front Door
&DEVC XYZ=5.452,0.115,1.2071, ID='DoorTemp_5/10', SETPOINT=398.,
QUANTITY='TEMPERATURE', INITIAL_STATE=.FALSE. /Far Hallway Top Device

&HOLE XB=4.995,5.909,0.0,0.115,0.81244,1.01555, COLOR='TAN',
DEVC_ID='DoorTemp_6/10' / Front Door
&DEVC XYZ=5.452,0.115,0.913995, ID='DoorTemp_6/10', SETPOINT=398.,
QUANTITY='TEMPERATURE', INITIAL_STATE=.FALSE. /Far Hallway Top Device

&HOLE XB=4.995,5.909,0.0,0.115,0.60933,0.81244, COLOR='TAN 1',
DEVC_ID='DoorTemp_7/10' / Front Door
&DEVC XYZ=5.452,0.115,0.710885, ID='DoorTemp_7/10', SETPOINT=398.,
QUANTITY='TEMPERATURE', INITIAL_STATE=.FALSE. /Far Hallway Top Device

&HOLE XB=4.995,5.909,0.0,0.115,0.40622,0.60933, COLOR='TAN 2',
DEVC_ID='DoorTemp_8/10' / Front Door
&DEVC XYZ=5.452,0.115,0.507775, ID='DoorTemp_8/10', SETPOINT=398.,
QUANTITY='TEMPERATURE', INITIAL_STATE=.FALSE. /Far Hallway Top Device

&HOLE XB=4.995,5.909,0.0,0.115,0.20311,0.40622, COLOR='TAN 3',
DEVC_ID='DoorTemp_9/10' / Front Door
&DEVC XYZ=5.452,0.115,0.30466, ID='DoorTemp_9/10', SETPOINT=398.,
QUANTITY='TEMPERATURE', INITIAL_STATE=.FALSE. /Far Hallway Top Device

&HOLE XB=4.995,5.909,0.0,0.115,0.0,0.20311, COLOR='TAN 4',
DEVC_ID='DoorTemp_10/10' / Front Door
&DEVC XYZ=5.452,0.115,0.1015, ID='DoorTemp_10/10', SETPOINT=398.,
QUANTITY='TEMPERATURE', INITIAL_STATE=.FALSE. /Far Hallway Top Device

&OBST XB=0.1143,1.0283,2.6482,2.725,0.0,2.0311, SURF_ID='DOORS'/ FRONT DOOR

&OBST XB=5.8322,5.909,1.157,2.071,0.0,2.0311, SURF_ID='DOORS'/ BEDROOM DOOR

&HOLE XB=4.995,5.909,1.024,1.16,0,2.0311/ Bedroom Door
&HOLE XB=0.0,0.118,1.811,2.725,0,2.0311/ Side Door

~~~~~~~~~~~~~~~~~~~HVAC~~~~~~~~~~~~~~~~~~~

&OBST XB=1.4,1.9,5.1953,5.6,0.16,0.43, COLOR='BLACK', SURF_ID='INERT'/ HVAC
&OBST XB=0.1,1.5,5.25,5.51,0.16,0.43, COLOR='BLACK', SURF_ID='INERT'/ HVAC_2
&HOLE XB=1.63,1.8,5.08,5.5001,0.2032,0.4032/ HVAC
&HOLE XB=0.0,1.8,5.3168,5.4692,0.2308,0.3903/ HVAC_2

~~~~~~~~~~~~~~~~~~~BEAN BAG~~~~~~~~~~~~~~~~~~~

&SPEC ID='POLYSTYRENE', FORMULA ='C8H8' /

&MATL ID='Polystyrene Beads'
       SPECIFIC_HEAT=1.5
       CONDUCTIVITY=0.034
       DENSITY=25.
     HEAT_OF_COMBUSTION=35600./

&SURF ID='BEANBAG'
       COLOR='GREEN'
       HRRPUA=152
       BURN_AWAY=.TRUE.
       IGNITION_TEMPERATURE=350.
       MATL_ID='Polystyrene Beads'
       THICKNESS=0.005/

&OBST XB= 1.1857, 1.8157, 1.457, 1.607, 0.00, 0.64, SURF_ID='BEANBAG' /
&OBST XB= 1.1857, 1.2857, 1.607, 2.067, 0.00, 0.44, SURF_ID='BEANBAG' /
&OBST XB= 1.68, 1.8167, 1.607, 2.067, 0.00, 0.44, SURF_ID='BEANBAG' /
&OBST XB= 1.2857, 1.7167, 1.457, 2.067, 0.00, 0.24, SURF_ID='BEANBAG' /

~~~~~~~~~~~~~~~~~~~BOOKCASE~~~~~~~~~~~~~~~~~~~

```
&MATL ID='PARTICLEBOARD'
      SPEC_ID='CELLULOSE'
      DENSITY=800.
      CONDUCTIVITY=0.14
      HEAT_OF_COMBUSTION=17.5
      SPECIFIC_HEAT=1.3 /

&SURF ID='Bookcase'
      COLOR='ORANGE'
      HRRPUA=120.
      MATL_ID='PARTICLEBOARD'
      RAMP_Q='bookcase_ramp'
      IGNITION_TEMPERATURE=230.
      THICKNESS=0.8 /

&SURF ID='Bookcase_Back'
      COLOR='ORANGE'
      HRRPUA=120.
      BURN_AWAY=.TRUE.
      RAMP_Q='bookcase_ramp'
      MATL_ID='PARTICLEBOARD'
      IGNITION_TEMPERATURE=230.
      THICKNESS=0.8 /

&RAMP ID='bookcase_ramp', T=107, F=1 /
&RAMP ID='bookcase_ramp', T=120, F=1.22 /
&RAMP ID='bookcase_ramp', T=140, F=1.28 /
&RAMP ID='bookcase_ramp', T=160, F=1.17 /
&RAMP ID='bookcase_ramp', T=180, F=1.15 /
&RAMP ID='bookcase_ramp', T=200, F=0.98 /
&RAMP ID='bookcase_ramp', T=220, F=0.91 /
&RAMP ID='bookcase_ramp', T=240, F=0.69 /
&RAMP ID='bookcase_ramp', T=260, F=0.55 /
&RAMP ID='bookcase_ramp', T=360, F=0.36 /
&RAMP ID='bookcase_ramp', T=390, F=0.27 /
&RAMP ID='bookcase_ramp', T=510, F=0.24 /
&RAMP ID='bookcase_ramp', T=540, F=0.29 /
&RAMP ID='bookcase_ramp', T=615, F=0.28 /
```

&OBST XB= 3.317, 4.017, 5.031, 5.081, 0.00, 1.06, COLOR='IVORY',
SURF_ID='Bookcase_Back' / Back End
&OBST XB= 3.267, 3.317, 4.751, 5.081, 0.00, 1.06, COLOR='IVORY', SURF_ID='Bookcase' /
Left End
&OBST XB= 4.017, 4.067, 4.751, 5.081, 0.00, 1.06, COLOR='IVORY', SURF_ID='Bookcase' /
Right End
&OBST XB= 3.317, 4.017, 4.751, 5.031, 1.01, 1.06, COLOR='IVORY', SURF_ID='Bookcase' /
Top
&OBST XB= 3.317, 4.017, 4.751, 5.031, 0.65, 0.70, COLOR='IVORY', SURF_ID='Bookcase' /
Top Shelf
&OBST XB= 3.317, 4.017, 4.751, 5.031, 0.34, 0.39, COLOR='IVORY', SURF_ID='Bookcase' /
Middle Shelf
&OBST XB= 3.317, 4.017, 4.751, 5.031, 0.00, 0.05, COLOR='IVORY', SURF_ID='Bookcase' /
Bottom

~~~~~~~~~~~~~~~~~~~DESK~~~~~~~~~~~~~~~~~~~

&MATL ID   ='PARTICLEBOARD1'
      SPECIFIC_HEAT   =1.3
      CONDUCTIVITY   =0.14
      DENSITY   =800
      SPEC_ID   ='CELLULOSE'/

&SURF ID   ='DESK'
      COLOR   ='WHITE'
      MATL_ID   ='PARTICLEBOARD1'
      BURN_AWAY   =.TRUE.
      THICKNESS   =0.025
      HRRPUA   =90.94
      RAMP_Q   ='DESK_ramp'
      IGNITION_TEMPERATURE   =232.2 /

&RAMP ID='DESK_ramp', T=144, F=1.630 /
&RAMP ID='DESK_ramp', T=377, F=1.750 /
&RAMP ID='DESK_ramp', T=960, F=0.341 /

&OBST XB= 3.595, 4.995, 1.157, 1.807, 0.695, 0.73, SURF_ID='DESK'/
&OBST XB=3.595, 3.645, 1.157, 1.807, 0.0, 0.695, SURF_ID='DESK'/
&OBST XB=3.945, 3.995, 1.157, 1.807, 0.0, 0.695, SURF_ID='DESK'/

&OBST XB= 4.945, 4.995, 1.157, 1.807, 0.00, 0.695, SURF_ID='DESK'/
&OBST XB=3.695, 3.995, 1.157, 1.807, 0.465, 0.5, SURF_ID='DESK' /
&OBST XB=3.695, 3.995, 1.157, 1.807, 0.0, 0.05, SURF_ID='DESK' /
&OBST XB=3.645, 3.945, 1.157, 1.807, 0.45, 0.5, SURF_ID='DESK'/
&OBST XB=3.645, 3.945, 1.157, 1.807, 0.0, 0.05, SURF_ID='DESK'/
&OBST XB=3.645, 3.945, 1.807, 1.857, 0.0, 0.7, SURF_ID='DESK'/

~~~~~~~~~~~~~~~~~~DESK CHAIR~~~~~~~~~~~~~~~~~~

&SPEC ID='POLYURETHANE'
    FORMULA='C25H42N2O6' /

&SPEC ID='POLYESTER'
    FORMULA='C10H8O4' /

&MATL ID='OAK'
    CONDUCTIVITY=0.17
    SPECIFIC_HEAT=2.38
    DENSITY=545.
    SPEC_ID='CELLULOSE'/

&MATL ID='PARTICLEBOARD_A'
    CONDUCTIVITY=0.078
    SPECIFIC_HEAT=1.3
    DENSITY=590.
    SPEC_ID='CELLULOSE'/

&MATL ID='FOAM'
    CONDUCTIVITY=0.034
    SPECIFIC_HEAT=1.4
    DENSITY=29.
    SPEC_ID='POLYURETHANE'/

&MATL ID='FABRIC'
    CONDUCTIVITY=0.2
    SPECIFIC_HEAT=1.3
    DENSITY=1345.
    SPEC_ID='POLYESTER'/

```
&SURF ID='SEAT_BOTTOM',
    COLOR='KHAKI',
    HRRPUA=704.0,
    IGNITION_TEMPERATURE=268.0,
    MATL_ID(1,1)='FABRIC',
    MATL_ID(2,1:2)='PARTICLEBOARD_A','FOAM',
    MATL_MASS_FRACTION(1,1)=1.0,
    MATL_MASS_FRACTION(2,1:2)=0.2,0.8,
    THICKNESS(1:2)=0.0009,0.5146
    RAMP_Q='chair_ramp' /

&SURF ID='WOOD LEGS',
    COLOR='BURNT SIENNA',
    HRRPUA=8.7,
    IGNITION_TEMPERATURE=260.0,
    MATL_ID(1,1)='OAK',
    MATL_MASS_FRACTION(1,1)=1.0,
    THICKNESS(1)=0.07 /


&RAMP ID='chair_ramp', T=60, F=0.7 /
&RAMP ID='chair_ramp', T=90, F=0.62 /
&RAMP ID='chair_ramp', T=112, F=0.1 /
&RAMP ID='chair_ramp', T=180, F=0.07 /
&RAMP ID='chair_ramp', T=240, F=0.0 /
&RAMP ID='chair_ramp', T=600, F=0.0 /

&OBST XB= 4.247, 4.787, 1.437, 1.857, 0.36, 0.47, SURF_ID='SEAT_BOTTOM' /
&OBST XB= 4.247, 4.787, 1.857, 2.017, 0.36, 0.97, SURF_ID='SEAT_BOTTOM' /
&OBST XB= 4.247, 4.317, 1.947, 2.017, 0.00, 0.36, SURF_ID='WOOD LEGS' /
&OBST XB= 4.247, 4.317, 1.437, 1.507, 0.00, 0.36, SURF_ID='WOOD LEGS' /
&OBST XB= 4.717, 4.787, 1.947, 2.017, 0.00, 0.36, SURF_ID='WOOD LEGS' /
&OBST XB= 4.717, 4.787, 1.437, 1.507, 0.00, 0.36, SURF_ID='WOOD LEGS' /


~~~~~~~~~~~~~~~~~~DRESSER~~~~~~~~~~~~~~~~~~

&MATL ID                ='WHITE PINE'
      SPEC_ID           ='CELLULOSE'
      SPECIFIC_HEAT     =2.5
```

```
            CONDUCTIVITY              =0.11
            DENSITY                   =435
        HEAT_OF_COMBUSTION     =18500/


&SURF ID                 ='Dresser'
        COLOR                  ='SEPIA'
        MATL_ID                ='WHITE PINE'
        THICKNESS       =0.04
        HRRPUA                 =437.94
        RAMP_Q                 ='DRESSER_RAMP'
        IGNITION_TEMPERATURE       =350/


&&RAMP ID='DRESSER_RAMP', T=299, F=1.610 /
&RAMP ID='DRESSER_RAMP', T=360, F=0.825 /
&RAMP ID='DRESSER_RAMP', T=450, F=0.750 /
&RAMP ID='DRESSER_RAMP', T=600, F=0.241 /
&RAMP ID='DRESSER_RAMP', T=900, F=0.151 /


&OBST XB=5.714, 6.214, 2.507, 2.577, 0.0, 0.93, SURF_ID='Dresser'/
&OBST XB=5.714, 6.214, 3.527, 3.597, 0.0, 0.93, SURF_ID='Dresser'/
&OBST XB=6.114, 6.214, 2.577, 3.527, 0.0, 0.93, SURF_ID='Dresser'/
&OBST XB=5.714, 6.214, 2.577, 3.527, 0.0, 0.06, SURF_ID='Dresser'/
&OBST XB=5.714, 5.764, 2.582, 3.527, 0.06, 0.325, SURF_ID='Dresser'/
&OBST XB=5.714, 6.214, 2.577, 3.527, 0.33, 0.36, SURF_ID='Dresser'/
&OBST XB=5.714, 5.764, 2.582, 3.527, 0.36, 0.625, SURF_ID='Dresser'/
&OBST XB=5.714, 6.214, 2.577, 3.527, 0.63, 0.66, SURF_ID='Dresser'/
&OBST XB=5.714, 5.764, 2.582, 3.527, 0.66, 0.925, SURF_ID='Dresser'/
&OBST XB=5.714, 6.214, 2.507, 3.597, 0.93,0.96, SURF_ID='Dresser'/



~~~~~~~~~~~~~~~~~~MATTRESS~~~~~~~~~~~~~~~~~~~


&MATL ID='POLYURETHANE_CORE'
        SPECIFIC_HEAT=1.4
        CONDUCTIVITY=0.02
        DENSITY=30
        SPEC_ID='POLYURETHANE'
        HEAT_OF_COMBUSTION=24200. /


&MATL ID='POLYESTER'
```

```
        CONDUCTIVITY=0.05
        SPECIFIC_HEAT=1.1
        DENSITY=525
        HEAT_OF_COMBUSTION=20300. /

&MATL ID='POLYURETHANE_COTTON'
        SPECIFIC_HEAT=1.4
        CONDUCTIVITY=0.02
        SPEC_ID='POLYURETHANE'
        DENSITY=575
        HEAT_OF_COMBUSTION=24200. /

&SURF ID='MATTRESS'
        COLOR='GRAY'
        HRRPUA=275
        BURN_AWAY=.TRUE.
        BACKING='EXPOSED'
        MATL_ID(1:2,1)='POLYESTER','POLYURETHANE_CORE'
        THICKNESS(1:2)=0.00038,0.1
        IGNITION_TEMPERATURE=245. /

&SURF ID='PILLOW'
        COLOR='BLACK'
        HRRPUA=325
        MATL_ID='POLYURETHANE_COTTON'
        THICKNESS=0.004
        BACKING='EXPOSED'
        BURN_AWAY=.TRUE.
        IGNITION_TEMPERATURE=190. /


&SURF ID='BOX SPRING'
        MATL_ID='WHITE PINE'
        THICKNESS=0.025 /

&OBST XB= 1.95, 3.474, 1.157, 3.189, 0.4318, 0.635, SURF_ID='MATTRESS' /
&OBST XB= 2.00, 2.6604, 1.157, 1.665, 0.635, 0.7366 SURF_ID='PILLOW' /
&OBST XB= 2.7, 3.3604, 1.157, 1.665, 0.635, 0.7366 SURF_ID='PILLOW' /
&OBST XB= 1.95, 2.05, 1.157, 3.189, 0.2318, 0.4318, SURF_ID='BOX SPRING' /
&OBST XB= 3.374, 3.474, 1.157, 3.189, 0.2318, 0.4318, SURF_ID='BOX SPRING'/
```

&OBST XB= 2.05, 3.474, 1.157, 1.257, 0.2318, 0.4318, SURF_ID='BOX SPRING'/
&OBST XB= 2.05, 3.474, 3.089, 3.189, 0.2318, 0.4318, SURF_ID='BOX SPRING'/
&OBST XB= 2.05, 3.474, 2.073, 2.173, 0.2318, 0.4318, SURF_ID='BOX SPRING'/

~~~~~~~~~~~~~~~~~~UPHOLSTERED CHAIR~~~~~~~~~~~~~~~~~~

&MATL ID='PINEWOOD'
    CONDUCTIVITY=0.15
    SPECIFIC_HEAT=2.805
    DENSITY=640.
    SPEC_ID='CELLULOSE'/

&SURF ID='upholstered_SEAT_CUSHION',
    COLOR='BURNT UMBER',
    HRRPUA=457.29,
    IGNITION_TEMPERATURE=407.0,
    MATL_ID='FABRIC','FOAM'
    THICKNESS=0.0009, 0.86
    RAMP_Q='upholsteredchair_ramp'/

&SURF ID='upholstered_WOOD LEGS',
    COLOR='MAROON',
    HRRPUA=14.03,
    IGNITION_TEMPERATURE=350.0,
    MATL_ID='PINEWOOD',
    THICKNESS=0.1
    RAMP_Q='upholsteredchair_ramp'/

&RAMP ID='upholsteredchair_ramp', T=270, F=1.0 /
&RAMP ID='upholsteredchair_ramp', T=312, F=0.01 /
&RAMP ID='upholsteredchair_ramp', T=1320, F=0.0 /

&OBST XB=5.794, 6.074, 4.091, 4.951, 0.15, 0.9, SURF_ID='upholstered_SEAT_CUSHION'/
Couch, back cushions
&OBST XB=5.294, 5.794, 4.801, 4.951, 0.15, 0.66, SURF_ID='upholstered_SEAT_CUSHION'/
Couch, right armrest
&OBST XB=5.294, 5.794, 4.091, 4.241, 0.15, 0.66, SURF_ID='upholstered_SEAT_CUSHION'/
Couch, left armrest

&OBST XB=5.294, 5.794, 4.241, 4.801, 0.15, 0.3, SURF_ID='upholstered_SEAT_CUSHION'/ Couch, seat bottom
&OBST XB=5.294, 5.791, 4.244, 4.798, 0.303, 0.46, SURF_ID='upholstered_SEAT_CUSHION'/ Couch, seat cushion
&OBST XB=5.294, 5.394, 4.801, 4.951, 0.0, 0.15, SURF_ID='upholstered_WOOD LEGS'/ F.R. Leg
&OBST XB=5.294, 5.394, 4.091, 4.241, 0.0, 0.15, SURF_ID='upholstered_WOOD LEGS'/ F.L. Leg
&OBST XB=5.974, 6.074, 4.801, 4.951, 0.0, 0.15, SURF_ID='upholstered_WOOD LEGS'/ B.R. Leg
&OBST XB=5.974, 6.074, 4.091, 4.241, 0.0, 0.15, SURF_ID='upholstered_WOOD LEGS'/ B.L. Leg

~~~~~~~~~~~~~~~~~~SIP~~~~~~~~~~~~~~~~~~

&SURF ID='SIP'
COLOR='MAGENTA'
HRRPUA=1105.7
RAMP_Q='fire_ramp' /

&RAMP ID='fire_ramp', T=0, F=0 /
&RAMP ID='fire_ramp', T=17, F=.75 /
&RAMP ID='fire_ramp', T=30, F=1 /
&RAMP ID='fire_ramp', T=40, F=.75 /
&RAMP ID='fire_ramp', T=60, F=0.675 /
&RAMP ID='fire_ramp', T=120, F=0.475 /
&RAMP ID='fire_ramp', T=180, F=0.4 /
&RAMP ID='fire_ramp', T=240, F=0.275 /
&RAMP ID='fire_ramp', T=300, F=0.225 /
&RAMP ID='fire_ramp', T=360, F=0.2 /
&RAMP ID='fire_ramp', T=420, F=0.2 /
&RAMP ID='fire_ramp', T=480, F=0.15 /
&RAMP ID='fire_ramp', T=540, F=0.125 /
&RAMP ID='fire_ramp', T=600, F=0.125 /
&RAMP ID='fire_ramp', T=660, F=0.1 /
&RAMP ID='fire_ramp', T=720, F=0.025 /
&RAMP ID='fire_ramp', T=780, F=0.020 /
&RAMP ID='fire_ramp', T=840, F=0.0 /

&OBST XB=5.214, 5.29, 4.306, 4.382, 0.00, 0.10, SURF_ID='SIP' /

~~~~~~~~SLICE/BOUNDARY FILES~~~~~~~~

&SLCF XB=2.5415,2.5415,1.157,6.081,0,2.44, QUANTITY='VELOCITY', VECTOR=.TRUE. / QUAD 1 WINDOW SLICE
&SLCF XB=2.5415,2.5415,1.157,6.081,0,2.44, QUANTITY='TEMPERATURE', VECTOR=.TRUE. / QUAD 1 WINDOW SLICE
&SLCF XB=2.5415,2.5415,1.157,6.081,0,2.44, QUANTITY='VOLUME FRACTION', SPEC_ID='OXYGEN', VECTOR=.TRUE. / QUAD 1 WINDOW SLICE

&SLCF XB=4.8425,4.8425,1.157,6.081,0,2.44, QUANTITY='VELOCITY', VECTOR=.TRUE. / QUAD 2 WINDOW SLICE
&SLCF XB=4.8425,4.8425,1.157,6.081,0,2.44, QUANTITY='TEMPERATURE', VECTOR=.TRUE. / QUAD 2 WINDOW SLICE
&SLCF XB=4.8425,4.8425,1.157,6.081,0,2.44, QUANTITY='VOLUME FRACTION', SPEC_ID='OXYGEN', VECTOR=.TRUE. / QUAD 2 WINDOW SLICE

&SLCF XB=5.338,5.338,-1.0,2.091,0,2.44, QUANTITY='VELOCITY', VECTOR=.TRUE. / DOORS
&SLCF XB=5.338,5.338,-1.0,2.091,0,2.44, QUANTITY='TEMPERATURE', VECTOR=.TRUE. / DOORS
&SLCF XB=5.338,5.338,-1.0,2.091,0,2.44, QUANTITY='VOLUME FRACTION', SPEC_ID='OXYGEN', VECTOR=.TRUE. / DOORS

&SLCF XB=2.116,5.268,5.0,5.0,0.857,2.097, QUANTITY='VELOCITY', VECTOR=.TRUE. / BOTH WINDOWS
&SLCF XB=2.116,5.268,5.0,5.0,0.857,2.097, QUANTITY='TEMPERATURE', VECTOR=.TRUE. / BOTH WINDOWS

&SLCF XB=4.995,5.909,0.2,0.2,0,2.0311, QUANTITY='VELOCITY', VECTOR=.TRUE. / FRONT DOOR
&SLCF XB=4.995,5.909,0.2,0.2,0,2.0311, QUANTITY='TEMPERATURE', VECTOR=.TRUE. / FRONT DOOR

&SLCF XB=0.0,6.3283,0.0,5.1953,1.8288,1.8288, QUANTITY='VELOCITY', VECTOR=.TRUE. / 6ft Z-plane
&SLCF XB=0.0,6.3283,0.0,5.1953,1.8288,1.8288, QUANTITY='TEMPERATURE', VECTOR=.TRUE. / 6ft Z-plane

&SLCF XB=0.0,6.3283,0.0,5.1953,1.8288,1.8288, QUANTITY='VOLUME FRACTION', SPEC_ID='OXYGEN', VECTOR=.TRUE. / 6ft Z-plane

&SLCF XB=0.0,6.3283,0.0,5.1953,2.4,2.4, QUANTITY='VELOCITY', VECTOR=.TRUE. / Ceiling Z-plane
&SLCF XB=0.0,6.3283,0.0,5.1953,2.4,2.4, QUANTITY='TEMPERATURE', VECTOR=.TRUE. / Ceiling Z-plane
&SLCF XB=0.0,6.3283,0.0,5.1953,2.4,2.4, QUANTITY='VOLUME FRACTION', SPEC_ID='OXYGEN', VECTOR=.TRUE. / Ceiling Z-plane

&BNDF QUANTITY='WALL TEMPERATURE'/
&BNDF QUANTITY='NET HEAT FLUX' /

&TAIL /